THE REPUBLIC OF TURKEY
BAHCESEHIR UNIVERSITY

THE TRANSIENT EFFECTS OF SWITCHING EVENTS ON THE DISTRIBUTION NETWORK WITH THE MICRO-GRID

Master's Thesis

EREN BAHARÖZÜ

ISTANBUL, 2018

THE REPUBLIC OF TURKEY

BAHCESEHIR UNIVERSITY

THE GRADUATE SCHOOL OF NATURAL AND APPLIED SCIENCES
M.S. ELECTRICAL AND ELECTRONICS ENGINEERING

THE TRANSIENT EFFECTS OF SWITCHING EVENTS ON THE DISTRIBUTION NETWORK WITH THE MICRO-GRID

Master's Thesis

EREN BAHARÖZÜ

Supervisor: Asst. Prof. Dr. GÜRKAN SOYKAN

ISTANBUL, 2018

THE REPUBLIC OF TURKEY

BAHCESEHIR UNIVERSITY

THE GRADUATE SCHOOL OF NATURAL AND APPLIED SCIENCE

ELECTRICAL AND ELECTRONICS ENGINEERING

Name of the Thesis: THE TRANSIENT EFFECTS OF SWITCHING EVENTS ON THE DISTRIBUTION NETWORK WITH THE MICRO-GRID
Name/Last Name of the Student: Eren BAHARÖZÜ
Date of Thesis Defense: 12.01.2018

This thesis has been approved by the Graduate School of Natural and Applied Science.

Prof. Dr. Nafiz ARICA
Graduate School Director

This is to certify that we have read this thesis and we find it fully adequate in scope, quality and content, as a thesis for degree of Master of Science.

Asst. Prof. Dr. Cavit Fatih KÜÇÜKTEZCAN
Program Coordinator

Examining Committee Members	Signature
Thesis Supervisor	
Asst. Prof. Dr. Gürkan SOYKAN	----------
Member	
Prof. Dr. Sadettin ÖZYAZICI	----------
Member	
Prof. Dr. Mustafa BAĞRIYANIK	----------

ACKNOWLEDGEMENT

My first debt of appreciation should go to my supervisor Asst. Prof. Dr. Gürkan Soykan for his support and encouragement through the not only my thesis but also my master program.

Also, I would like to thank my family for their support and encouragement, without them I cannot complete this thesis.

Istanbul, 2018 Eren BAHARÖZÜ

ABSTRACT

THE TRANSIENT EFFECTS OF SWITCHING EVENTS ON THE DISTRIBUTION NETWORK WITH THE MICRO-GRID

Eren Baharözü

Electrical and Electronics Engineering

Thesis Supervisor: Asst. Prof. Dr. Gürkan Soykan

January 2018, 75 Pages

Sustainable and clean energy has come into the forefront with the increasing demand especially for last two decades. In this duration, distributed energy resources (DERs) have started to become the common energy sources to generate power slowly in all over the world. Especially, DERs such as photovoltaic (PV) systems and wind energy systems (WESs) are started to use on the customer side. With this usage, the micro-grid (MG) concept was born on the distribution side of the power system. As all new concepts of power systems, power quality phenomenon has come to the prominence with this new concept. In this regard, many researchers have studied the effects of different types of micro-grids to power quality phenomenon. Yet, the majority of these studies has not considered the all necessities to obtain the accurate results especially for analyzing the transient events on power systems. Because of this, in this study detailed and frequency dependent models were used to fulfill all the necessities to simulate the real system. An AC micro-grid system, consisting of PV system, WES, energy storage system and loads, was used to analyze the effects of transient events to the main-grid and micro-grid. Switching, lightning and faults events are considered in terms of the power quality phenomenon. Thus, they are simulated as different cases by using the EMTP-RV software in this thesis. At the end of the simulations, the results of on/off grid operation and single-phase fault with multiple MGs cases show that any MG has a positive influence on the voltage profile. On the other hand, when transient events are considered more distortions and fluctuations on the voltage are seen at the bus of the MG for all cases. Finally, it can be deducted that MGs are more vulnerable to transient events and they are affected by such events considerably.

Keyword: Distributed Energy Resources, Faults, Lightning, Micro-Grid, Switching, Transient

ÖZET

ANAHTARLAMA OLAYLARIYLA MEYDANA GELEN GEÇİCİ OLAYLARIN MİKRO-ŞEBEKELİ DAĞITIM ŞEBEKESİNDEKİ ETKİSİ

Eren Baharözü

Elektrik-Elektronik Mühendisliği

Tez Danışmanı: Yrd. Doç. Dr. Gürkan Soykan

Ocak 2018, 75 Sayfa

Özellikle son yıllarda, yüksek enerji talebi ile beraber sürdürülebilir ve temiz enerji anlayışı ön plana çıkmıştır. Bu süre zarfında, dağıtık enerji kaynakları (DER'ler) elektrik üretimi için yavaş yavaş yaygın enerji kaynakları olmaya başlamıştır. Özellikle fotovoltaik (PV) sistemler ve rüzgar enerjisi sistemleri (WES) gibi dağıtık enerji kaynakları müşteri tarafında kullanılmaya başlanmıştır. DER'lerin güç dağıtım sistemlerinde kullanımı ile de mikro şebeke (MG) konsepti doğmuştur. Tüm yeni güç sistemleri konseptlerinde olduğu gibi, güç kalitesi fenomeni bu yeni konsept için de ön plana çıkmıştır. Bu bağlamda birçok araştırmacı, farklı mikro-şebeke türlerinin güç kalitesine etkilerini incelemiştir. Ancak, bu çalışmaların çoğu özellikle geçici olayların güç sistemleri üzerindeki analizleri göz önünde bulundurulduğunda, doğru sonuçlar elde etmek için gereken tüm gereksinimleri dikkate almamıştır. Bu nedenle bu çalışmada, gerçek bir dağıtım sistemini yansıtacak benzetimin tüm gereksinimleri, detaylı ve frekans bağımlı modeller kullanılarak sağlanmıştır. Geçici olayların ana şebeke ve mikro şebeke üzerindeki etkilerini analiz etmek için PV sistemi, WES, enerji depolama sistemi ve yüklerden oluşan bir AC mikro şebeke kullanılmıştır. Anahtarlama, yıldırım ve arıza olayları güç kalitesi fenomeni açısından değerlendirilmiştir. Bu olayları içeren farklı vaka çalışmaları bu tez çalışmasında EMTP-RV yazılımı kullanılarak simüle edilmiştir. Özellikle, mikro şebekenin ana şebekeye bağlı/şebekeden bağımsız (ada mod) işletimi ve birden fazla MG'nin kullanıldığı şebekede tek faz hatası vaka çalışmaların sonuçları, MG'nin gerilim profilleri üzerinde olumlu bir etkiye sahip olduğunu göstermektedir. Bununla birlikte, geçici olaylar göz önüne alındığında, tüm vaka çalışmalarında MG barasında daha fazla bozulma ve gerilim dalgalanmaları görülmektedir. Dolayısıyla yapılan vaka çalışmaları ışığında, MG'lerin geçici olaylara karşı daha savunmasız oldukları ve önemli ölçüde etkilendiği sonucuna varılabilmektedir.

Anahtar Kelimeler: Arızalar, Dağıtık Enerji Kaynakları, Yıldırım, Mikro Şebeke, Anahtarlama, Geçici Olaylar

CONTENTS

TABLES

FIGURES

ABBREVIATIONS

ASUI	:	Average Service Unavailability Index
ASAI	:	Average Service Availability Index
AC	:	Alternating Current
CAES	:	Compressed Air Energy Storage
CAIDI	:	Customer Average Interruption Duration Index
CP	:	Constant Parameter
DC	:	Direct Current
ESS	:	Energy Storage System
ENS	:	Energy Not Supplied
FD	:	Frequency Dependent
IEC	:	International Electrotechnical Commission
IEEE	:	The Institute of Electrical and Electronics Engineers
IG	:	Induction Generator
MG	:	Micro-grid
N	:	N-Type Semiconductor
NOX	:	Nitrogen Oxide
P	:	P-Type Semiconductor
PI	:	Proportional Integral Controller
PM	:	Permanent Magnet
PV	:	Photovoltaic
PWM	:	Pulse Width Modulation
SAES	:	Superconducting Magnetic Energy Storage
SAIDI	:	System Average Interruption Duration Index
SAIFI	:	System Average Interruption Frequency Index
SG	:	Synchronous Generator
WES	:	Wind Energy System

SYMBOLS

A	:	Current
C	:	Capacitance
L	:	Inductance
P	:	Power
R	:	Resistance
V	:	Voltage
Ω	:	Resistance
λ	:	Flux Linkage
ω	:	Angular Velocity

1. INTRODUCTION

Day by day consumption of energy is increasing. In order to provide sustain and continuous energy, different resources have been using. Currently, fossil fuels are still main energy sources for supplying energy. However, plenty of countries changed their energy policies especially for last two decades. They aimed to achieve clean and sustainable energy. Thus, renewable energy resources like wind and solar took people's interest. Also, there is a fact that fossil fuels will be run out following decades. To fulfill of fossil fuels place and accomplish these new targets, distributed energy resources (DERs) are installed all over the World. Most of the distributed energy resources, especially small scaled ones, are located near the customers. Wind energy systems, PV panels, batteries and micro-generators are used as main DERs. Such aggregation of DERs with loads named as micro-grids. Micro-grids can be operated both grid-connected and islanded. Normally grid-connected mode is preferred but for islands and some rural areas, renewable energy sources are the only option to provide energy or electricity. Depending on its operation mode micro-grids can offer a lot of benefit related power quality problems for customers and utilities.

These benefits can be summarized as decreased negative environmental effects, higher reliability, higher energy efficiency, minimization of losses and improvement of endurance of network to faults. On the contrary, due to the usage of power electronic devices in micro-grid, harmonic currents and voltage distortions can be seen. Based on usage purpose of micro-grids and scenarios, both positive and negative effects can be changed. Also, micro-grids became more vulnerable systems if they operated as an islanded mode. Most of the studies in the literature focus on power quality issues to last more than 1 cycle and not focus on temporary events like transients. Yet, transient events have an influence on the power system and should be studied.

The concept of the transient is a term used for undesirable and instantaneous events. In power systems, transient happens when the network changes from steady-state to unsteady-state. In general, the transient events that occur in the system have two different sources: lightning strike and switching. Thus, transients are classified into two distinct categories; impulsive transients and oscillating transients. Another considered criterion

when making this classification is the wave characteristics of the transients that these two transient sources will create. Thus, it can be said that these transient categories reflect the characteristics of the waveform of current and voltage which will happen during the transient event. The transient voltage that can be created by the lightning strike is called as an impulsive transient, and the transient voltage that can be created by the switching events in the network is called as an oscillatory transient.

In this thesis to fulfill the gap in the literature, both oscillatory and impulsive transient events are modeled and simulated with details for power grid which includes connected micro-grids. Then the simulation results are evaluated.

1.1 LITERATURE REVIEW

In order to understand effects of micro-grids, lots of studies were done especially related to power quality issues. In this part, studies which can be found in the literature were reviewed.

For example, in (Davodi et al., 2010), wind energy system was used as an only energy resource of micro-grid. The designed micro-grid system was modeled in PSCAD software and five different cases simulated which were connection and disconnection of WES, single phase fault, load disconnection and micro-grid disconnection from the infinite bus. The result of these cases was evaluated in terms of wind turbine active and reactive power reactions.

In (Belkacemi et al., 2015), micro-grid which consists of wind energy system, PV panel and more 10 rotating machines was tested for three-phase fault analysis by considering both on and off-grid operations of it. The main purpose of this study was to investigate the stability of system based on operation mode during faults. To do so, real-time test system which including hardware and software (Labview, Visual Studio and photovoltaic power profile emulation PPPE) was used. 4 scenarios were tested and results indicated that micro-grid is more vulnerable to faults if it is in off-grid mode.

Several papers (Singh et al., 2016), (Zhang et al., 2016) and (Majumder et al., 2009) focused on load shedding scenarios. These scenarios were performed in ETAP, Matlab/Simulink and PSCAD respectively. Load shedding is the term that is used for disconnection of some loads from micro-grid when it is in off-grid mode (islanded). The

point of origin of this concept is to prevent frequency changes due to a mismatch between generation and consumption. Generally, when micro-grid is islanded, load became higher than a generation and this causes decreasing in frequency. In order to keep frequency at grid frequency, either load shedding should be done or micro generator or diesel generators should be installed.

Besides the effects of load shedding scenarios, some studies (Ghosh et al., 2009), (Majumder et al., 2010), (Goyal and Gupta, 2012) and (Kumar and Gupta, 2016) were concerned with control management systems of micro-grid for load shedding. In these studies, different control schemes were proposed and examined to find most suitable one in terms of their benefits to load shedding and management process.

There are other research papers that analyzed the power quality problems and improvements only considering micro-grid itself. For instance, positive effects of supercapacitor as an energy storage were investigated (Zheng et al., 2015). Their effects on power quality improvement were tested and evaluated for fault and switching conditions. Test cases were modeled and simulated by using PSCAD software. Results showed that energy storage systems improve the reliability of micro-grid when transient events are considered. Another study which was done by Rasheed, B., M., Awais, M. and Jawaid, N., in 2016, examined the stability of micro-grid under different loads. Four cases were tested by using PSCAD. From test analysis, it was deducted that balanced loads and distributed energy resources decrease power losses and increase the stability of micro-grid.

Some studies addressed the positive effects of micro-grids to the power grid. Matlab software was used to simulate and test the influence of micro-grids. In first study (Tuffana and AlMuhaini, 2015), reliability indices (SAIFI, SAIDI, CAIDI, ASUI, ASAI, ENS) were investigated with and without micro-grid and the results indicate that in general all indices are improved with the usage of DG in the micro-grids. In the second study (Miron et al., 2016), PV panels were used as only DERs in the micro-grid structure. Weak Romanian distribution network was modeled and 10 scenarios were tested in terms of different load curves. The results of simulations showed that although the PV panels cause some drawbacks like an injection of harmonic currents, effects of PV panels to the power grid are positive generally. In the third study (Seritan et al., 2016), ETAP software

was used to investigate effects of micro-grid. By considering different load and generation curves, assessment of the influence of micro-grid was done. Test results point to benefits of micro-grid in terms of harmonic indexes, losses and reactive power.

When the studies that are mentioned above are evaluated, it is seen that the micro-grid concept has the influence of power quality issues and pros and cons of micro-grids vary from case to case. Depending on the designed network, different case scenarios should be studied. Yet, in these studies, designed networks were modeled as basic models (not considering frequency dependent models or complete distribution grid) and case studies were tested for considering only one of the main DERs.

1.2 OBJECTIVE OF THESIS

There are two objectives in this thesis. The first one is modeling the electrical structure and operation of the designed micro-grid system in EMTP-RV software by considered main distributed resources which are wind energy system, photovoltaic system and energy storage system. The second and the main objective of this thesis is to simulate the transient events which can be occurred in the grid-connected micro-grid system and evaluate the influence of micro-grid to these events in terms of power quality by modeling both the main grid and micro-grid as frequency dependent. It is expected that this thesis is able to contribute the literature by investigating the effects of transient events with more accurate modeling of the power system by using EMTP-RV and considering all main DERs.

1.3 THESIS ORGANIZATION

The thesis consists of six chapters. In the first chapter, background information and recent implementation of the micro-grid system are presented. Other studies and research related to the micro-grid system in the literature are reviewed from the point of their contribution and focus areas. Besides these, the aim of the thesis, and the scope of the thesis are given in this chapter. Micro-grid types are defined and explained in the following chapter with regards to electrical structure, operation modes and control methods. Main components of the micro-grid system are described as a PV system, WE, ESS, cables and load in chapter three. Then, they are scrutinized by considering their electronic models. Control systems of DERs are modeled in EMTP by using state equation and built-in blocks. The photovoltaic system is modeled with MPPT while traditional PI control is used for wind

energy system. This control system information is also given in this chapter. In the fourth chapter, information and illustration of detailed modeling of the micro-grid system in EMTP-RV are given. In the fifth chapter, different possible transient case scenarios and their potential effects on the main power grid and micro-grid are defined. Moreover, the simulation results of the test cases which are done by using EMTP-RV software, are indicated. Also, evaluation and explanation of these simulation results are done in this chapter. The conclusion of the thesis with the recommendations is presented in chapter six.

2. MICRO-GRID SYSTEMS

Micro-grid is basically the low voltage distribution system where power generation systems are located to customer side. They are operated at the LV, and their total installed generation capacity generally less than the MW range. Micro-grid consists of different components which are DGs, ESSs, loads and cables (Su and Wang, 2012). A micro-grid is capable of functioning both grid-connected and islanded (emergency situation) mode of operation. Currently, the concept of micro-grid has grown in importance especially in last two decades. Due its lower cost, reliability and efficiency, micro-grids have around 3.2 gigawatts power capacity today (Dorf, 2005). With the increasing of the micro-grid applications, they are categorized in various subjects such as electrical structure and operation modes.

2.1 TYPES OF MICRO-GRIDS IN TERMS OF ELECTRICAL STRUCTURE

The electrical structure of the grid, it has been always questioned when the DC and AC system were introduced (Watson, 2007). Since then, different researchers defended these different structures. Beside these two well-known electrical structures, a new electrical structure called as a hybrid electrical structure which is composed of a combination of AC and DC electrical system, came into consideration. These all three electrical structures are available in the micro-grid applications (Hossain et al., 2014; Lasseter, 2010). Their detailed information is given in following subsections.

2.1.1 AC Micro-Grids

AC micro-grids are the most commonly used micro-grid architecture in the power system. In this type micro-grid, DERs, ESS and loads are connected to one main AC bus. Then this AC bus is connected to the distribution side of grid via a switch. The basic structure of AC micro-grid is given below as Figure 2.1.

Figure 2.1: AC Micro-Grid Structure

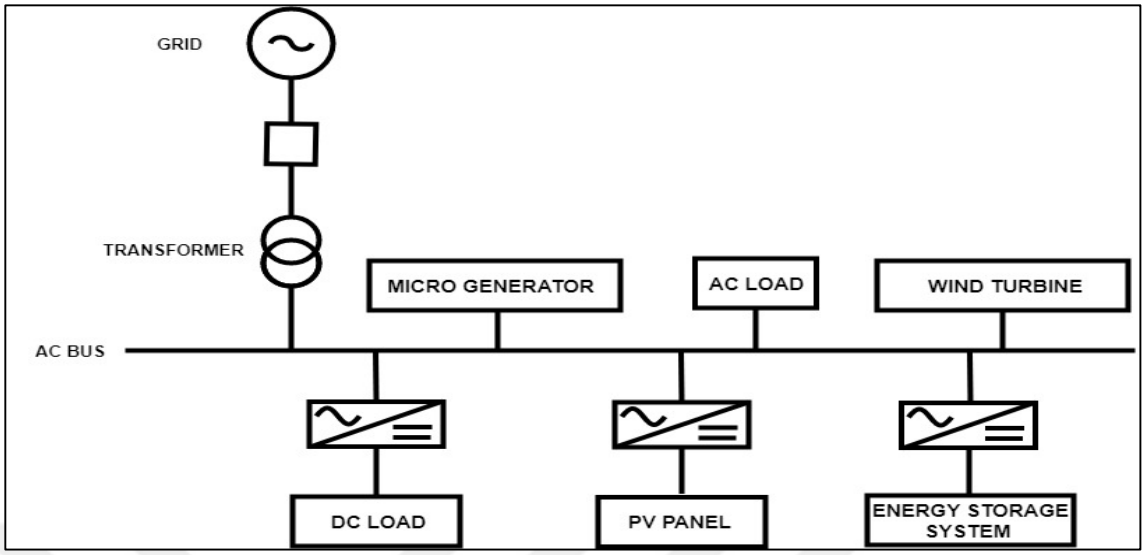

2.1.2 DC Micro-Grids

In this type of micro-grid, unlike the AC micro-grids, all components are linked to main DC bus. This main DC bus is connected utility grid with the bi-directional converter. If loads of micro-grid mainly consists of DC form, DC micro-grids are more efficient than AC micro-grids because of usage of less power electronic devices. Illustration of DC micro-grid is shown in Figure 2.2.

Figure 2.2: DC Micro-Grid Structure

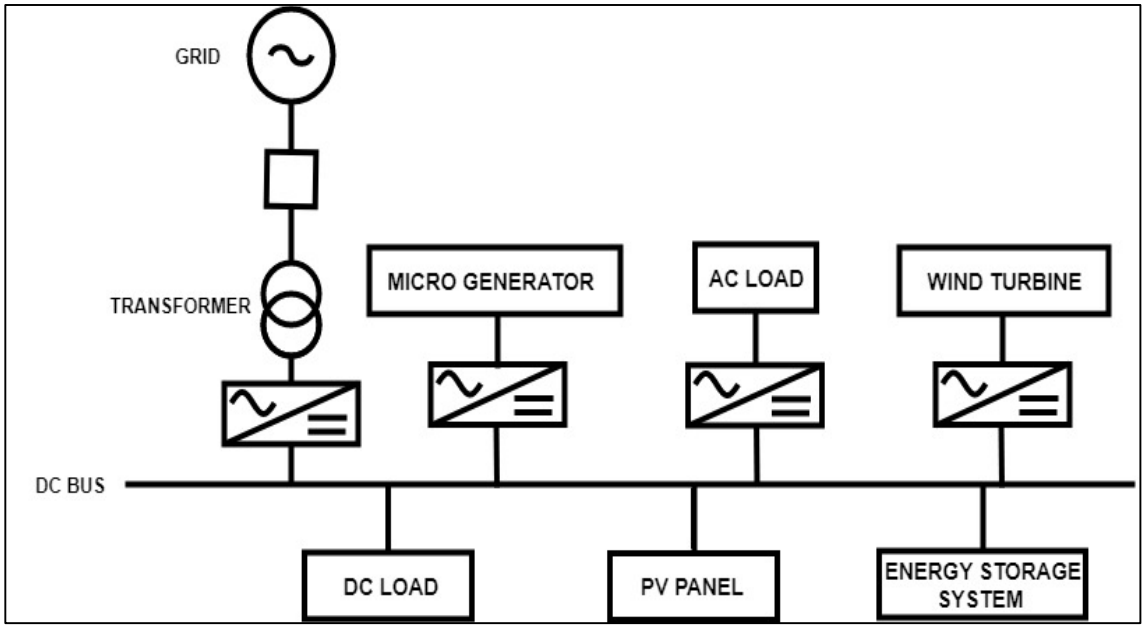

2.1.3 Hybrid Micro-Grids

Hybrid micro-grids is a combination of DC bus where DC components like ESSs, PVSs and DC loads are located on it, and AC bus where AC components like WES, AC loads are connected to it. The bi-directional converter is used between AC and DC buses (Eghtedarpour and Farjah, 2014; Liu et al., 2011). The main configuration of Hybrid Micro-grid is shown in below as Figure 2.3.

Figure 2.3: Hybrid Micro-Grid Structure

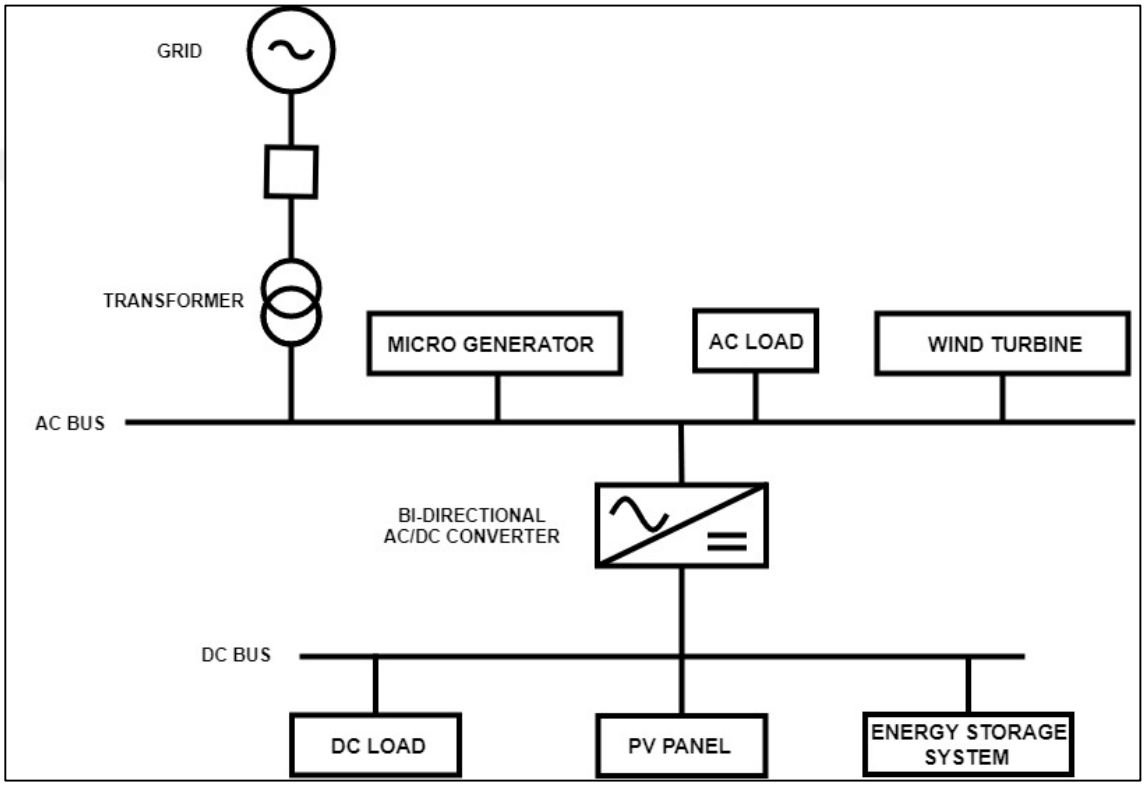

2.2 TYPES OF MICRO-GRIDS IN TERMS OF OPERATION MODE

Micro-grids can be operated in two different modes. These are grid-connected mode and islanded mode. When micro-grid is capable of operation at grid-connected mode, it can be operated as an islanded mode as well by changing the main switch after PCC.

2.2.1 Grid-Connected Mode

The most of the future micro-grids will be operated in a grid-connected mode, except for those which installed on physical islands or rural areas where there is no main electrical grid. The main advantages of the micro-grids come in sight when they are operated in

grid-connected mode. The electrical configuration of AC micro-grid for grid-connected mode is indicated in below as Figure 2.4.

Figure 2.4: Grid Connected Mode of AC Micro-Grid

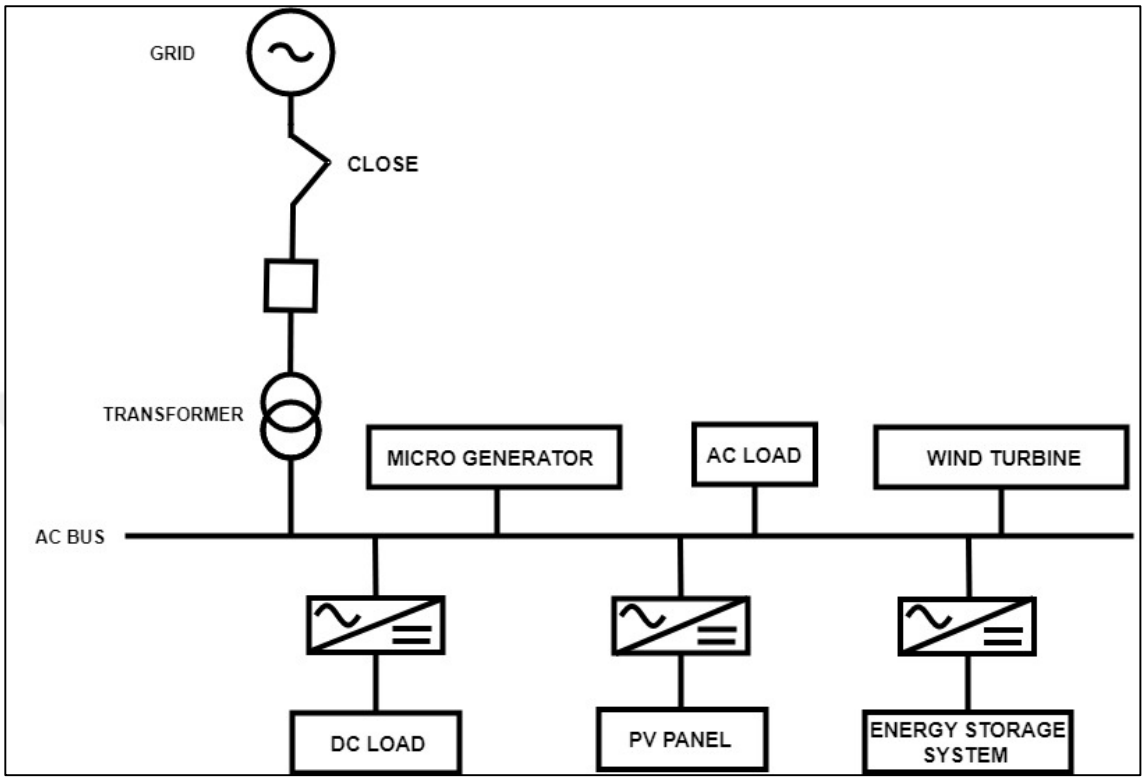

2.2.2 Islanded Mode

Islanded mode operation was born due to the obligation. People who live in islands or rural areas installed renewable energy sources in order to get electricity and energy. Thus, they created islanded mode micro-grid. However, long-term islanded mode operation requires accurate and satisfying storage and generation capacity in order to continue supplying the necessary energy to all loads. That's why without any emergency or obligation, islanded mode operation is not preferred. The electrical configuration of AC micro-grid for islanded mode is indicated in below as Figure 2.5.

Figure 2.5: Islanded (Off-Grid) Mode of AC Micro-Grid

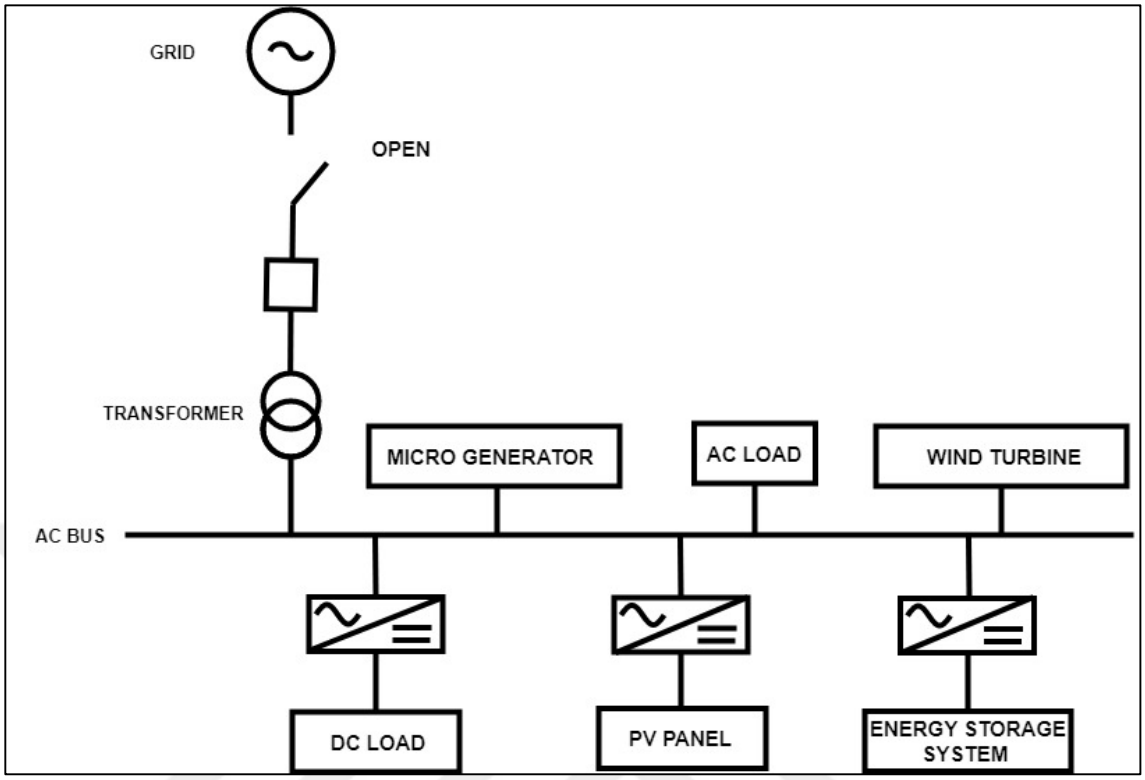

3. COMPONENTS OF MICRO-GRID SYSTEM

3.1 PHOTOVOLTAIC SYSTEM

Currently obtained energy from solar panels got priority like other distributed energy resources. Photovoltaic systems are the best known and common used one in order to generate electrical power from the sun. Its history goes to over 170 years back. Since then, PV system concept has been changed and improved with their efficiency. Currently, PV systems consist of four main component which is PV cells, maximum power point tracking (tracker) (MPPT), DC-DC converter and inverter. These elements are explained below subsections with more detailed way.

3.1.1 PV Cell

Solar panels are made of semiconductors. N-type and P-type two semiconductor are connected to each other and when photons come to the surface of this connected area, current occurs and flows at the external circuit. In theoretically, when photons hit the joint area, electrons of the semiconductor will get more energy. While negative electrons rise in N-type, positive ions rise in P-type. Therefore, a potential difference occurs and it causes the current flow between them. Current flows from P-type semiconductor to N-type semiconductor. Schematic representation of PV cell is given in Figure 3.1. This current is occurred in DC form and should be converted into AC form in order to use in the distribution network. Also, PV cells are connected electrically in series and parallel to each other to obtain higher current, voltage and power value. These connected cells create PV modules which are enduring the environmental effects and provide impermeability. Then, PV modules linked to each other with electrically and create PV arrays.

Figure 3.1: PV Cell Representation

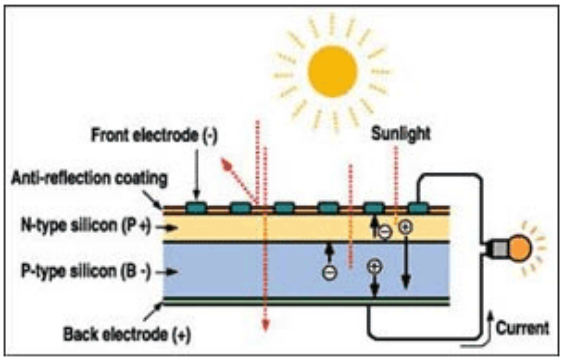

Source:http://www.engineering.com

Efficiency and cost of these PV cells or panels are mainly based on the type of semiconductor and manufacturing process of them. Semiconductor materials presently used for photovoltaic cells are monocrystalline silicon, polycrystalline silicon, amorphous silicon, cadmium telluride, and copper indium gallium selenide/sulfide (Jacobson, 2009). With the development of multi-junction concentrator cell, highest efficiency percentage of cells which is %46 is achieved in 2014 (NREL, 2013).

The equivalent circuit of the PV cell is given in Figure 3.2. It consists of series resistance, shunt resistance, current source and diode. As mentioned before, a group of PV cells creates PV arrays. Following formulas which are shown in Eq. (3.1), Eq. (3.2), Eq. (3.3) and Eq. (3.4), are used for PV arrays and describe current and voltage relationship of PV arrays (Sharma et al., 2015; Pandiarajan et al., 2012; Ramos et al., 2012; Villalva et al., 2009).

Figure 3.2: Equivalent Circuit of PV Cell

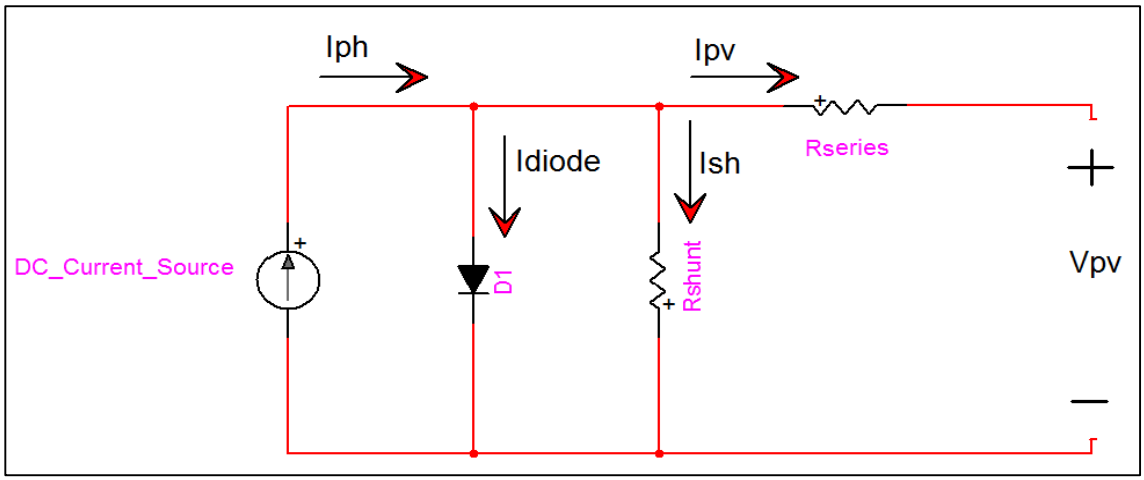

$$I = N_p.I_{ph} - N_p.I_s\left[exp\left(\frac{q.\left(\frac{V}{Ns} + I.R_s\right)}{\frac{N_p}{K.Temp.n}}\right) - 1\right] - \frac{\left(\frac{V.Np}{Ns} + I.R_s\right)}{R_{sh}} \quad (3.1)$$

Where;

I is the current of PV array

N_p is the number of parallel PV cells

I_{ph} is the photocurrent

I_s is the cell saturation current

q is the electron charge which is 1.6×10^{-19} C

N_s is the number of series PV cells

V is the voltage of PV array

K is the Boltzmann's constant which is 1.38065×10^{-23} J/Kelvin

Temp is the actual temperature (Kelvin)

n is the ideal factor of diode

R_s is the series resistance (ohm)

R_{sh} is the shunt resistance (ohm)

I_{ph} is occurred from photoelectric events and calculated as follows;

$$I_{ph} = \left[I_{sc} + K_i.\left(Temp - Temp_{ref}\right)\right].G \quad (3.2)$$

Where;

$Temp_{ref}$ is the reference temperature (298 Kelvin)

I_{sc} is the short circuit current at reference temperature and irradiance

K_i is the temperature short circuit current constant

G is the ratio of actual irradiance to reference irradiance (1 kW/m^2)

Cell saturation currents change depending on the temperature and formulated as;

$$I_s = I_{RS}.\left(\frac{Temp}{Temp_{ref}}\right)^3 . exp\left[\frac{q.E_g.\left(\frac{1}{Temp_{ref}} - \frac{1}{Temp}\right)}{K.n}\right] \quad (3.3)$$

Where;

I_{RS} is the reserve saturation current of PV cell at reference temperature and irradiance

E_g is the band gap energy of silicon which is 1.2

The final formula related with PV cells is the reserve saturation current which can be described as;

$$I_{RS} = \frac{I_{sc}}{\left[exp\left(\frac{q.V_{oc}}{N_s.K.Temp.n}\right) - 1\right]} \quad (3.4)$$

Where; V_{oc} is the open circuit voltage of the PV array.

The most important two parameters in the PV systems are open circuit voltage and short circuit current. They are main factors to affect the maximum power of PV array at the reference temperature and irradiance (Priyadarshanee, 2012).

3.1.2 MPPT

Maximum power point tracking (MPPT) is crucial equipment in the PV systems. As it mentioned above, PV systems have nonlinear behavior and their maximum power point changes with radiation and temperature. That's why MPPT control systems are used to extract maximum power from PV panels. By applying some methods or algorithms, MPPT controller changes the output voltage of PV. In other words, it changes the duty cycle of a transistor inside DC-DC boost converter. The basic connection structure of

MPPT control unit with PV array and the DC-DC converter is shown below in Figure 3.3.

Figure 3.3. MPPT Controller Connection with PV and DC Chopper

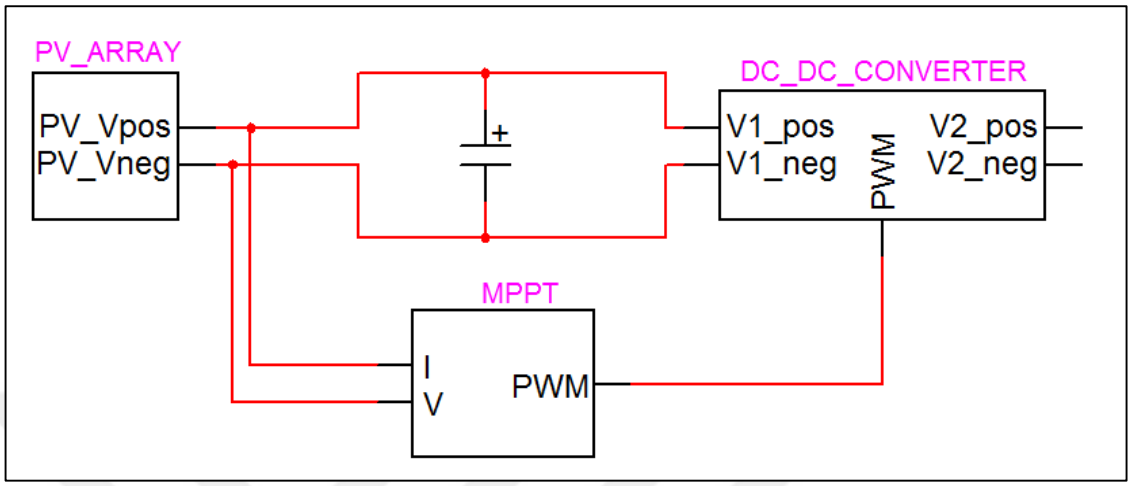

In the literature, plenty of maximum power point tracking methods are available. These methods are categorized as direct and indirect methods. Most commonly known and used ones are perturbation and observation (P&O) for a direct method and fractional open circuit method (FOC) for an indirect method (Faranda and Leva, 2008; Esram and Chapman, 2007; Sera et al., 2006).

In FOC, it is assumed that voltage location of maximum power point is always fixed and proportional to the magnitude of open circuit voltage. Between the 75% and 85% of open circuit voltage is selected as voltage magnitude of maximum power point. The main disadvantage of this technique is to not delivering power to load when measuring the magnitude of open circuit voltage.

Figure 3.4: Flow Chart of P&O Algorithm

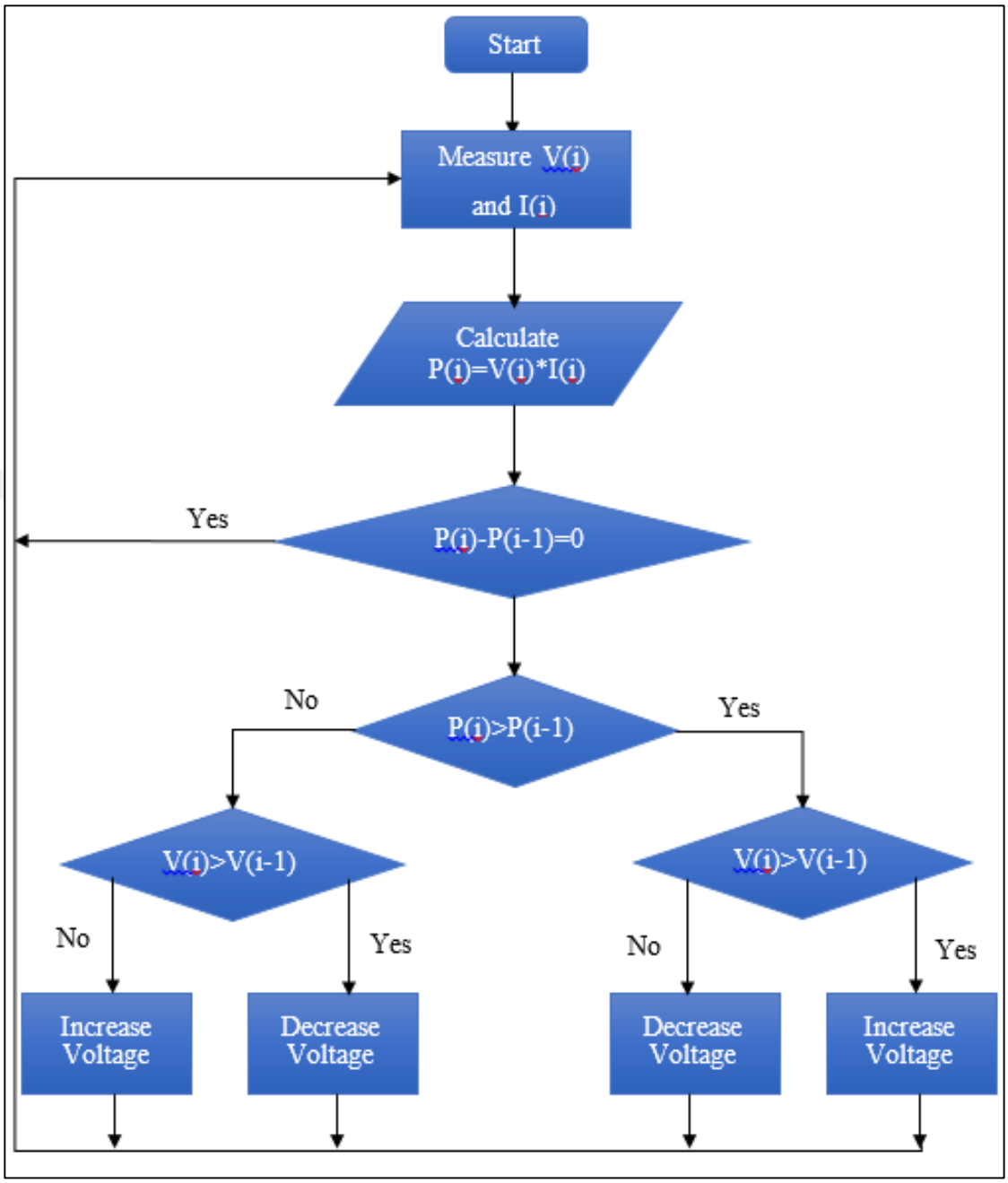

On the other hand, P&O method increases or decreases the PV array output voltage. By changing it, current can be changed and the new power of PV system occurs. Then by comparing PV output power and voltage with previous values, algorithm decide to increase or decrease the voltage magnitude. To better understanding, a flowchart of the P&O algorithm is given in Figure 3.4. When PV array output power change in a positive way (P(i)>P(i-1)), algorithm check voltage differences (V(i)>V(i-1)). If the voltage difference is positive, the output voltage of PV array continues to increase. Otherwise,

the output voltage of PV array continues to decrease. Same way, if the output power of PV decreases with the change of voltage magnitude, PV output voltage starts to change in opposite direction. The main advantage of this method is its simplicity and outperformance. The main disadvantage of this method is causing fluctuations in the maximum power point. Thus, prohibit these fluctuations, step size of the algorithm should be chosen low enough. In this thesis, P&O algorithm is used when modeling and analyzing the micro-grid system.

3.1.3 DC-DC Boost Converter

The boost converter is also known as a step up converter. That means voltage magnitude is increased in the output side of the converter. In order to achieve such increment, one diode and one transistor must be used. Figure 3.5 shows a schematic demonstration of the DC-DC boost converter.

Figure 3.5: DC-DC Boost Converter

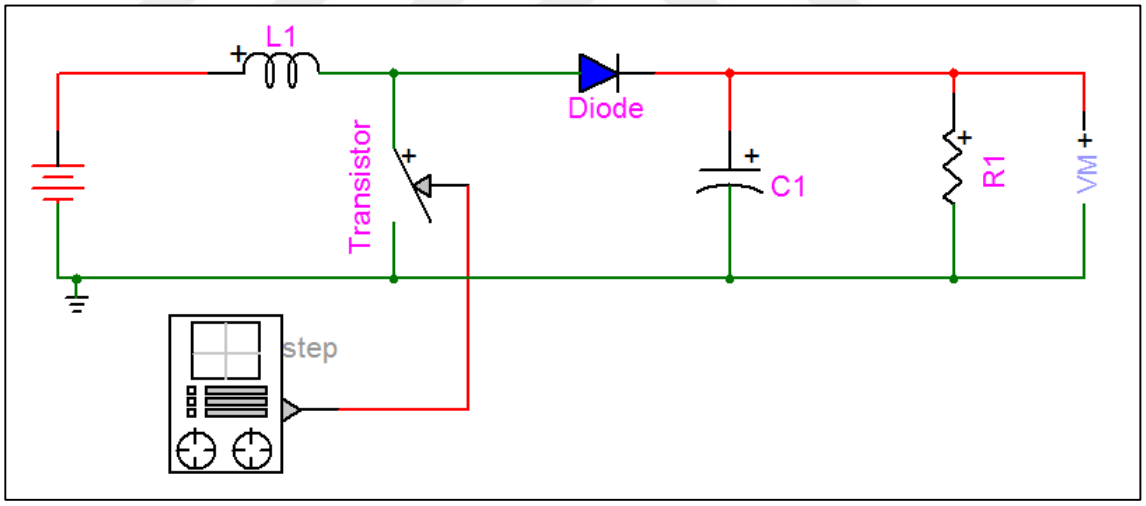

As it can be seen that capacitor and inductance are used as a filter to decrease voltage fluctuations. The basic working principle of the DC-DC boost converter is explained below:

i. When the transistor switch is closed, the current through the inductance (L1) increases and energy begins to be stored on the inductance.
ii. When the transistor switch is opened the current passing from inductance (L1) starts to flow through the diode to the capacitor C1 and to the load (R1).

iii. The inductance discharges its energy and the polarity of the voltage on the inductance became the same as the polarity of the voltage source and is connected to the load via a diode. Thus, the level of the output voltage is increased.

Figure 3.6 and Figure 3.7 show the two distinct stages of DC-DC boost converter which are the switch is closed and the switch is opened respectively.

Figure 3.6: Closed Switch State of Converter

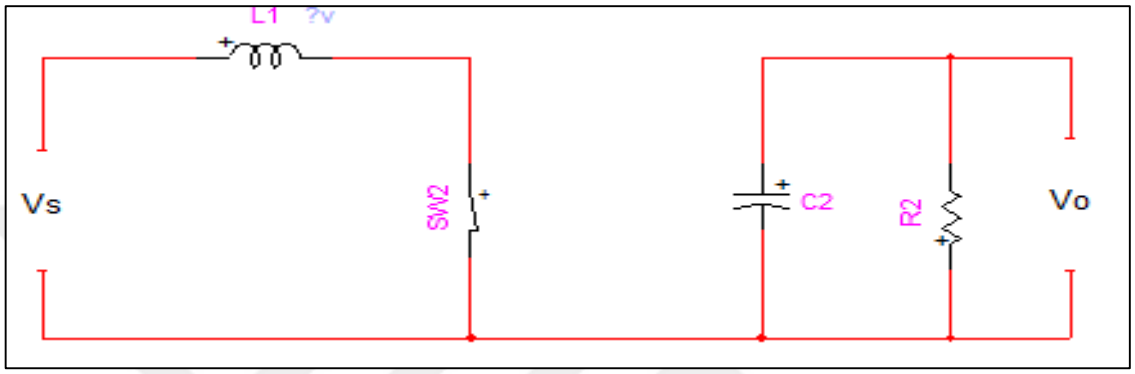

Figure 3.7: Open Switch State of Converter

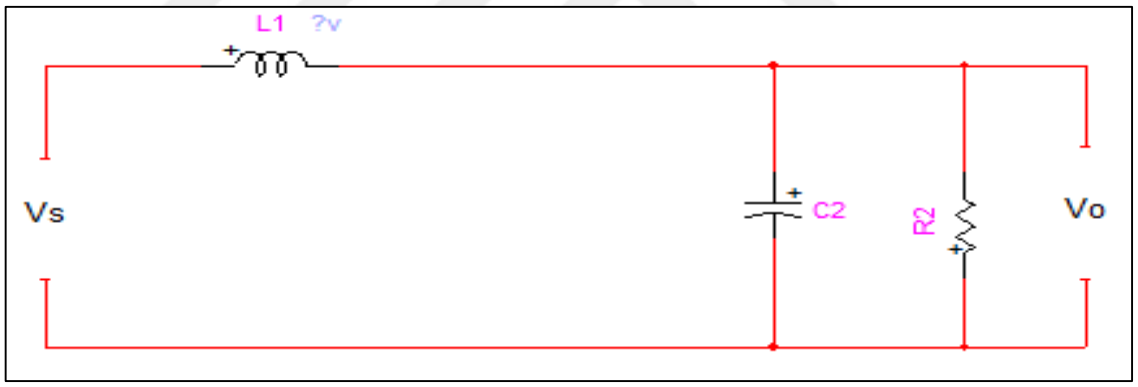

If there is an MPPT circuit in the PV system, transistor or switch is controlled with the help of it. The main purpose of it, changing the voltage magnitude of PV system and obtaining maximum power from PV systems.

3.1.4 Inverter

The inverter is used for converting DC to AC. A basic three-phase inverter consists of three single-phase inverter switches, each connected to one of three AC terminals. Generally, carrier-based PWM techniques are applied due to having fewer harmonics. Electrical illustration of 3 phase inverter is given in Figure 3.8.

Figure 3.8: Electrical Representation of Three Phase Inverter with IGBTs

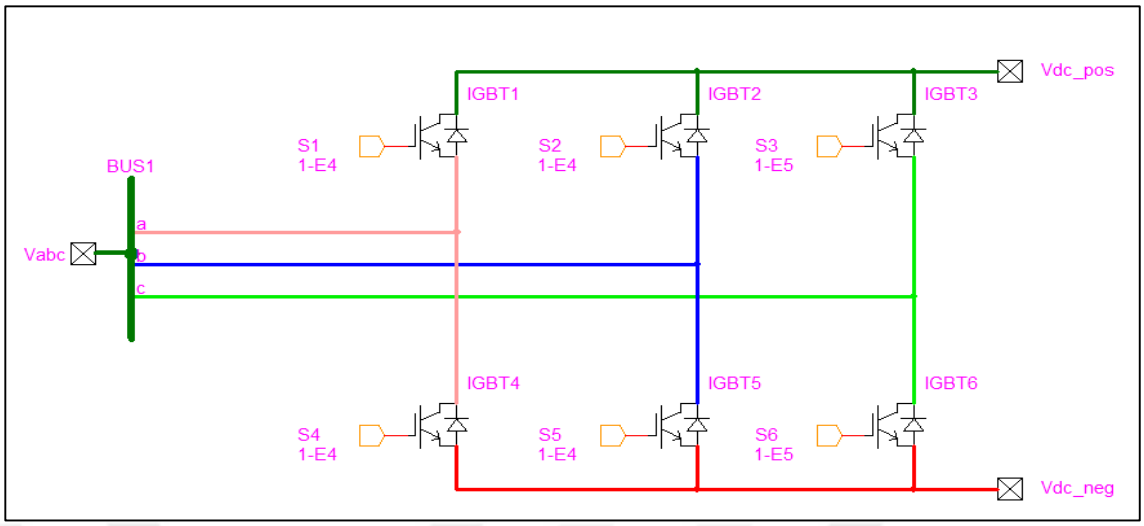

For controlling switches (IGBTs), there are two modes of conduction which are 120° and 180°. In this thesis, 180° mode of conduction is used. Every device is in conduction state for 180° where they are switched on at every 60° intervals. Status for six switches is given in Table 3.1 as “On” or “Off”.

Table 3.1: Status of Switches

Switch Interval	S1	S2	S3	S4	S5	S6
0° to 60°	On	Off	Off	Off	On	On
60° to 120°	On	On	Off	Off	Off	On
120° to 180°	On	On	On	Off	Off	Off
180° to 240°	Off	On	On	On	Off	Off
240° to 300°	Off	Off	On	On	On	Off
300° to 360°	Off	Off	Off	On	On	On

3.2 WIND ENERGY SYSTEM

Wind energy systems have been matured past decades with the help of environmental concerns and new regulations. Usage of wind as an energy source goes back up to 900 AD when Persians used windmills. Now, WESs have the biggest slice of the World renewable energy market and still continue to growth (Manwell et al., 2011). The capacity of installed WESs exceeded over 486 GW at the end of 2016. Yearly installed capacities of WESs from 2001 to 2016 are shown in Figure 3.9. Europe and Asia together have 365 GW of installed wind power capacity which is 75% of total installed power capacity.

Figure 3.9: Yearly Installed Capacities of WES

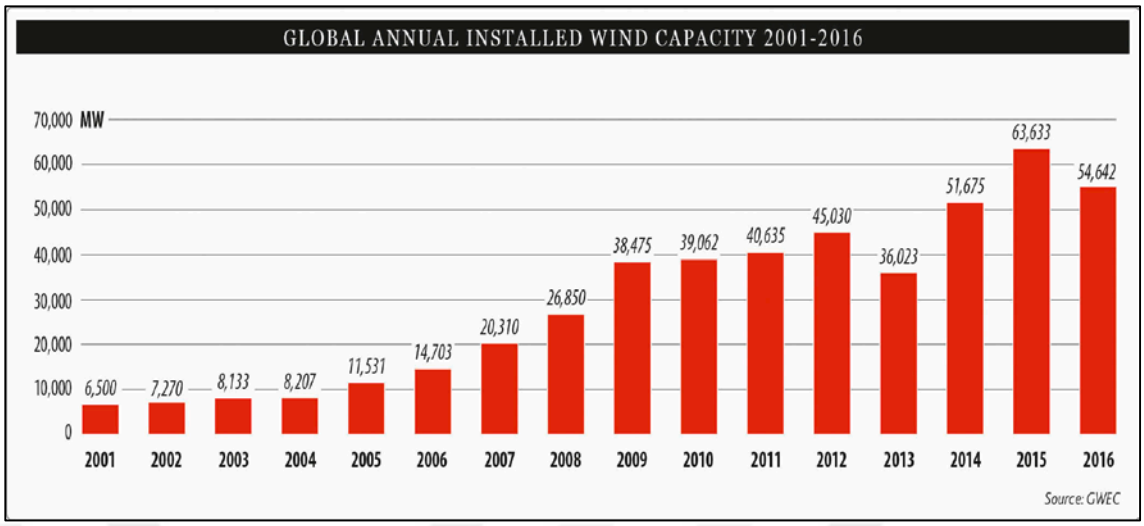

Source: http://gwec.net/global-figures/graphs

Basically, energy obtained from winds can be calculated following formula for wind turbines:

$$P_{wind} = \frac{\rho . A}{2} v_{wind}^3 c_p(\lambda, \beta) \tag{3.5}$$

Where;

P_{wind} is the generated wind power (W),

ρ is the air density (kg/m^3),

A is the turbine blades swept area (m^2),

c_p is the performance coefficient,

v_{wind} is the wind speed (m/s),

λ is the ratio of tip speed to wind speed and,

β is the pitch angle of blades (degree).

In this thesis, equation of c_p is taken from (Heier, 2009) and it is given below as Eq. (3.6).

$$c_p(\lambda, \beta) = 0.5176x(116/\lambda_i - 0.4\beta - 5)e^{-21/\lambda_i} + 0.0068\lambda \tag{3.6}$$

$$\frac{1}{\lambda_i} = \frac{1}{\lambda + 0.08\beta} - \frac{0.035}{\beta^3 + 1} \tag{3.7}$$

In these two equations, maximum c_p value is achieved as 0.48 when pitch angle is zero and λ is equal to 8.1. To better understanding of the relationship between c_p and λ, their characteristic curve is given below in Figure 3.10.

Figure 3.10: Relation between c_p and λ Depending on Pitch Angle

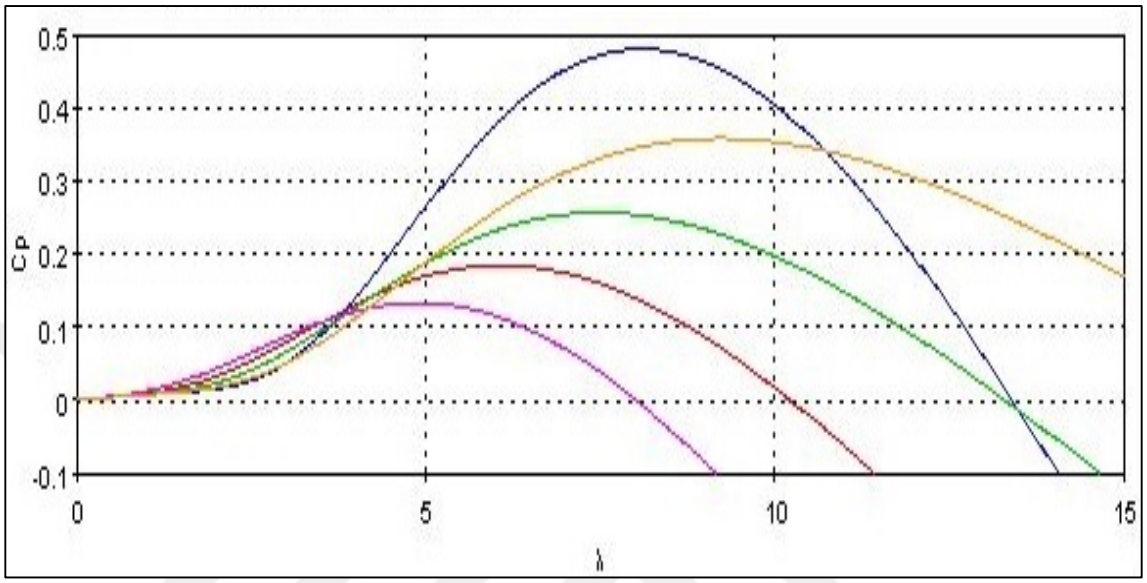

Since first WESs were used, their power capabilities, structures and control types have been changed continuously. Wind energy systems are mainly classified into four parts in terms of rotate type, speed control, power control and structure.

3.2.1 Blade Rotate Types

Wind energy systems or wind turbines categorized into two groups in terms of their rotating axis. They are called as horizontal axis wind turbines (HAWTs) and vertical axis wind turbines (VAWTs) (Riegler, H., 2003). Both have been technologically advanced in parallel but HAWTs got more attention than VAWTs. Currently, HAWTs are used for wind energy systems which have higher power capacity, while VAWTs are used for small wind energy systems which have less power capacity (Shikha and Kothari, 2005).

i. Horizontal Axis Wind Turbines

Figure 3.11: Basic View and Structure of Horizontal Axis Wind Turbines

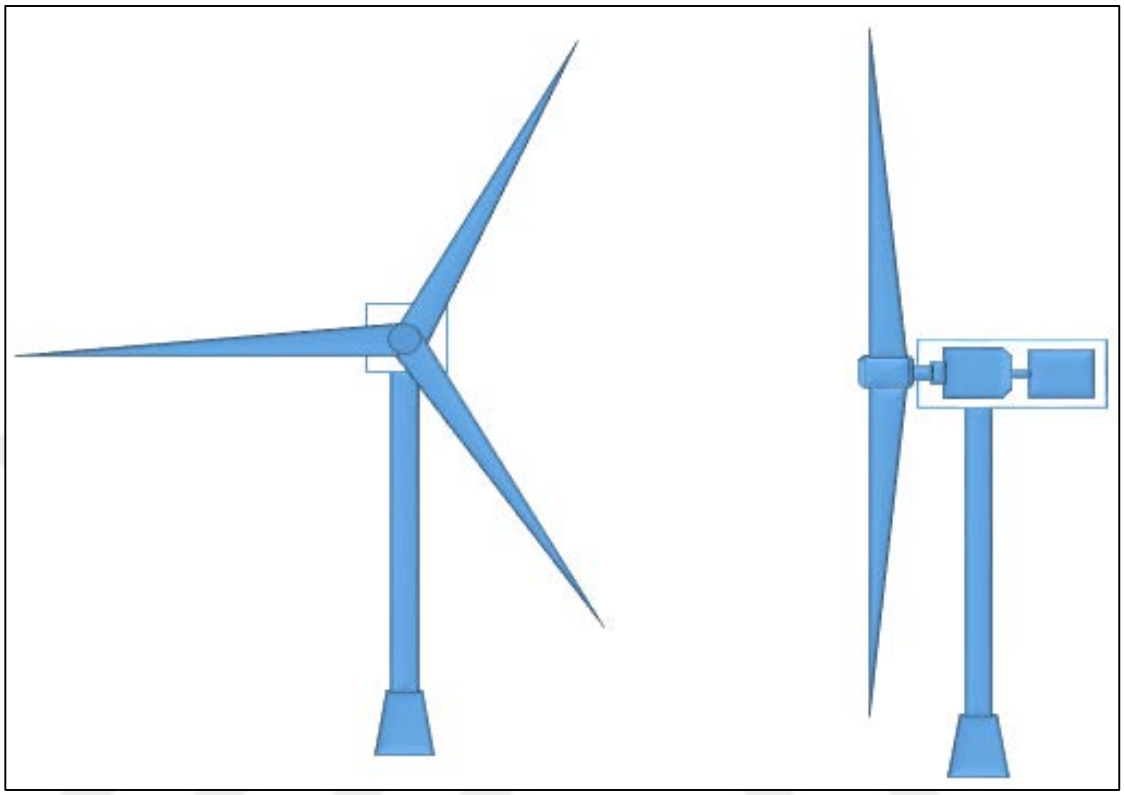

Horizontal axis wind turbines are the ones which are used more commonly in the world. They have a rotor and asynchronous generators are mounted at the top of the tower. Generally, most of HAWTs have three blades are located on the rotor horizontally and gearbox between rotor and generator. The rotor of the turbine is placed in the opposite of the wind direction. In this way, blades can turn with wind and generate electricity by rotating generator. The typical structure of this type wind energy systems is presented in Figure 3.11.

ii. Vertical Axis Wind Turbines

Unlike the HAWTS, rotor placed vertically in VAWTs. Thus, wind direction becomes non-important. As it is seen from Figure 3.12, generator and gearbox usually mounted near the ground which makes installation and maintenance easy. The main drawback of this type of wind turbines is producing less energy (Shikha and Kothari, 2005). That's why they are preferred for building installations with small power capacities.

Figure 3.12: Basic View and Structure of Vertical Axis Wind Turbines

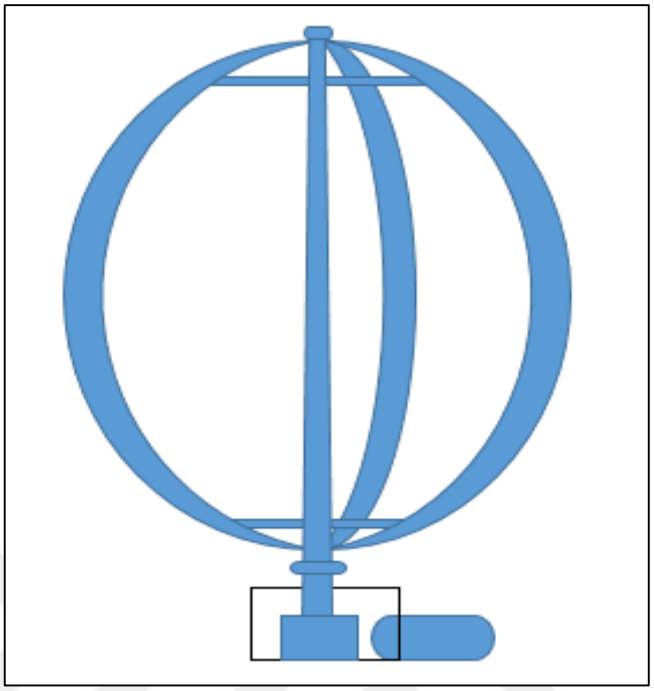

3.2.2 Speed Control

There are two-speed control categories in wind energy systems which are fixed speed and variable speed.

i. Fixed Speed

Up to the end of 80's majority of the wind energy systems consists of the standard asynchronous generator (induction generators) which operated with a fixed speed. This induction generator is connected to the electrical network directly without any converter. In such systems, the rotor speed is fixed and independent from wind speed. Therefore, they achieve maximum efficiency for only one specific wind speed (Hansen et al., 2004).

Fixed speed wind energy systems have both pros and cons. Lower cost and simplicity are main benefits of them. On the other hand, ungovernable reactive power consumption and voltage fluctuations caused by wind speed changes are main disadvantages of fixed speed wind energy system (Larsson, 2000).

ii. Variable Speed

On the contrary of fixed speed, maximum efficiency is achieved for a variety of wind speeds. Torque is kept almost constant and fluctuations are prevented in variable speed wind energy systems. These systems include power converters between generator and electrical network (Hansen et al., 2004).

Same as fixed speed WESs, variable speed WESs have advantages and disadvantages. While higher cost and losses are main drawbacks of them, controllable power, reduction of voltage fluctuations and obtaining maximum power in variable wind speeds are prominent benefits of them (Sorensen et al., 2000).

3.2.3 Power Control

Power control of the WESs is also known as blade control of the WESs and divided into 3 classes. They are used in order the protect wind turbine and keep the power of WESs in a specified boundary.

i. Passive Stall Control

It is the simplest way of power control in the WESs. The angle of blades is kept as stable and rotor continues to stall when wind speed exceeds wind turbine's limits.

ii. Active Stall Control

When the power of WES is larger than rated power value, blades pitched with a larger angle of attack to keep power in rated. On the other hand, when wind speed is low, blades pitched again in order to obtain maximum power. With the increase of power capacities of wind tribunes, this type of power control mechanism came into use.

iii. Pitch Control

The main working principle is same with active stall control system. Blades pitched either to obtain optimal power at current wind speed or to limit power at rated power value. The difference from active stall control is the turning of blades into opposite direction (Hoffmann, 2002).

3.2.4 Wind Structure

In the literature, wind turbine structures are mainly classified into 4 classes namely A, B, C, D (Hansen et al., 2004). Their topologies and basic structures are given in Figure 3.13.

Currently, type C dominates the market of WESs. However, Type D is the new trend and the installation capacities of type D are increasing especially in Europe and Asia (Lacal-Arrntegui, 2014; Jansuya and Kumsuwan, 2013).

i. Type A

In this type of WESs, squirrel cage induction generator (SCIG) is used. They are fixed speed wind turbines and as mentioned before they are connected to the electrical network directly without any converter.

ii. Type B

This type of WESs has variable speed control through variable rotor resistance. Wound rotor induction generator (WRIG) is used in type B WESs. They are directly connected to network same as type A.

iii. Type C

They are known as doubly fed induction generators (DFIG) in the market. Generally, WRIG is used in this type of WESs. Unlike the type A and type B, the rotor is controlled with converter while the stator is directly connected to the electrical network.

iv. Type D

The generator is connected to the main electrical network via frequency controlled converter in this configuration. Generator type can be permanent magnet synchronous generator (PMSG) or electrically excited synchronous generator (EESG). On the contrary of other types, some of D type WESs don’t have a gearbox.

Figure 3.13: Wind Turbine Topologies (Lacal-Arrntegui, 2014)

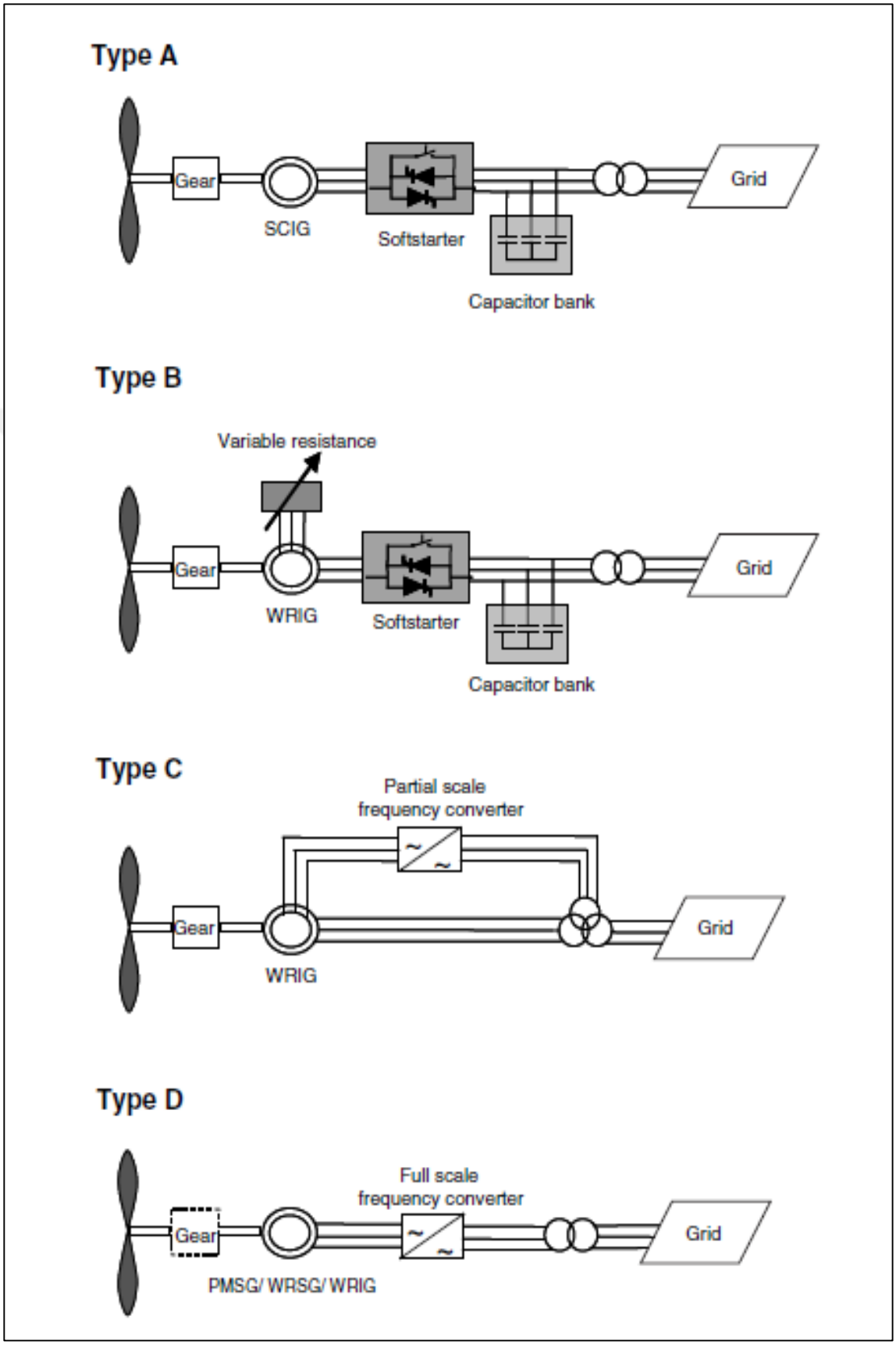

3.3 ENERGY STORAGE SYSTEM

With the integration of renewable resources into the network, energy storage systems have gained the great importance. Energy storage devices at the distribution and end-user levels are beginning to provide clean energy and increase reliability. A common goal in all storage systems is to ensure that the generated energy is stored at a specified time, and then to use this stored energy in a different time interval for the desired purpose. There are several types of energy storage systems like batteries, ultracapacitors, flywheels, pumped hydro, compressed air energy storage (CAES) and superconducting magnetic energy storage (SMES). Depending on their characteristics, usage areas of energy storage systems are changed. They are used for peak shaving, solving power quality issues and providing support for renewable energy resources. In Figure 3.14, main characteristics of main energy storage systems are given.

Figure 3.14: Main Characteristics of Energy Storage Systems (Wong et al., 2011)

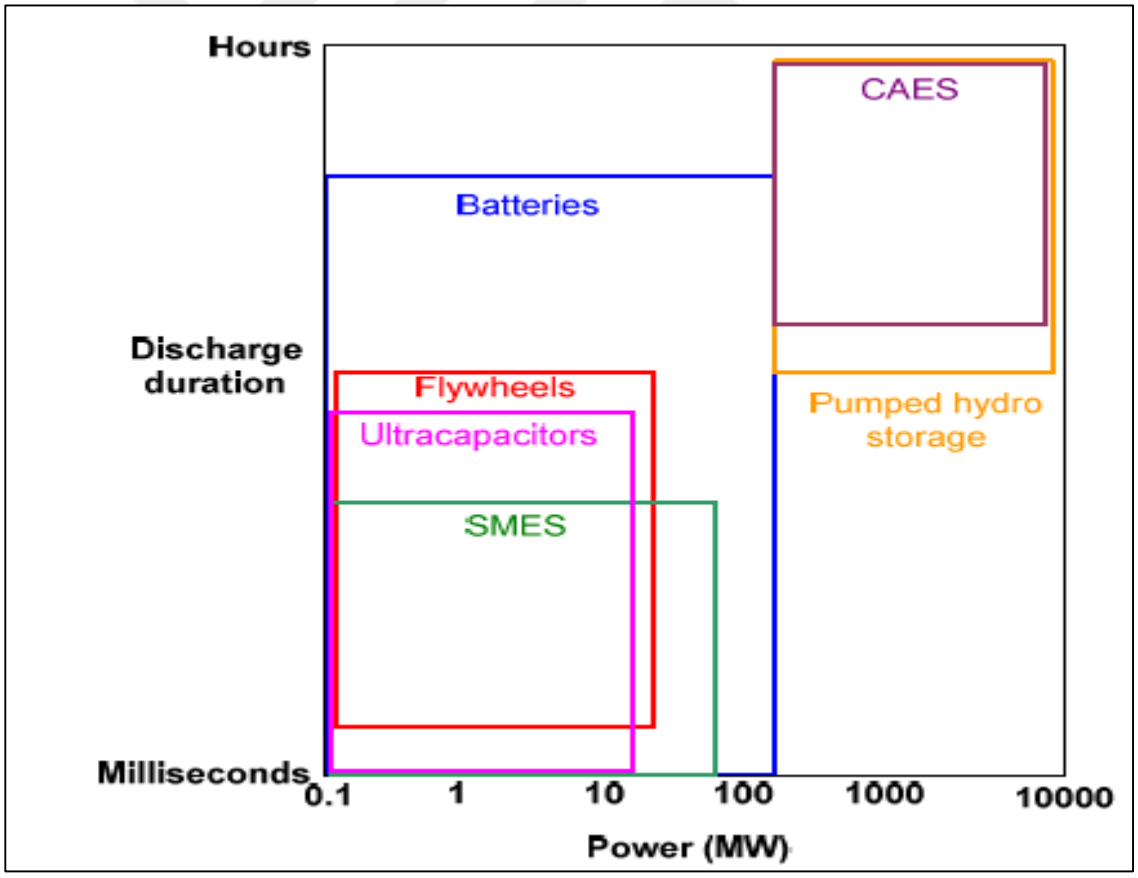

When energy storage systems are compared, batteries come into prominence due to their discharge and power characteristics. Also, when distribution level micro-grid

applications are considered, it can be seen that majority of ESS are batteries (Mariam et al., 2013). In such applications, batteries store the energy when energy is available in the network. According to their management system, they can be charged directly from the grid during off-peak hours or from renewable energy resources. When energy is needed, batteries supply energy to dc or ac loads and increase the reliability of micro-grid and grid. Beside these functionalities, they are also providing valuable capabilities for micro-grids such as smoothing intermittent PV power flow, reactive power support and more than that they give the opportunity to earn revenue from arbitrage.

Figure 3.15: Increment of Energy Density Values of Batteries (Bradford, 2009)

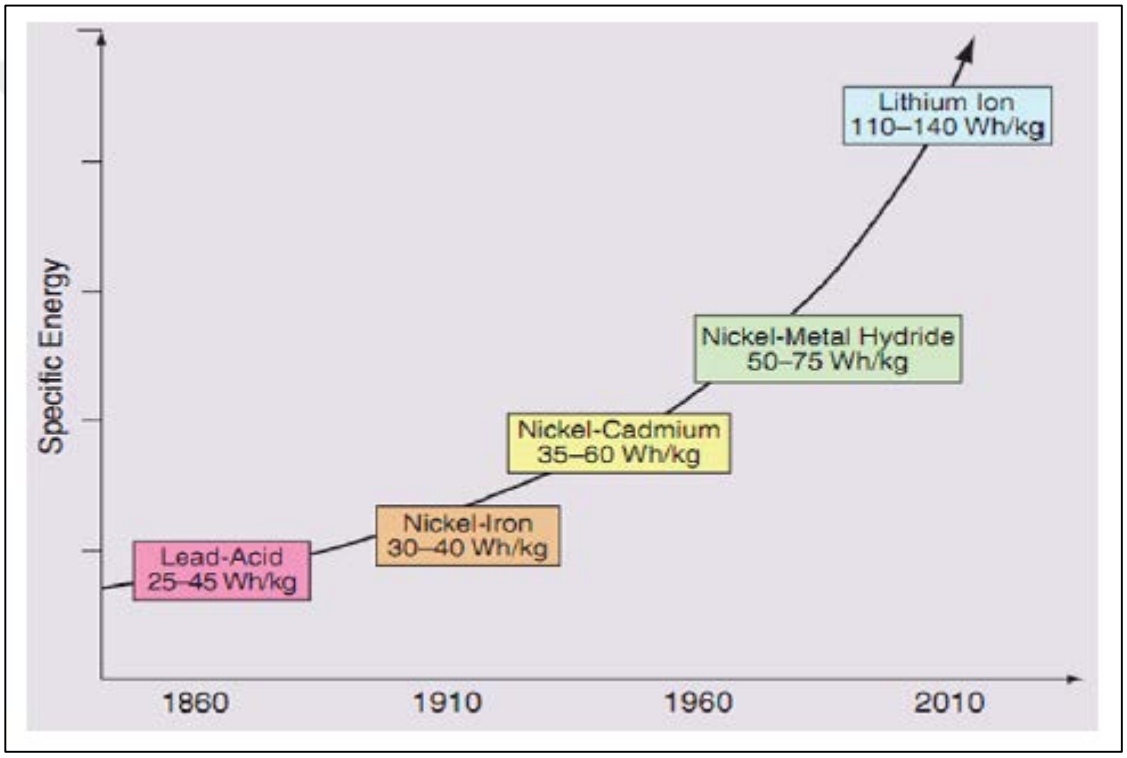

Batteries can be classified into four main types which are Lithium-Ion, Nickel-Metal, Lead-acid, Nickel-iron, and Nickel–Cadmium. Firstly, lead-acid batteries are introduced in the 19th century. Since then, energy densities of batteries have been increased and new types of batteries came to exist. The logarithmic increment of energy density values of batteries is presented in Figure 3.15 (Bradford, 2009). Batteries should have some qualifications such as having a higher energy density, fast charging process, enough life cycle and low cost. Lithium-Ion batteries have all of these fundamentals but low cost (Singh et al., 2016; Plett, 2004). Thus, in thesis Lithium-Ion battery is chosen as an energy storage to supply energy the loads when micro-grid is in island mode. Built-in Lithium-

Ion battery is used for modeling in EMTP-RV. As all batteries, threshold state of charge and bottom of state of charge are assigned as 80% and 20% respectively.

3.4 UNDERGROUND CABLES / OVERHEAD LINES

Overhead lines and underground cables are the main parts of the network which carry the electricity and power to end users. Overhead lines have their own towers. Length of their tower and distance between phases on their tower affect impedance value of overhead lines. Same as overhead lines, the distance between phases is important for underground cables. Proximity and skin effect change with this distance. Thus, the accurate representation of all of these should be taken into consideration.

3.5 LOADS

Loads are essential parts of the electrical network. In the literature mainly, loads are categorized into 3 section which are constant power load, constant current load and constant impedance load (Willis, 2004; Willis, 2002). Depending on this categorization, active and reactive power values of loads can change. In order to find new calculated active and reactive power of loads, formulization which is given below as Eq. (3.8) and Eq. (3.9) can be used.

$$P = P_0 x \left(\frac{V}{Vbase}\right)^{n_p} \tag{3.8}$$

$$Q = Q_0 x \left(\frac{V}{Vbase}\right)^{n_q} \tag{3.9}$$

Where;

P is the actual active power,

Q is the actual reactive power,

P_0 is the nominal active power,

Q_0 is the nominal reactive power,

V is the actual voltage level,

Vbase is the base voltage level,

n_p is the active power exponent and,

n_q is the reactive power exponent.

Although lots of value can be assigned for n_p and n_q values, there are 3 main n_p and n_q values are used depending on load types which mentioned above. These values are 0, 1, and 2. When n_p and n_q are chosen as 0, it means that load is constant power. When n_p and n_q are chosen as 1, it means that load is constant current. If n_p and n_q are chosen as 2 it means that load is constant impedance (Lal and Mubeen, 2015)

As a simple example, when n_p and n_q are assumed to be 0, the values of P and Q will be equal to P_0 and Q_0. Thus, active and reactive powers will be same with the powers that the user specifies.

If the values of n_p and n_q are taken as 1 and the value of the voltage at the load which obtained after load flow was 0.5 pu. (half of nominal voltage 1 p.u.), the new power values will be obtained as half of the power value that nominal power or the user has assigned. Thus, while both the voltage and the power values will be reduced by half, the load current which is drawn from the network will remain constant.

In last type power which is constant impedance n_p and n_q values are taken as 2. When the voltage value is accepted as 0.5 p.u., the value of the new power value will be one-fourth of nominal power values. However, the impedance value will remain constant due to the fact that impedance is equal to the square of voltage divided by power.

4. MODELING OF SIMULATION SYSTEM IN EMTP-RV

Firstly, a model of electrical power grid system is shown in Figure 4.1. Then, EMTP-RV model of AC micro-grid is indicated in Figure 4.3. After, explanations of the power grid and micro-grid structures, specifications and model of the components of AC micro-grid are presented with the help of applied built-in blocks, functions and formulas in EMTP-RV.

The main electrical grid consists of the main source, transmission substation (154-34.5 kV Transformer), lines, distribution substation (34.5-0.4 kV Transformer), lines, loads, and micro-grids. In EMTP-RV, same electrical components are used with frequency dependent model as mentioned previously. EMTP-RV model of the power grid is given in Figure 4.1. Between source and transmission substation (145-34.5 kV Transformer) 10 km frequency dependent overhead line is used. After transformer 7 outgoing feeders are modeled. These 7 outgoing feeders are connected to double busbar system of transmission substation. While some of these distribution feeders are modeled as lump model, others are modeled more detailed. More detailed model of distribution centers located inside of subcircuits which named DM. For lump models, MV underground cable is connected between transmission substation and transformer (34.5-0.4 kV). Then a load of that feeder is linked to transformer directly (Figure 4.1).

On the other hand, detailed model of the distribution center is given in Figure 4.2. Although the configuration of it seems like loop, with the open switch at the bottom, distribution centers are operated as a radial system. Underground cables are used as lines same with lump models.

Micro-grid system is located inside of DM subcircuit which connected Bus 9. Detailed information of micro-grid model is explained in the following part.

Figure 4.1: EMTP-RV Model of Power Grid

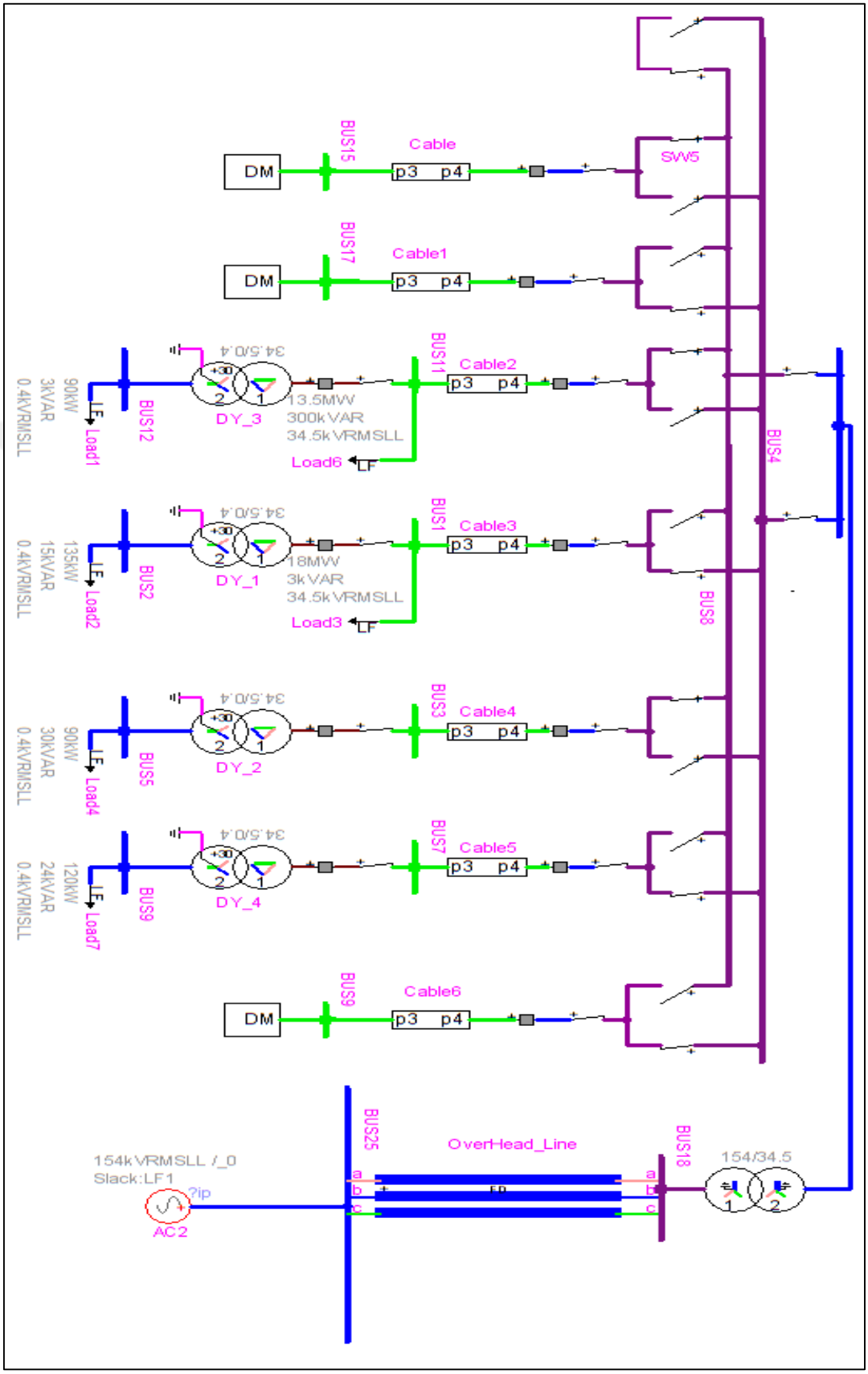

Figure 4.2: Detailed EMTP-RV Model of Distribution Center

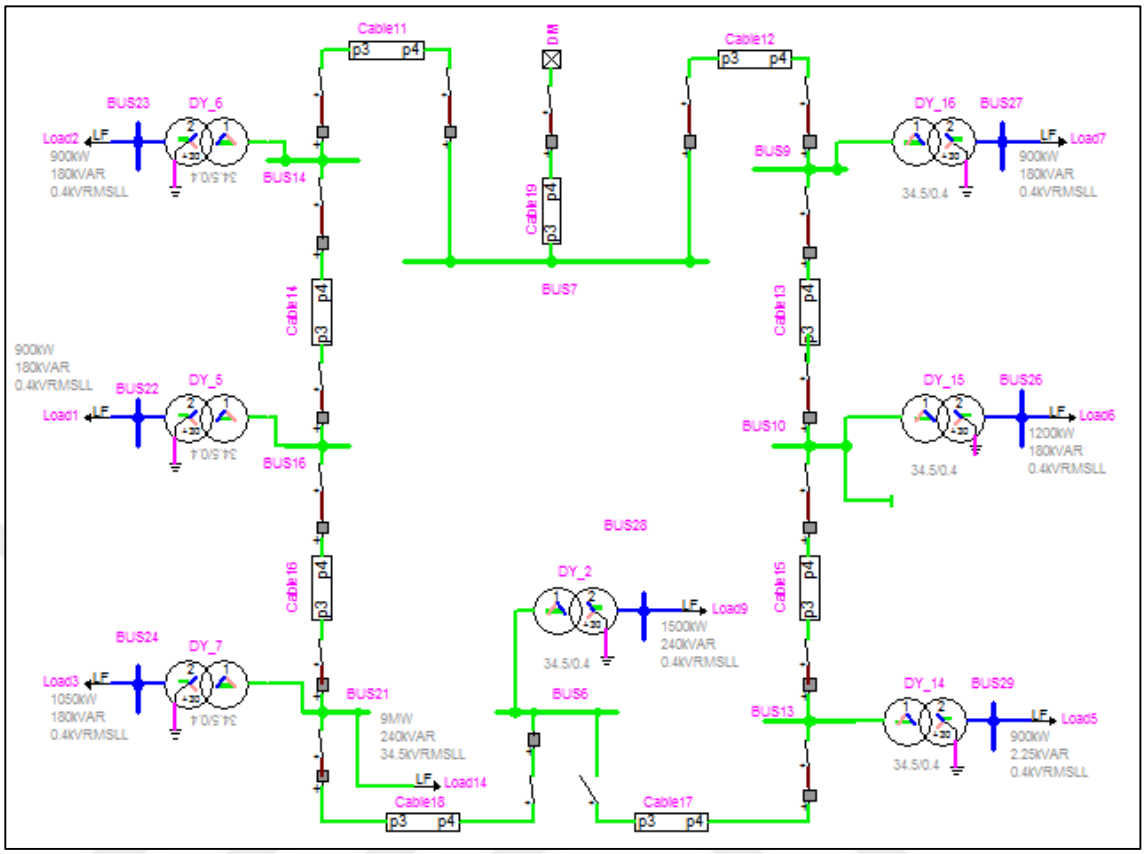

4.1 MODELED STRUCTURE OF MICRO-GRID

In this thesis, AC micro-grid system is modeled. In AC bus, wind turbine, micro generator and AC loads are connected directly. On the other hand, PV panel, battery and DC loads are connected through DC-AC converter to the main AC bus. Then, main AC bus linked to the electrical grid with protection devices. The basic structure of designed micro-grid is shown in Figure 4.3. This structure is located inside of DM which is given in Figure 4.1 and connected to Bus 9. The exact location of micro-grid is Bus 13. Loads are removed from the bus and micro-grid is linked to that bus.

Figure 4.3: Designed Micro-Grid Structure

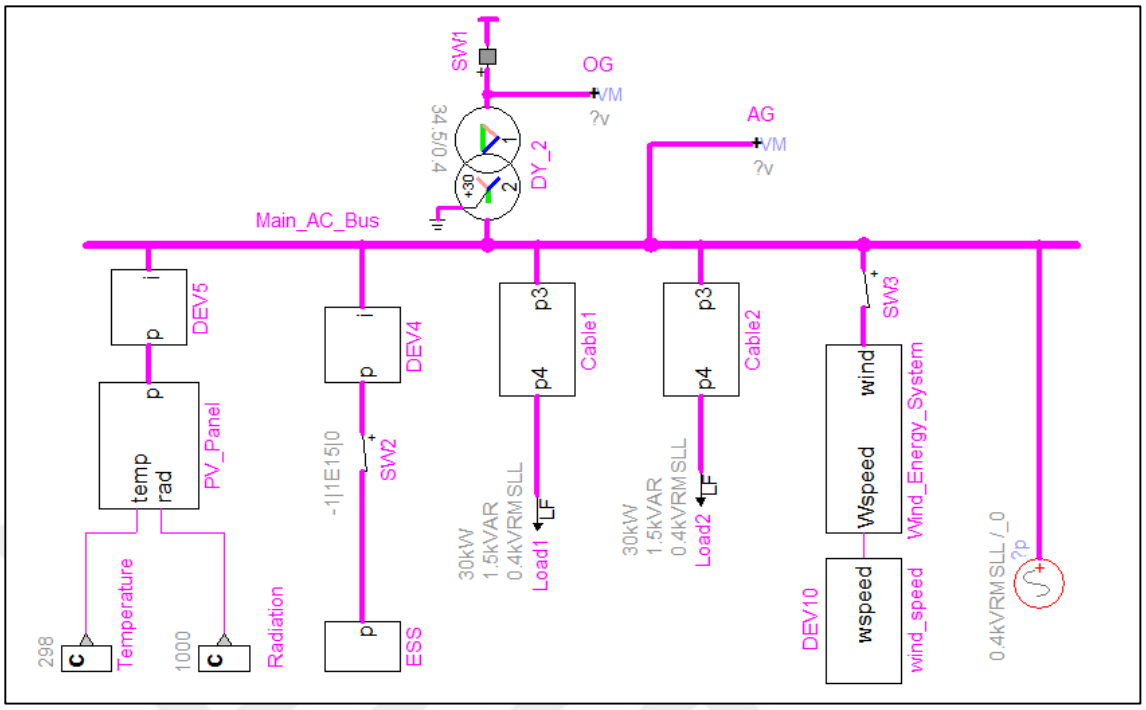

4.1.1 The Model of Wind Energy System

In this designed micro-grid system, pitch controlled and directly connected squirrel cage induction generator is chosen and modeled as wind turbine system. To control the pitch angle of blades, PI control block is modeled. Related parameters of modeled wind turbine are given in Table 4.1. Also, EMTP-RV implementation of a wind turbine is given as Figure 4.4.

Figure 4.4: EMTP-RV Model of Wind Turbine

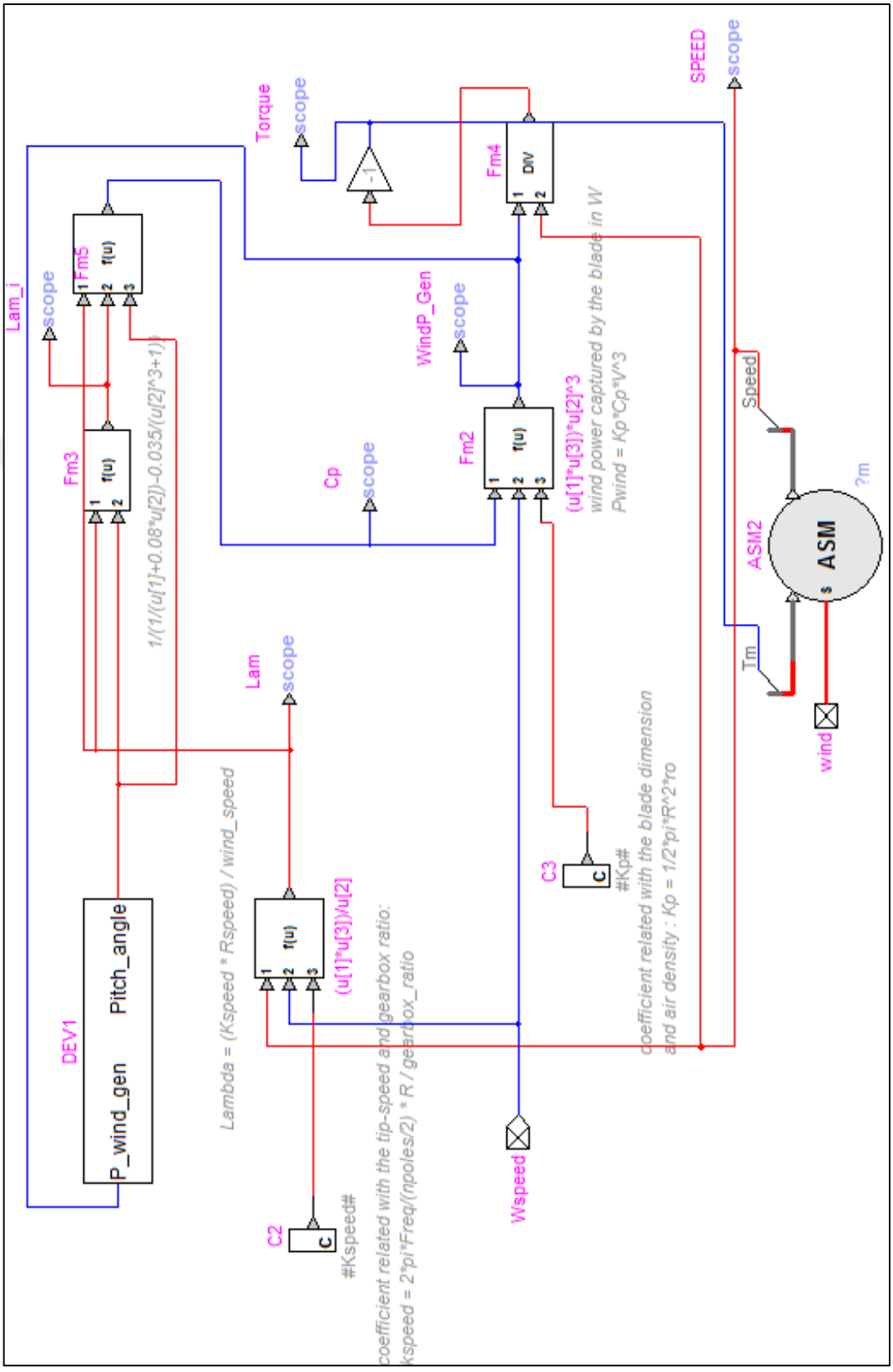

Table 4.1: Wind Turbine Parameters

Parameters	Values
Rated Wind Power (kW)	109
Voltage Level (kV)	0.4
Rated Wind Speed (m/s)	12
Blade Radius (m)	8.25

For wind energy system, wind speed, c_p and generated wind power graphs are given in Figure 4.6 and Figure 4.7 respectively. When wind speed is equal to rated wind speed which is 12 m/s2, c_p is equal to 0.48 and wind power is equal to rated wind power. However when speed is more or less than rated wind power, c_p value is changed. For example, when wind speed is increased to 13 m/s2 at the 1.5 second of simulation, c_p value starts to decrease to maintain rated power. Main reason of this changing of the pitch angle of wind energy system. Recovering the generated wind power and keep it at rated power takes around 0.2 second. On the other hand, when wind speed is decreased to 10 m/s2 c_p value is also decreased compared to c_p value at rated wind speed. This new c_p value became more than c_p value at 13 m/s2 wind speed and less than c_p value at 12 m/s2 wind speed. On the contrary of the previous situation, the only reason of this is the wind speed which is less than rated wind speed. It means that pitch angle stays zero same as rated wind power. A change of pitch angle is also shown in Figure 4.8.

Figure 4.5: Variable Wind Speed with Time

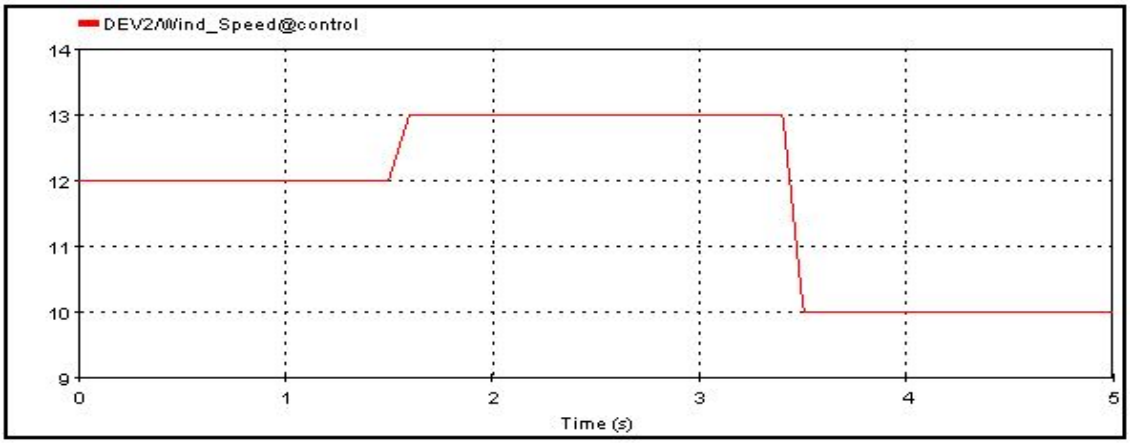

Figure 4.6: Changed Occurred in CP Depending on Wind Speed

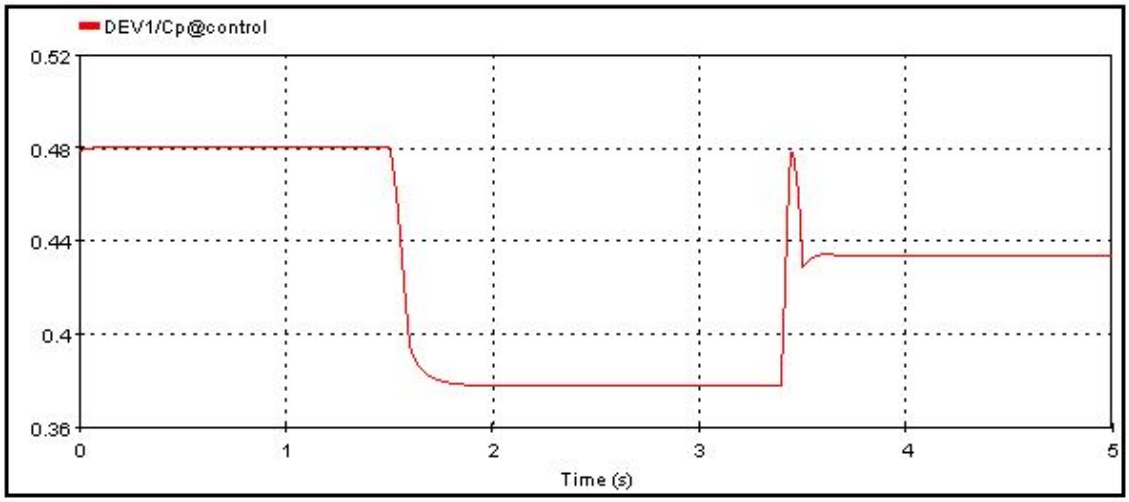

Figure 4.7: Changes in the Generated Wind Power Depending Variable Wind Speed

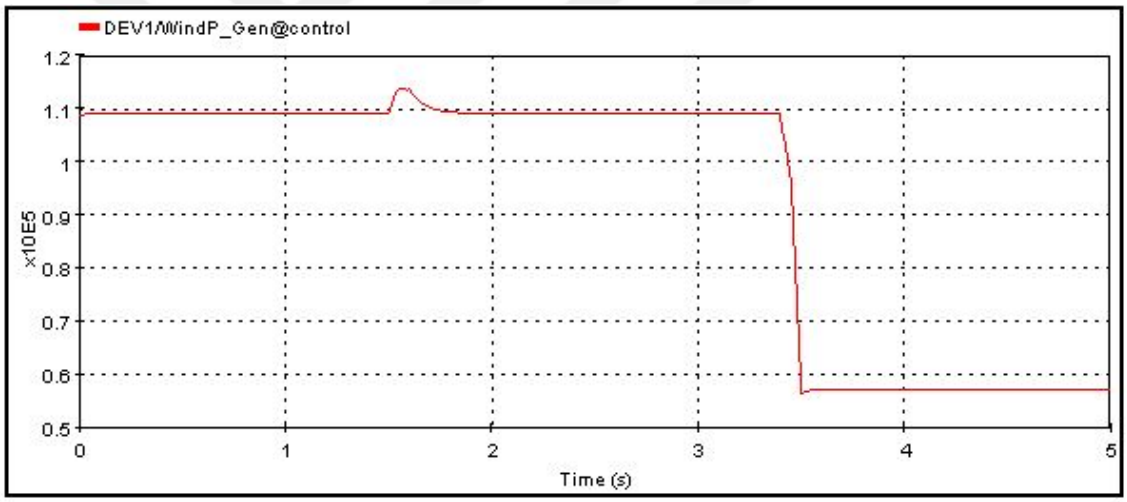

Figure 4.8: Pitch Angle Values

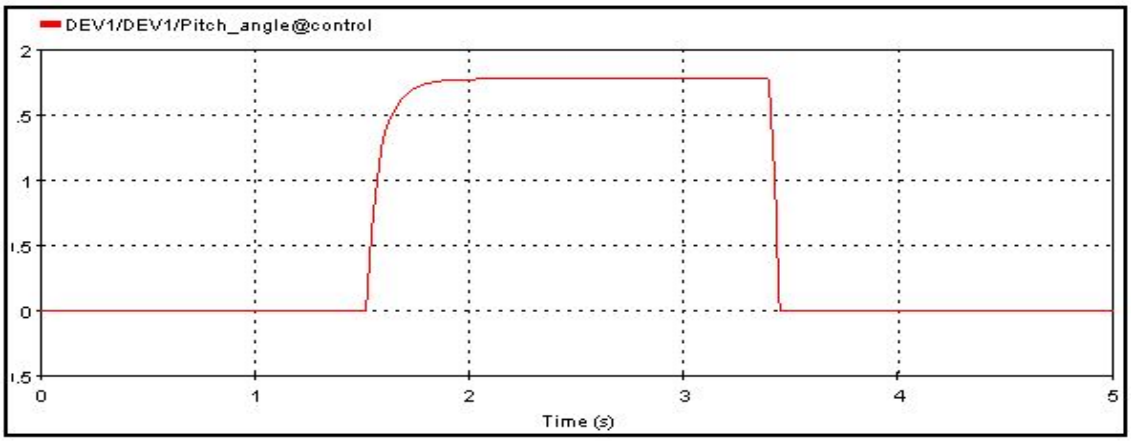

4.1.2 The Model of PV System

Specifications of modeled PV panel characteristics are also given to evaluate and understand simulation results. They are shown in below as Table 4.2. EMTP-RV implementation of PV panel is given in Figure 4.9. Wind speed value for wind energy system and irradiance or temperature values for PV system are changed during the simulation in order to be sure that modeling is correct.

Table 4.2: PV System Characteristics

Parameters	**Value**
Open Circuit Value (V)	197.4
Short Circuit Current (A)	49.26
The voltage at Peak Power (V)	182
Current at Peak Power (A)	48.125
Peak Power (kW)	8750
Temperature Coefficient (A/°C)	0.0032
Series Resistance (ohm, Ω)	0.2
Shunt (Parallel) Resistance (ohm, Ω)	414

For PV panel, I-V characteristic curves of it for different irradiance and temperature is indicated in Figure 4.10 and Figure 4.11 respectively. From these figures, it can be deducted that irradiance and power value of PV panel are directly proportional to each other. With the increasing temperature, it can be seen that there is little change in the short circuit or power while open circuit voltage values decrease.

Figure 4.9: EMTP-RV Model of PV Panel

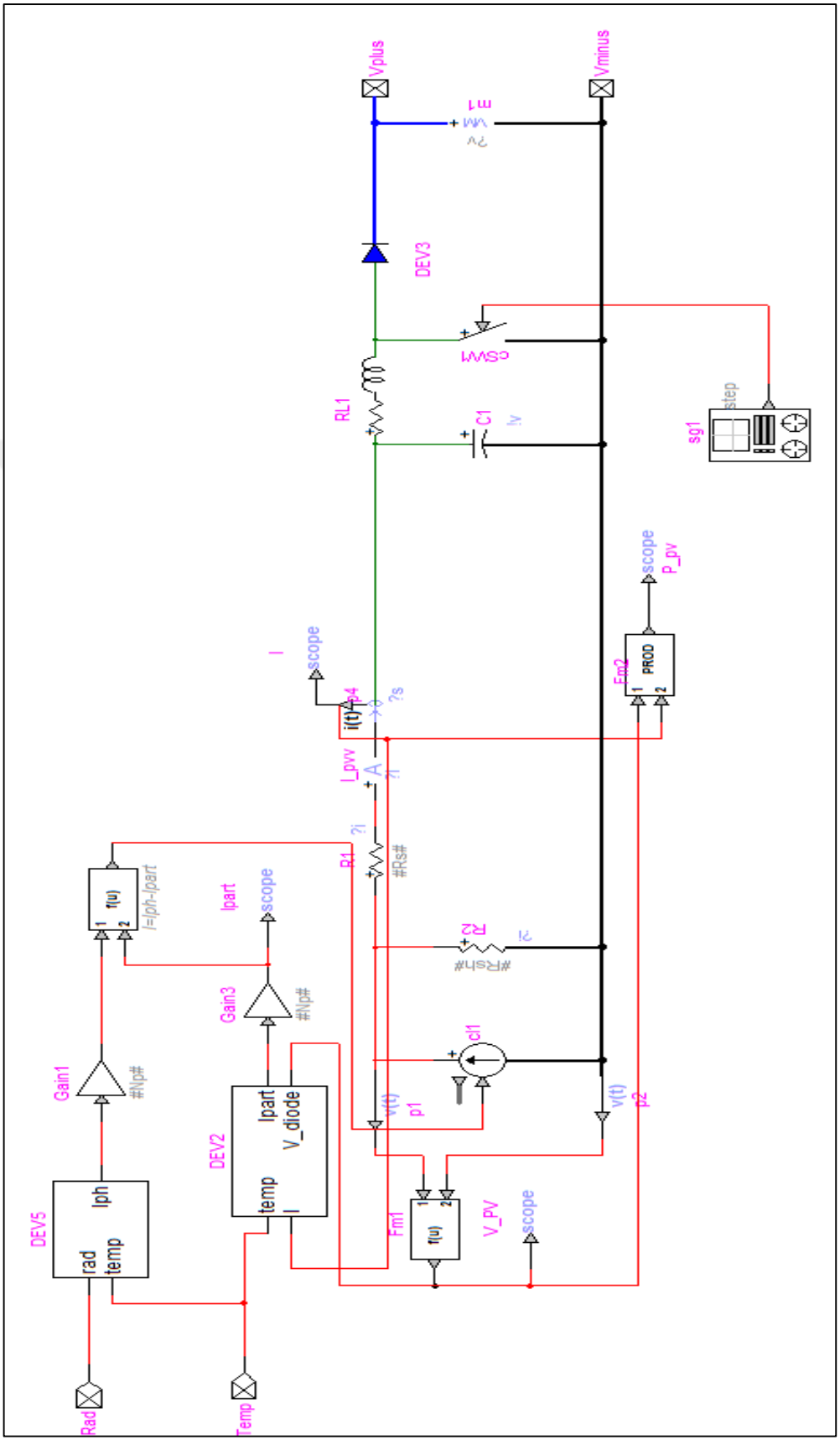

Figure 4.10: I-V characteristic of PV Panel Depending on Irradiance

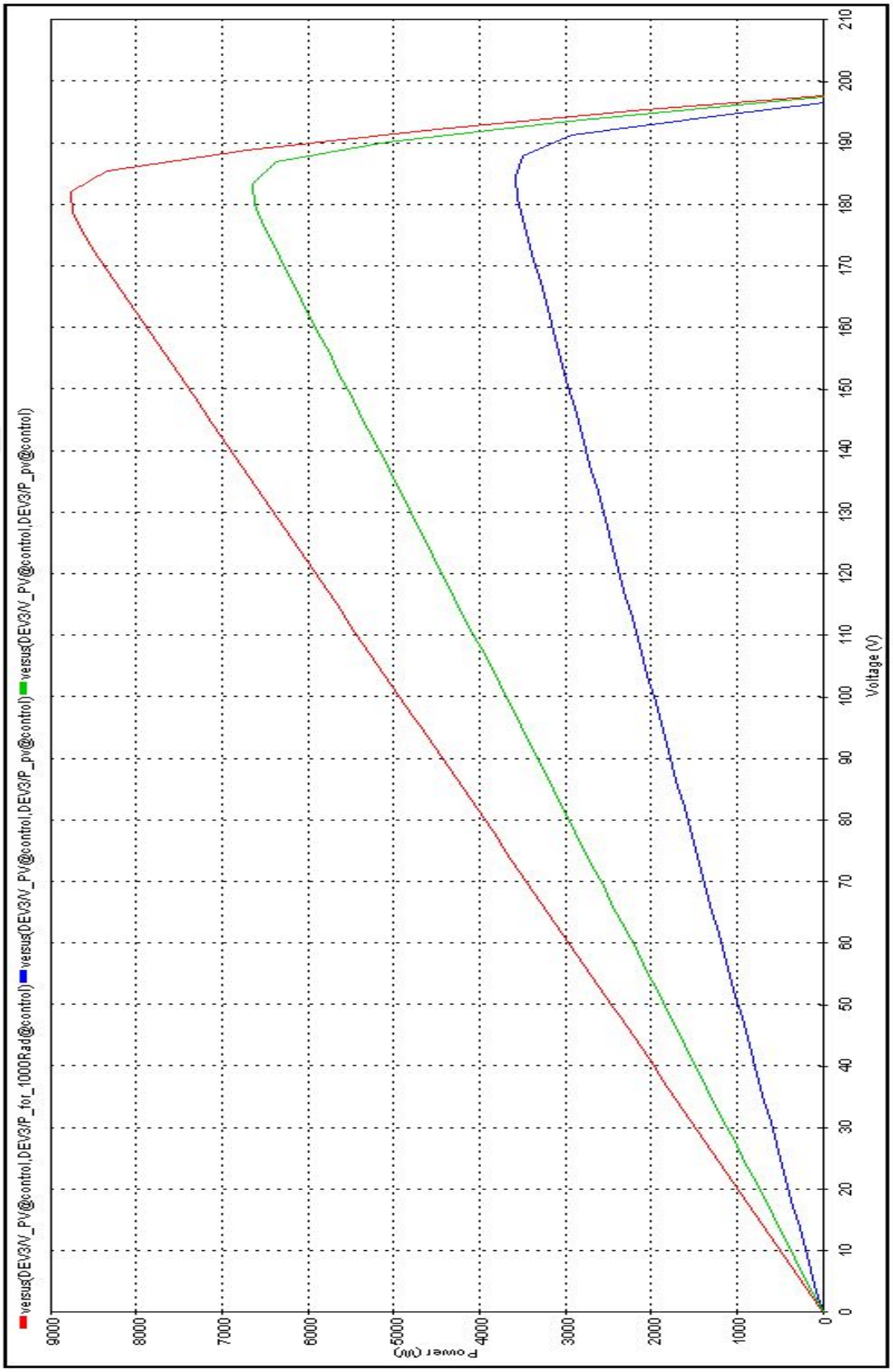

Figure 4.11: I-V characteristic of PV Panel Depending on Temperature

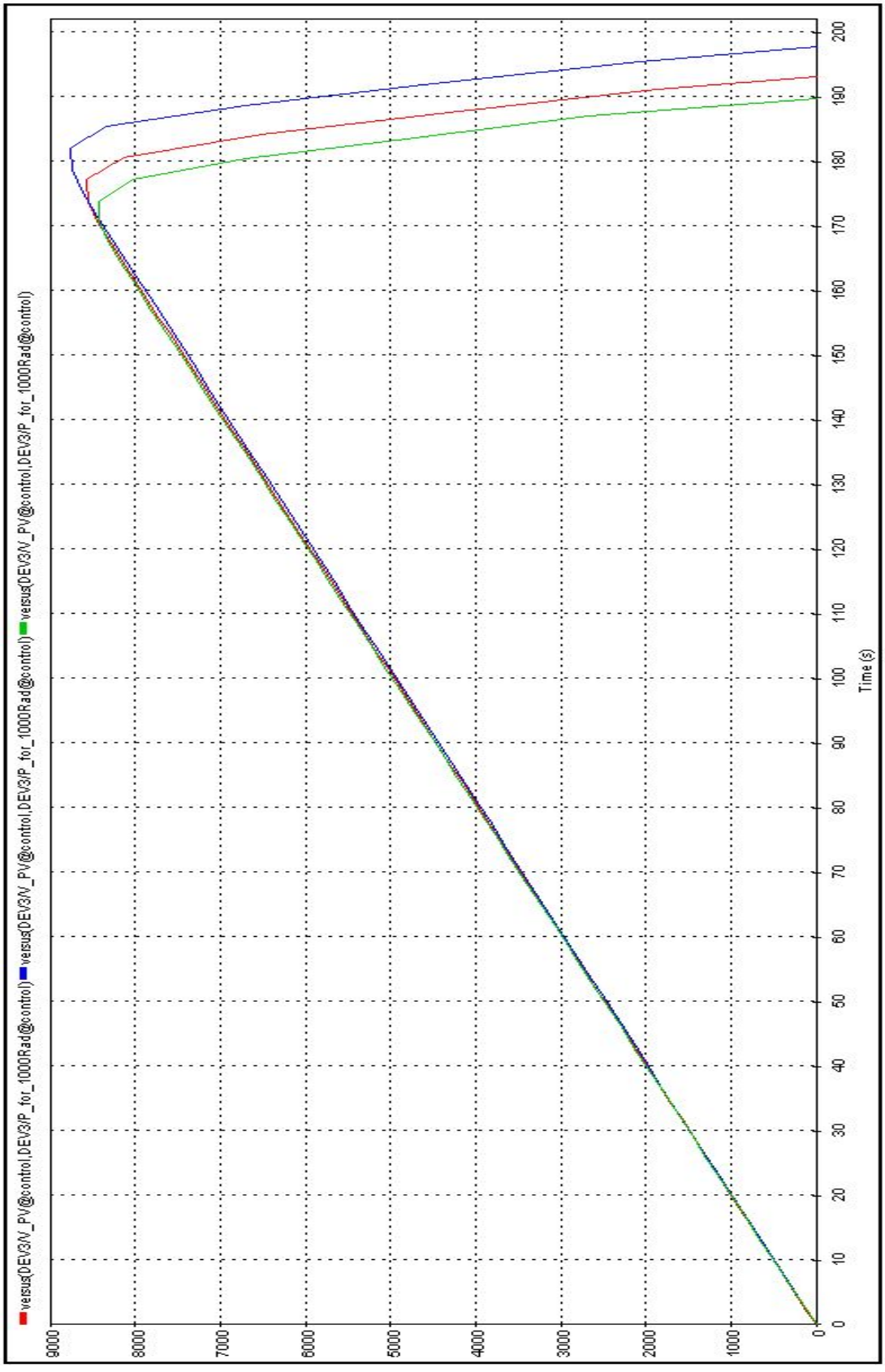

4.2 TRANSFORMER

In EMTP-RV, transmission or distribution transformers are used as a built-in function. In this model; connection type (Wye-Wye, Wye-Delta, etc.) of the transformer, its nominal power, primary and secondary voltage magnitudes can be changed easily. Also, primary, secondary and magnetizing impedance values can be assigned. This block function consists of three identical non-ideal one phase transformers. Illustration of the transformer in EMTP-RV software is indicated below as Figure 4.12.

Figure 4.12: Transformer as a Built-in Function

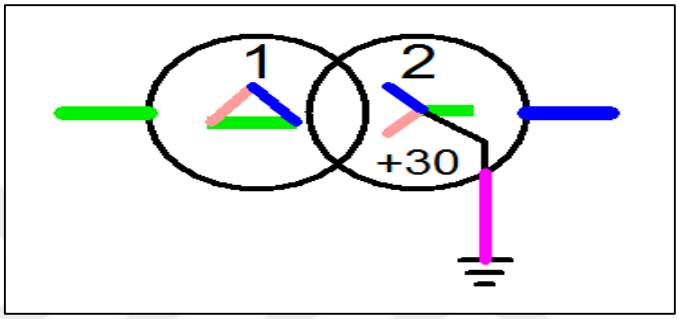

4.3 THE MODEL OF LOADS AND LINES

4.3.1 Load Model

In EMTP-RV, loads which are used for load flow and time domain simulations can be used directly from the library as a built-in function. Illustration of the load is given in Figure 4.13. In order to assign load, active power, reactive power n_p and n_q values should be defined. Load data tab which these values entered is indicated below as Figure 4.14.

Figure 4.13: Load as a Build-in Function

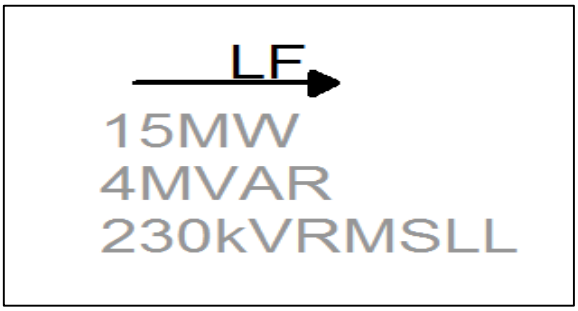

Figure 4.14: Load Data Tab

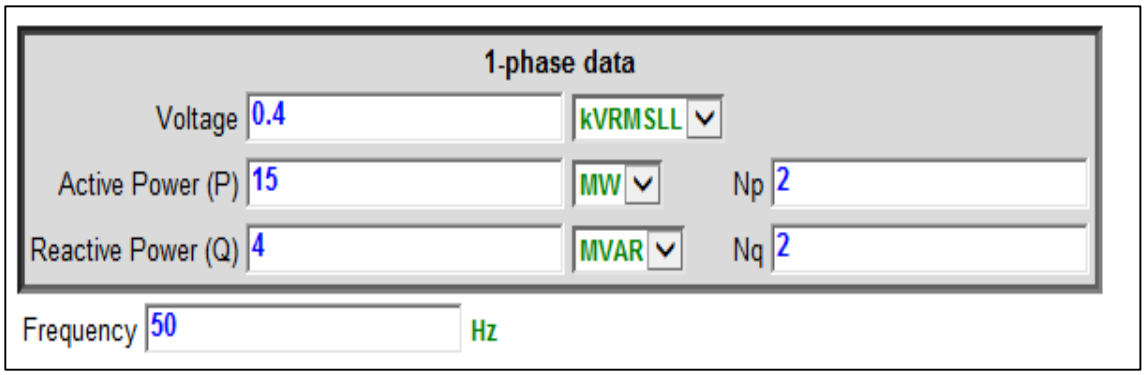

4.3.2 Overhead Line Model

For lines, there are two options which are constant parameter (CP) and frequency dependent (FD) models. In FD line model, resistance and inductance of line are calculated by considering frequency, skin effect and ground return conditions. On the other hand capacitance value accepted as constant. Also, shunt conductance value is taken into consideration as 0.2x10-9 S/km. Characteristic line impedance formula is given in below as Eq. (4.1):

$$Z_c = \frac{R + j\omega L}{G + j\omega C} \tag{4.1}$$

In CP line model, R, L and C values are calculated at assigned frequency and keep constant. While L and C are distributed on the line, R values assigned to line ends with R/4 value and middle of the line with R/2 value. Shunt conductance is ignored. When FD and CP line models are compared, it can be said that frequency dependent models are more accurate than CP line models. Thus, FD line model is used in this thesis. FD line model representation is shown in Figure 4.15.

Figure 4.15: Frequency Dependent Overhead Line

4.3.3 Underground Cable Model

Same as line models, there are CP and FD models for cables. While C, R, L and G values are taken into consideration with the change of frequency in FD cable model, R, L, C and G (equal to zero) values are taken as constant. In this thesis, FD cable models are used for more accurate simulations. FD cable representation is indicated in below as Figure 4.16.

Figure 4.16: Frequency Dependent Underground Cable

5. SIMULATIONS AND RESULTS

In this thesis, different transient case studies are investigated. These case studies are categorized under 3 topics as switching, lightning and faults. Purpose of case studies under these topics is to evaluate both effects of transient events on micro-grid and effects of micro-grid to the customer and main power grid under such events.

5.1 SWITCHING EVENTS

5.1.1 Micro-Grid Disconnection and Connection with Main Power Grid

In this case, designed micro-grid is connected to the main electrical grid while all distributed energy resources and loads are connected. Then at instant t=0.4 second, micro-grid is disconnected from main grid till at instant t=0.6 second. During this case, voltage magnitudes and shapes for all 3 phases in micro-grid are obtained. Obtained graphs are indicated in Figure 5.1 and Figure 5.3 for MV side of micro-grid and in Figure 5.2 and Figure 5.4 for LV side of micro-grid.

Figure 5.1: Voltage Graph at MV Side of Micro-Grid at Off-Grid

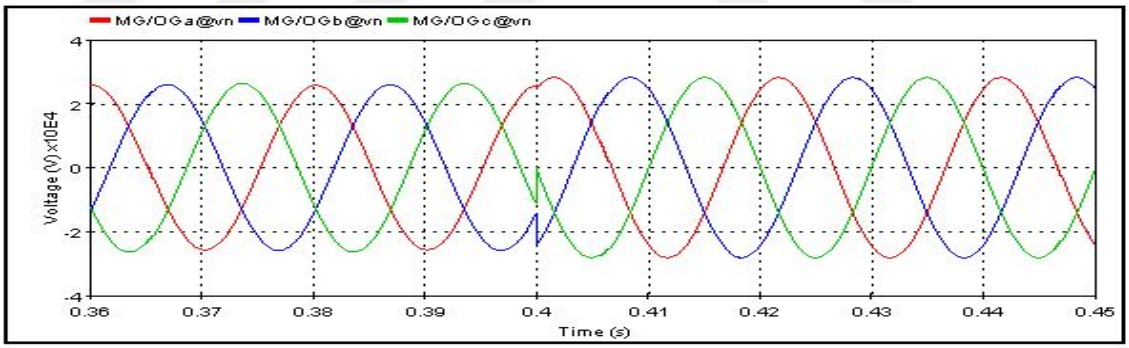

Figure 5.2: Voltage Graph at LV Side of Micro-Grid at Off-Grid

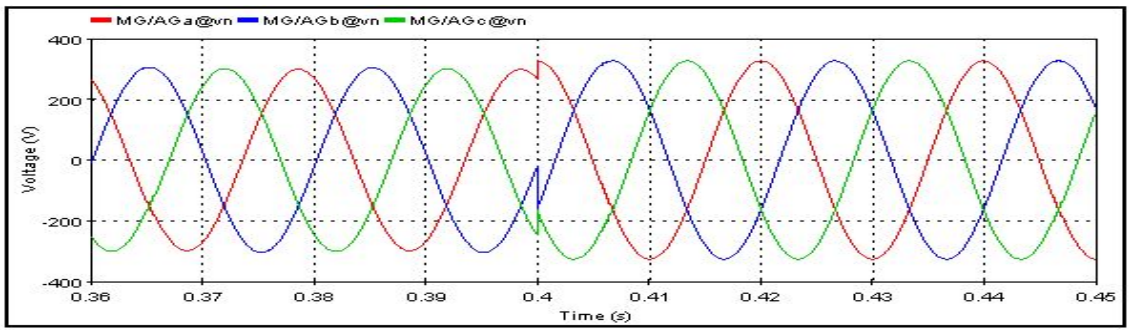

Figure 5.3: Voltage Graph at MV Side of Micro-Grid

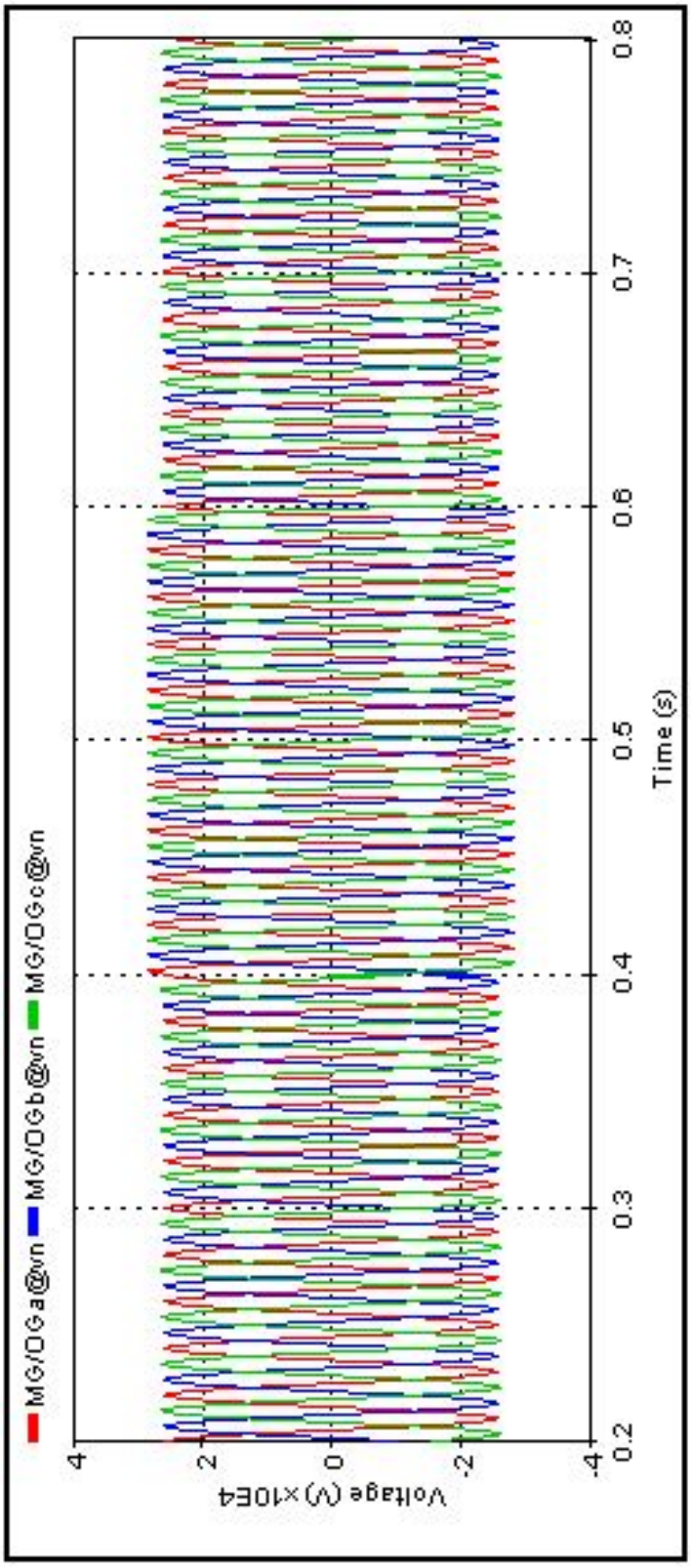

Figure 5.4: Voltage Graph at LV Side of Micro-Grid

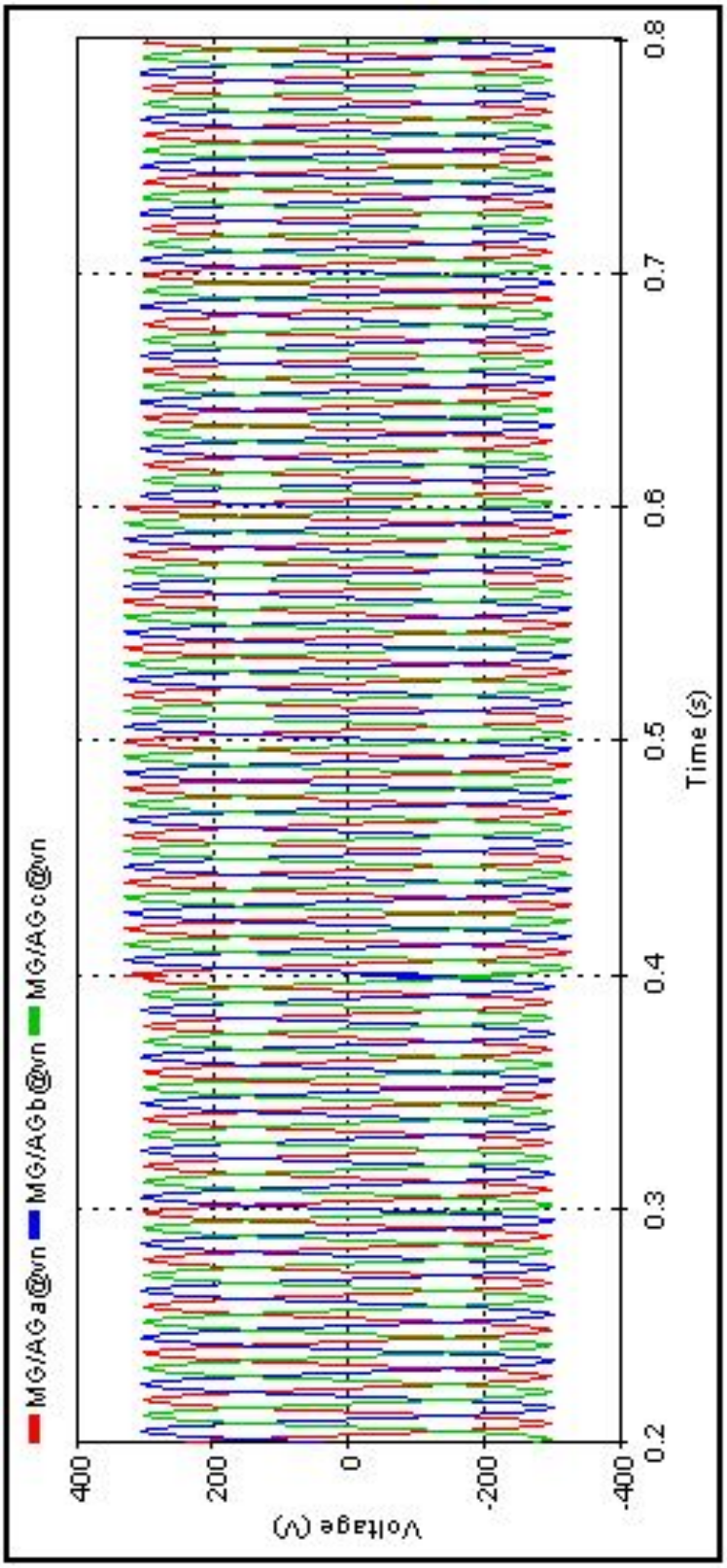

From the figures of this case, two situations can be seen. One of them is magnitude change which can be seen in Figure 5.1 and Figure 5.4 clearly. In the off-grid mode, the voltage magnitude of micro-grid is increased. This situation occurs because, in on-grid mode, the main bus of AC micro-grid is affected by other loads which cause a voltage drop in the grid. However, when micro-grid became an island and its main supply became DERs, it is affected by only its own loads which cannot cause a voltage drop.

The second situation which is observed is a phase shift. It can be seen in Figure 5.3 and Figure 5.2. When micro-grid is completely disconnected from the main grid at instant 4 seconds, phase shift at all phases occurs. To avoid such satiation phase control management should be done.

5.1.2 Unsynchronized Micro-Grid Disconnection

In the second case, unsynchronized switching condition is simulated. Firstly, all distributed energy resources are removed from the model. Then, at 0.1 second, the status of two switches are changed to make maneuver between two feeders. To simulate unsynchronized switching, 1 phase of bottom switch opened with 0.1-second delay. Modeling illustration of these two feeders is given in below as Figure 5.5. Also, voltage shapes for LV and MV side of MG location are indicated in Figure 5.6 and Figure 5.7 respectively.

Figure 5.5: Black Switch Opened While Red Switch Closed With 0.1 Second Delay at Phase C

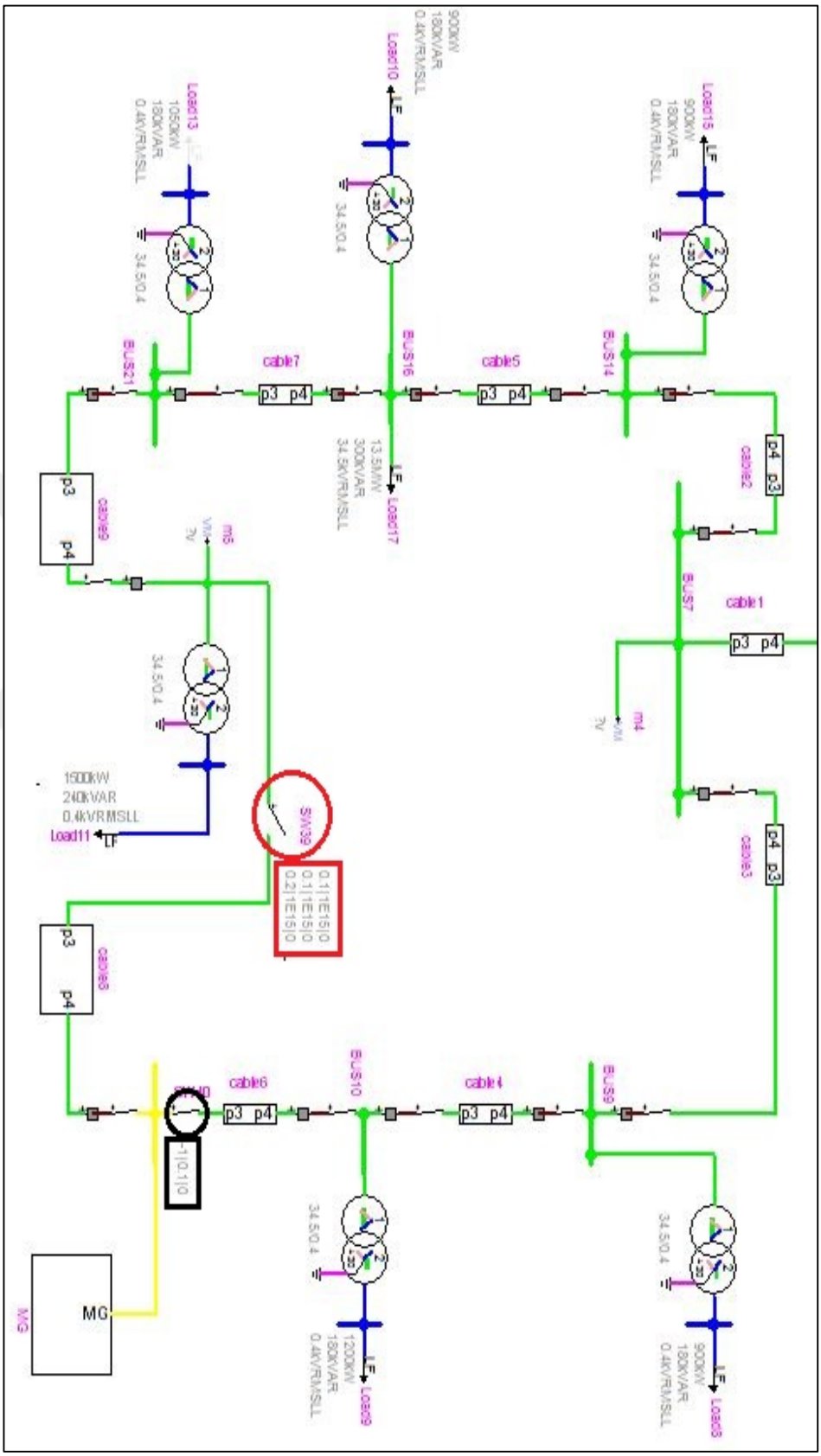

Figure 5.6: Voltage Graph at LV Side of Micro-Grid When Only Loads are Connected

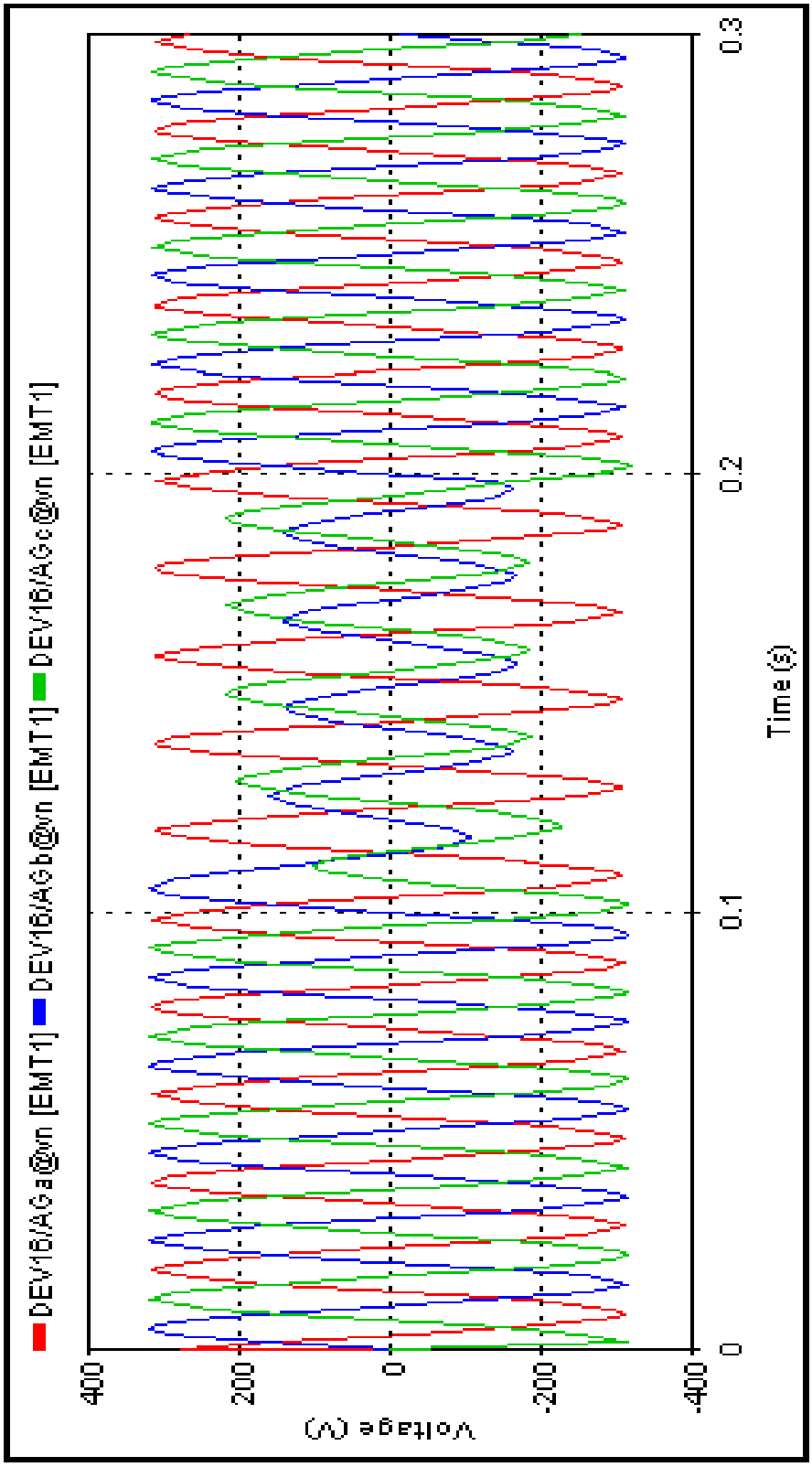

Figure 5.7: Voltage Graph at MV Side of Micro-Grid When Only Loads are Connected

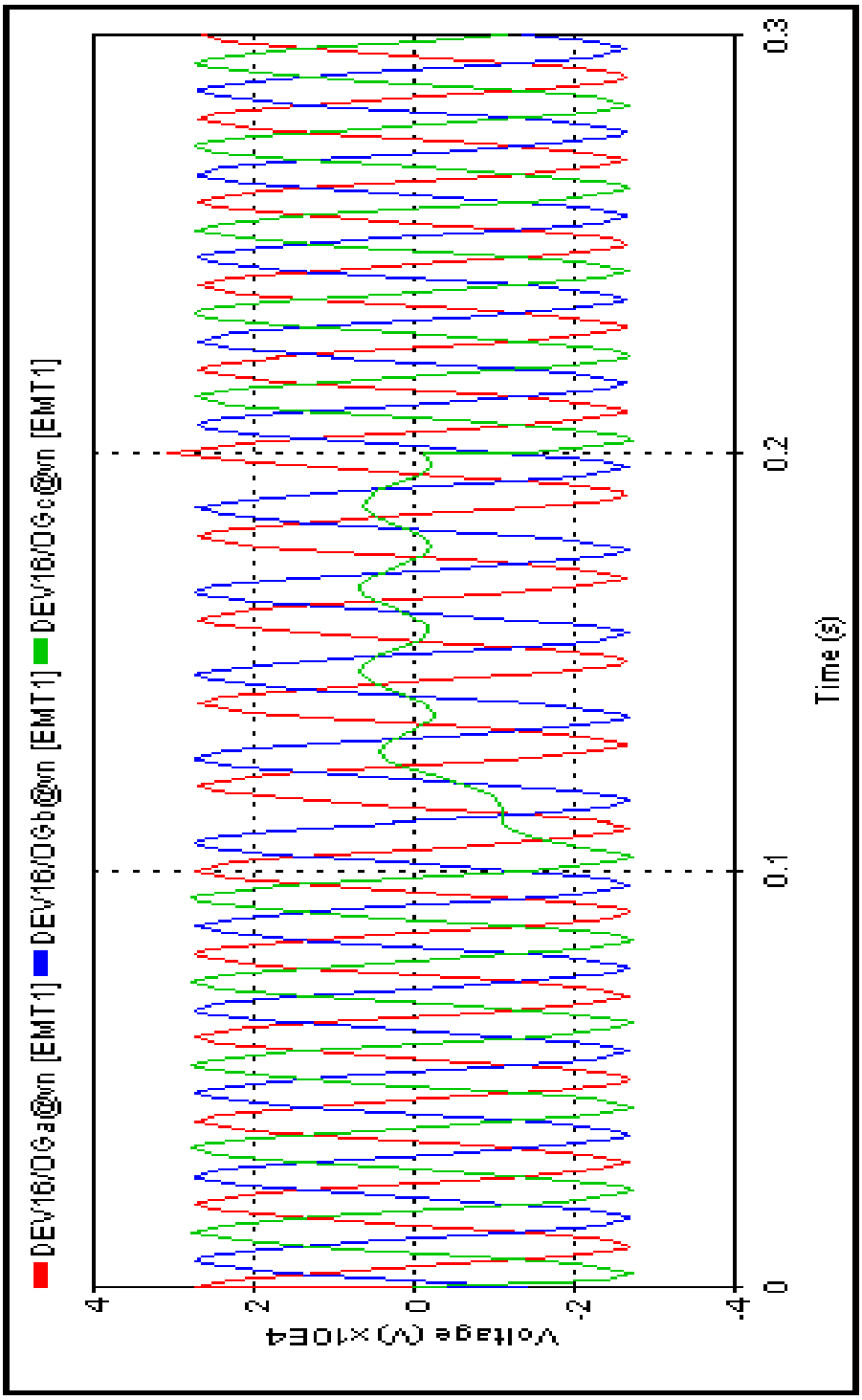

For comparison and seeing the effect of micro-grid, the same case is simulated again when all distributed energy resources (WES, PV, ESS) are connected. Obtained voltage graphs are given in below as Figure 5.8 and Figure 5.9.

Figure 5.8: Voltage Graph at MV Side of Micro-Grid

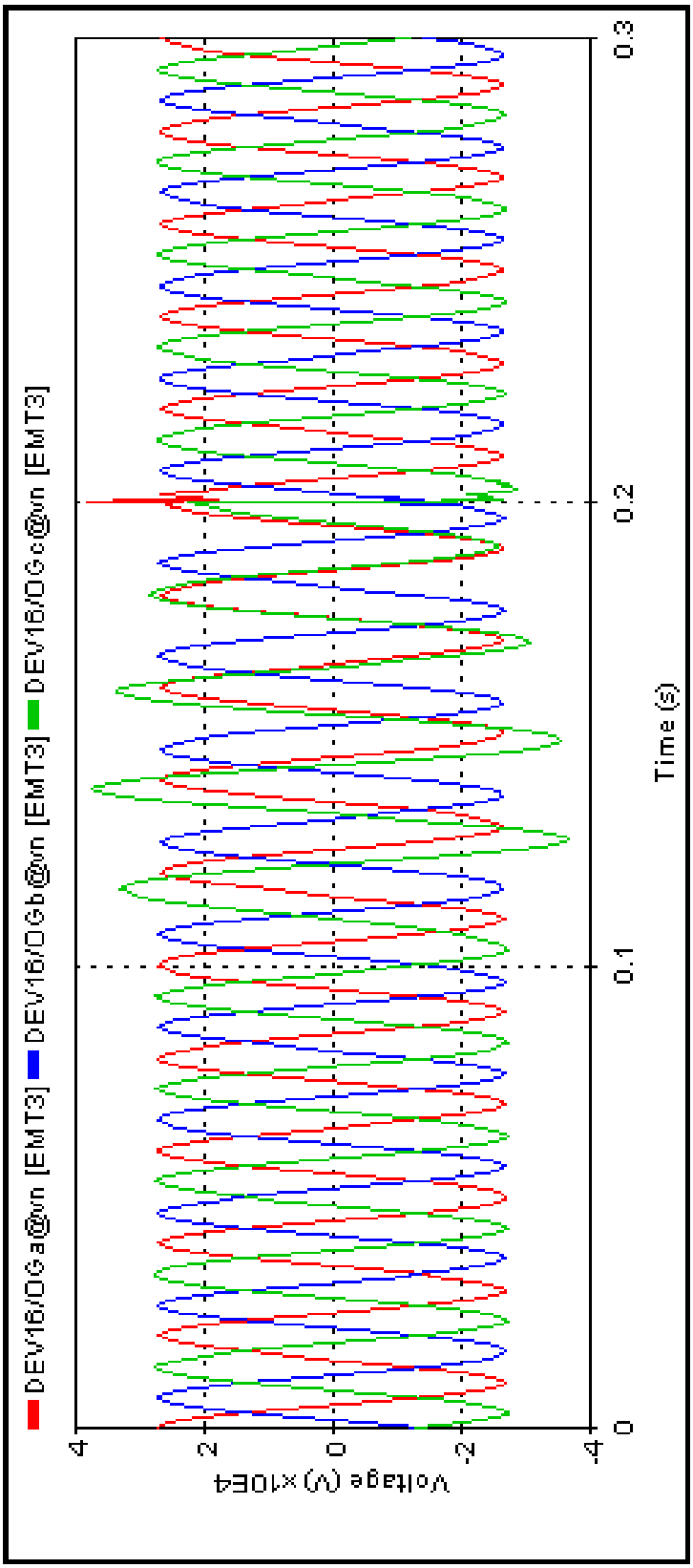

Figure 5.9: Voltage Graph at LV Side of Micro-Grid

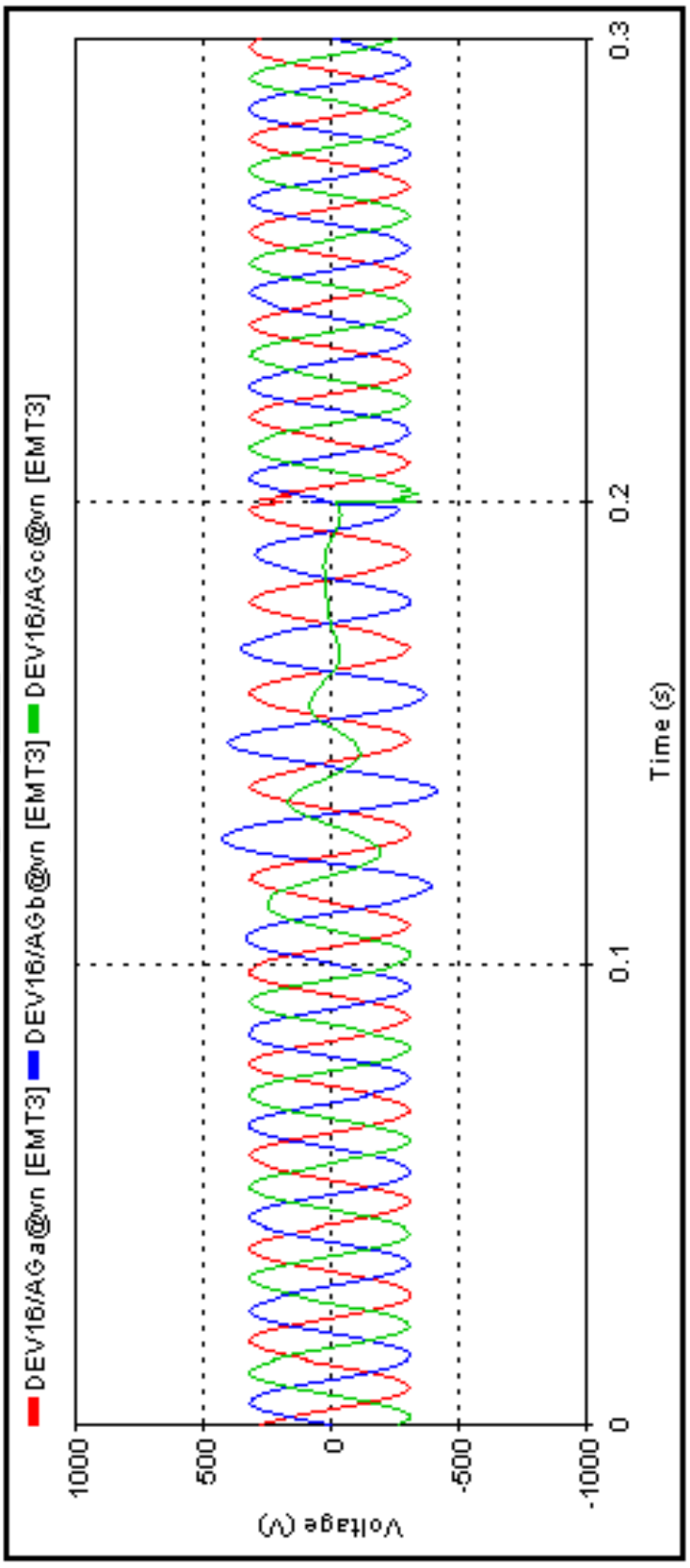

For not considering DERs or micro-grid, 0.1-second delay at switching causes voltage sag at the phase which delay is occurred. On the other hand, when micro-grid is considered, not only voltage swell is seen but also transient event at the end of switching is observed at the same phase. From this case, it can be said that effects of renewable energy resources should be studied especially when micro-grid is operated as grid connected. To avoid such negative effects, micro-grid can be operated in the islanded mode before the switching is started and continue to be operated as islanded mode until all switching process is finished. In this case, the micro-grid will not be affected by such negative influences.

5.1.3 Load Connection and Disconnection from Main Power Grid

In this third case, 18 MW load is connected to the system at 0.1 second and stay connected till 0.3 second. This load is linked to Bus 10 in Figure 4.2 with 3 phase switch. The transient event is seen clearly especially when the load is connected to the system at 0.1 second. While the load is connected to the grid, the voltage drop is also seen. After disconnection from power grid at 0.3 second, almost 1-period temporary voltage swell event occurs. When this voltage swell event and voltage fluctuations which occurred during load connection and disconnection are compared for different buses, it is obvious that load connection and disconnection affected to MG bus more than other buses due to DERs and power electronic equipment in the micro-grid structure. The obtained voltage graphs for different buses are given in Figure 5.10, Figure 5.11, Figure 5.12 and Figure 5.13. In Figure 5.10, voltage measurements are shown for Bus 7 while in Figure 5.11 voltage measurements which is taken from Bus 6 are shown. For this case, the obtained voltage shapes for MV side of micro-grid are shown in two figures which are Figure 5.12 and Figure 5.13. Purpose of this is to read graphs easily and show the influence of the case on the micro-grid bus more clearly.

Figure 5.10: Voltage Graph at Bus 7 During Load Connection and Disconnection

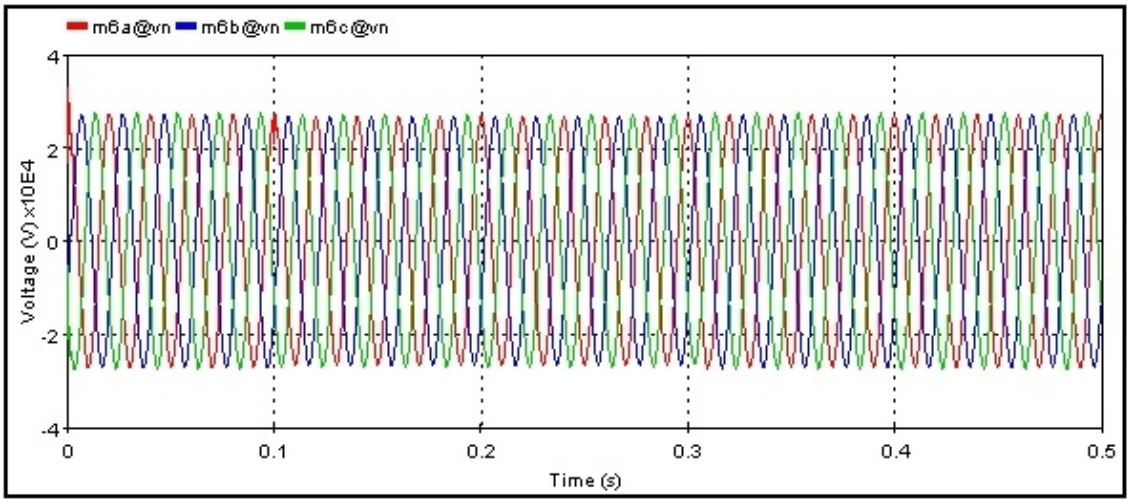

Figure 5.11: Voltage Graph at Bus 6 During Load Connection and Disconnection

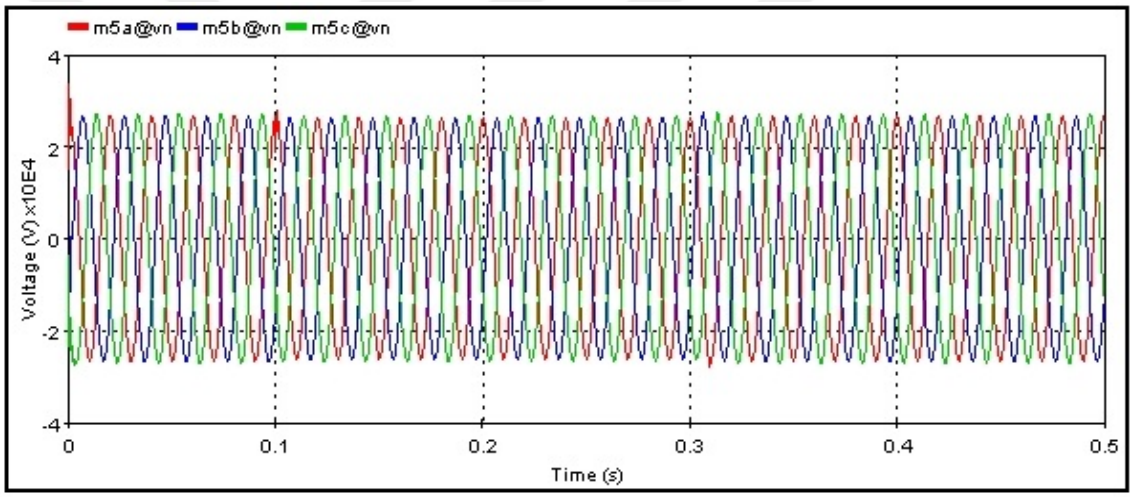

Figure 5.12: Voltage Graph at MV Side of Micro-Grid During Load Connection and Disconnection

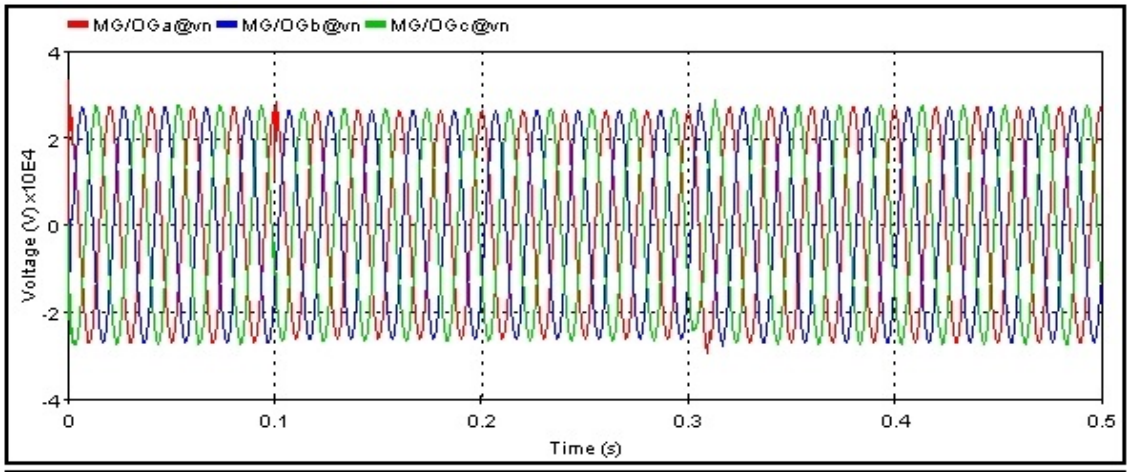

Figure 5.13: Closer and Clear Voltage Graph at MV Side of Micro-Grid During Load Connection and Disconnection

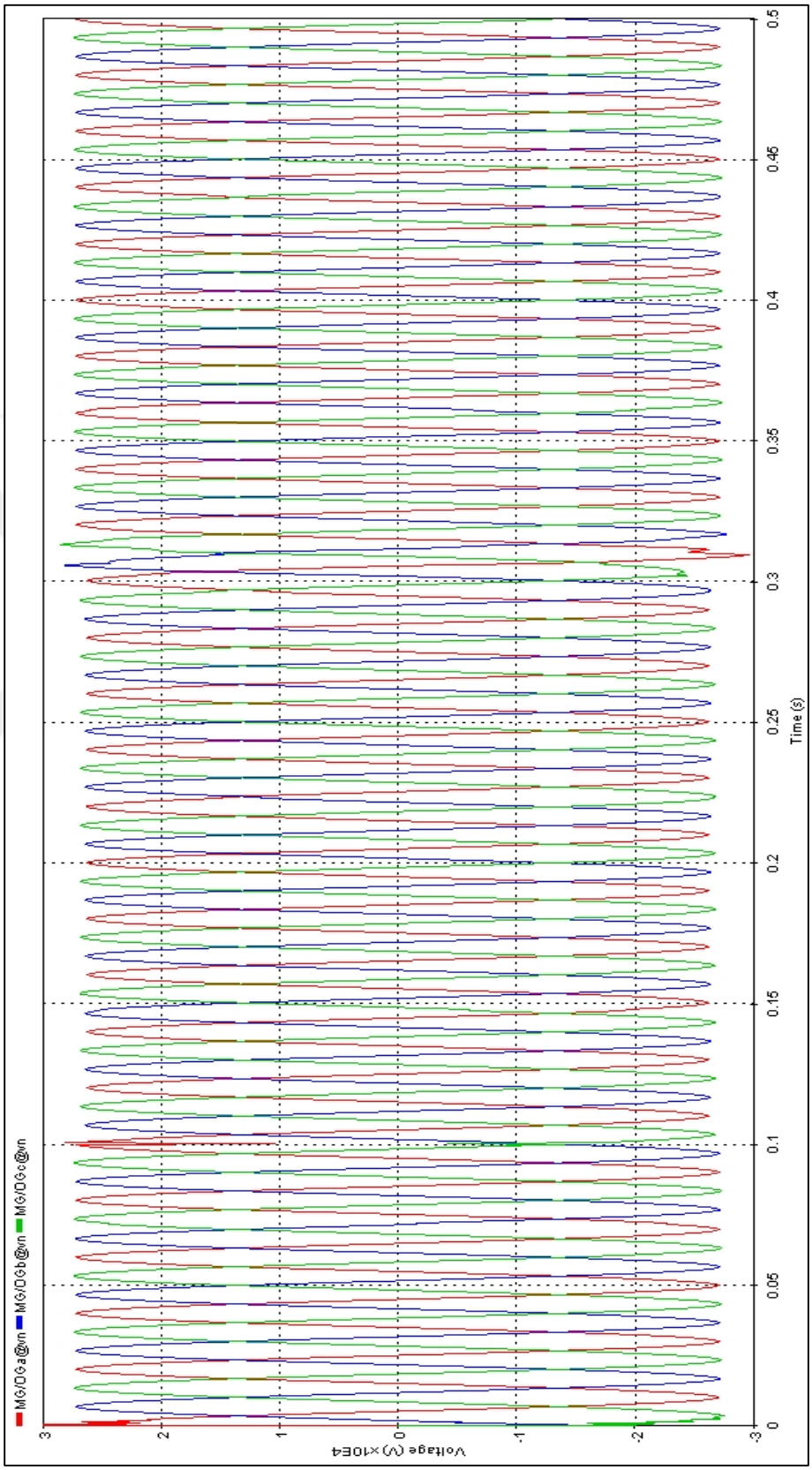

5.1.4 De-energization and Re-energization of Transmission Transformer

In this case, the transformer at transmission substation is de-energized and re-energized by changing the status of switches located between Bus 18 and Bus 4 in Figure 4.1. This switching operation occurs from 0.21 second to 0.25 second. Thus, the system became non-energized during 0.04 second. Obtained voltage graphs at Bus 7, Bus 6 and MV side of micro-grid for this event are indicated in Figure 5.14, Figure 5.15 and Figure 5.16. When transient events are compared for these 3 different locations, the worst situation in terms of fluctuations and swell issues is seen at MV side of micro-grid. Although the duration of the transient event is almost same for 3 locations, voltage magnitudes and voltage fluctuations especially for re-energization vary from bus to bus. While the voltage magnitude at swell goes up to 4kV in Bus 6 and Bus 7, voltage magnitude at swell goes up to 5 kV in MG. Also, fluctuations are more obvious for MG location than other two buses. To see transient effects clearly, closer voltage graph is given in Figure 5.17 for MV side of Micro-grid.

Figure 5.14: Voltage Graph at Bus 6 During Transformer De-energization and Re-energization

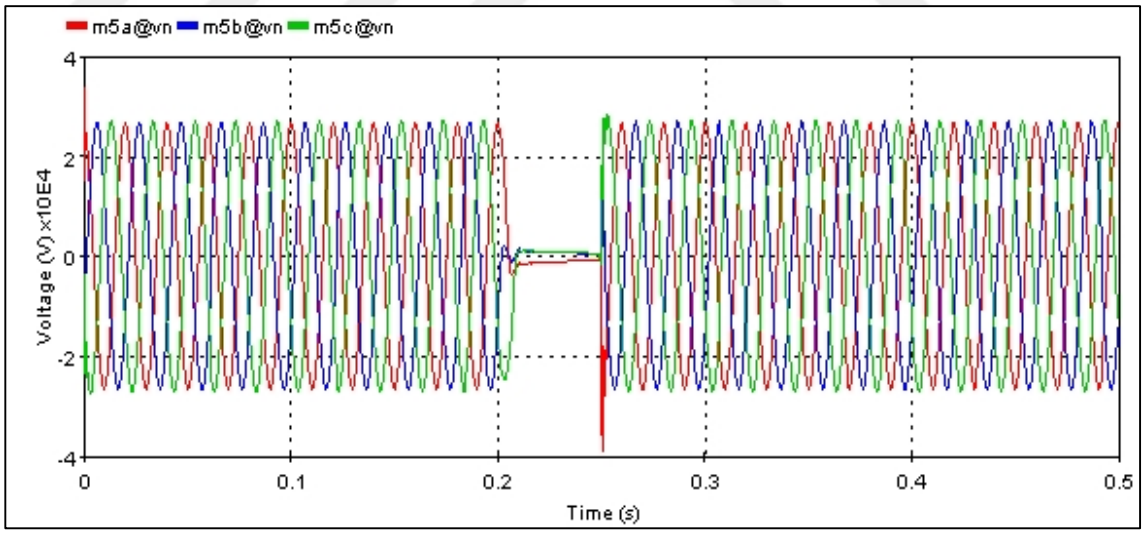

Figure 5.15: Voltage Graph at Bus 7 During Transformer De-energization and Re-energization

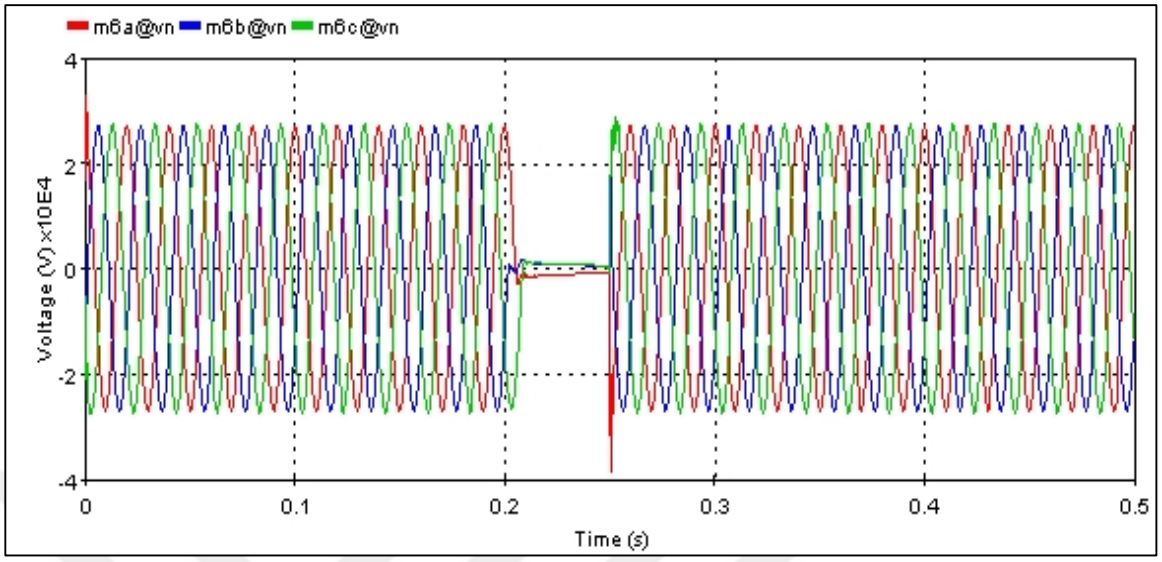

Figure 5.16: Voltage Graph at MV Side of Micro-Grid During Transformer De-energization and Re-energization

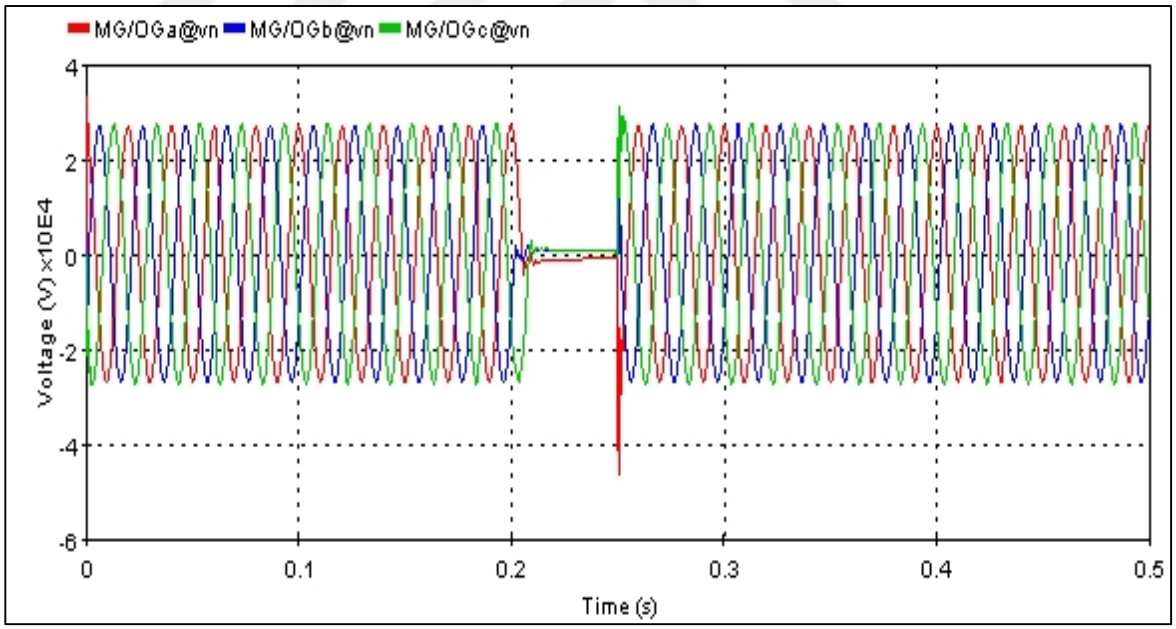

Figure 5.17: Zoomed Voltage Graph at MV Side of Micro-Grid During Transformer De-energization and Re-energization

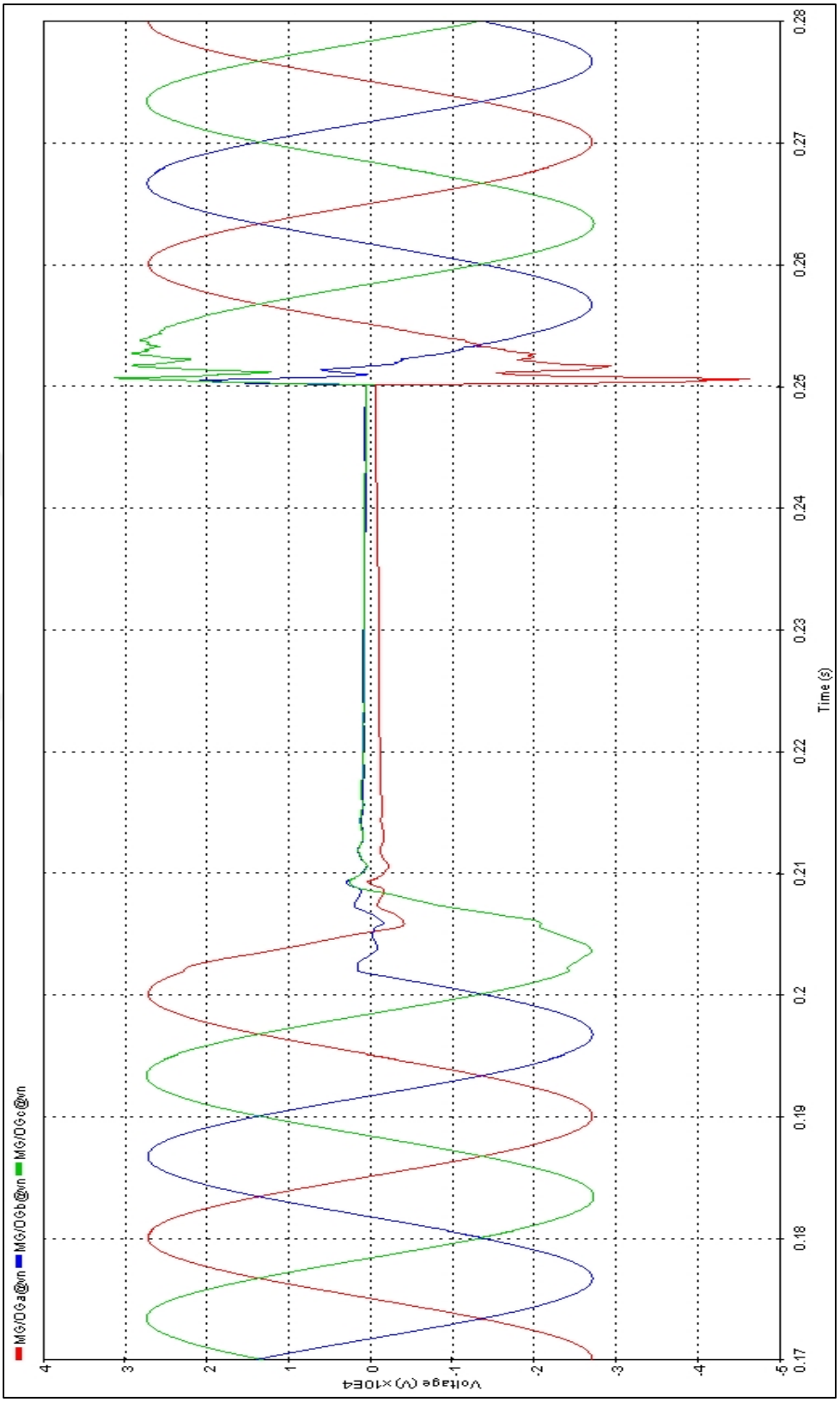

5.2 LIGHTNING EVENT

In this case, a lightning stroke the one phase of the overhead line at transmission system level. This event is occurred at 100 ms and lasted 300 µs. For this case, CIGRE lighting current source is used. The current characteristics of built-in CIGRE model in EMTP-RV software are shown below in Figure 5.18.

Figure 5.18: EMTP-RV Model of CIGRE Lightning Current Source

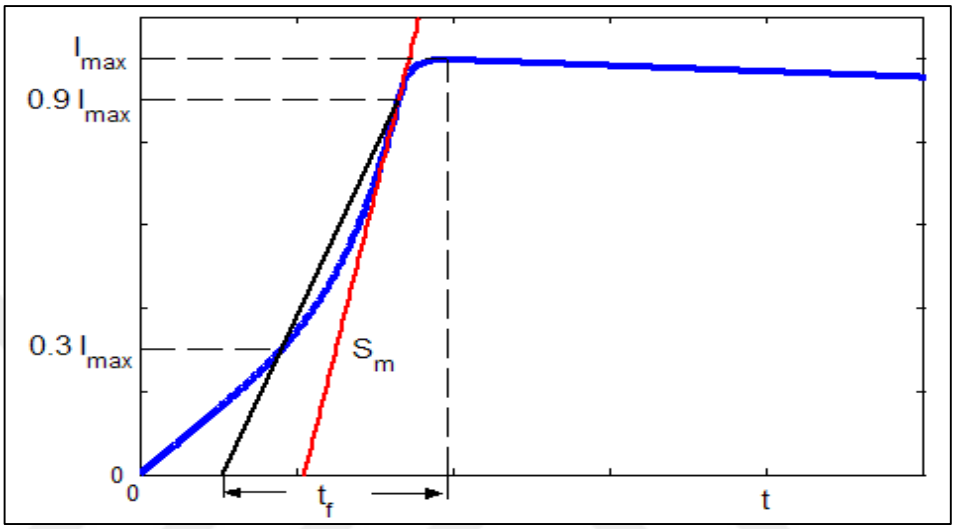

Simulation results in terms of voltage graphs for 3 buses which are Bus 4, MG Bus and Bus 6 are given in Figure 5.19, Figure 5.20 and Figure 5.21 respectively. As expected, higher voltage magnitude occurs near the overhead line and lower voltage magnitude occurs farthest from the overhead line. For Bus 4 which is located after the secondary side of 154/34.5 kV transformer, 5620 kV is seen at phase which lightning is stroke. While 5266 kV occurs for MV side of micro-grid, 4731 kV occurs for Bus 6 at the same phase. Such voltage magnitudes are obtained less than 20 µs after lightning stroke. So it is clear that even micro-grid is located far from the lightning event, it affected substantially. Due to the fact that micro-grids are consists of power electronic devices, such high voltage swell can influence electronic boards and cause burning or malfunction of them. Thus, necessary power protection equipment should be used to prevent such situations.

Figure 5.19: Voltage Graph at Bus 4

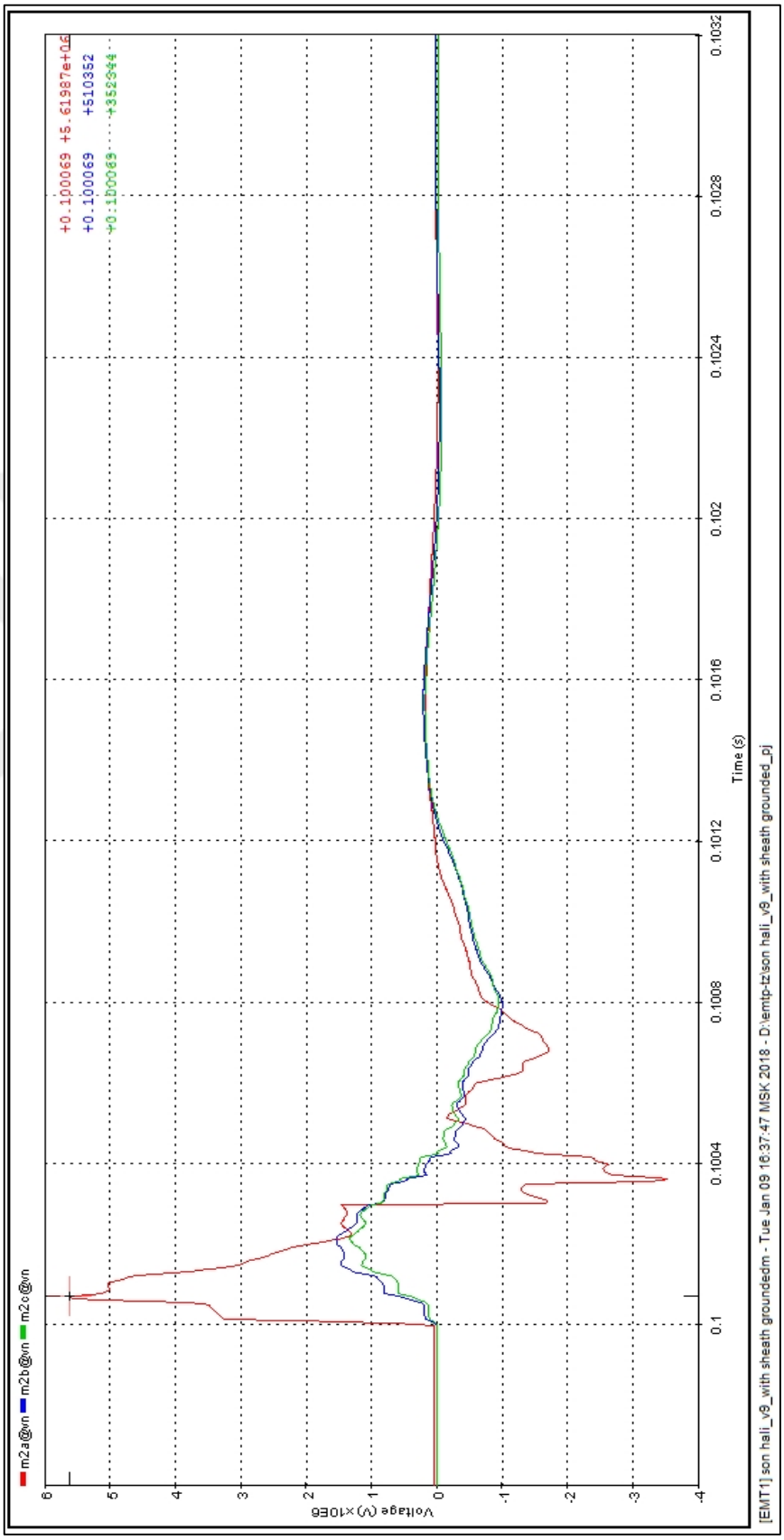

Figure 5.20: Voltage Graph at MV Side of Micro-Grid

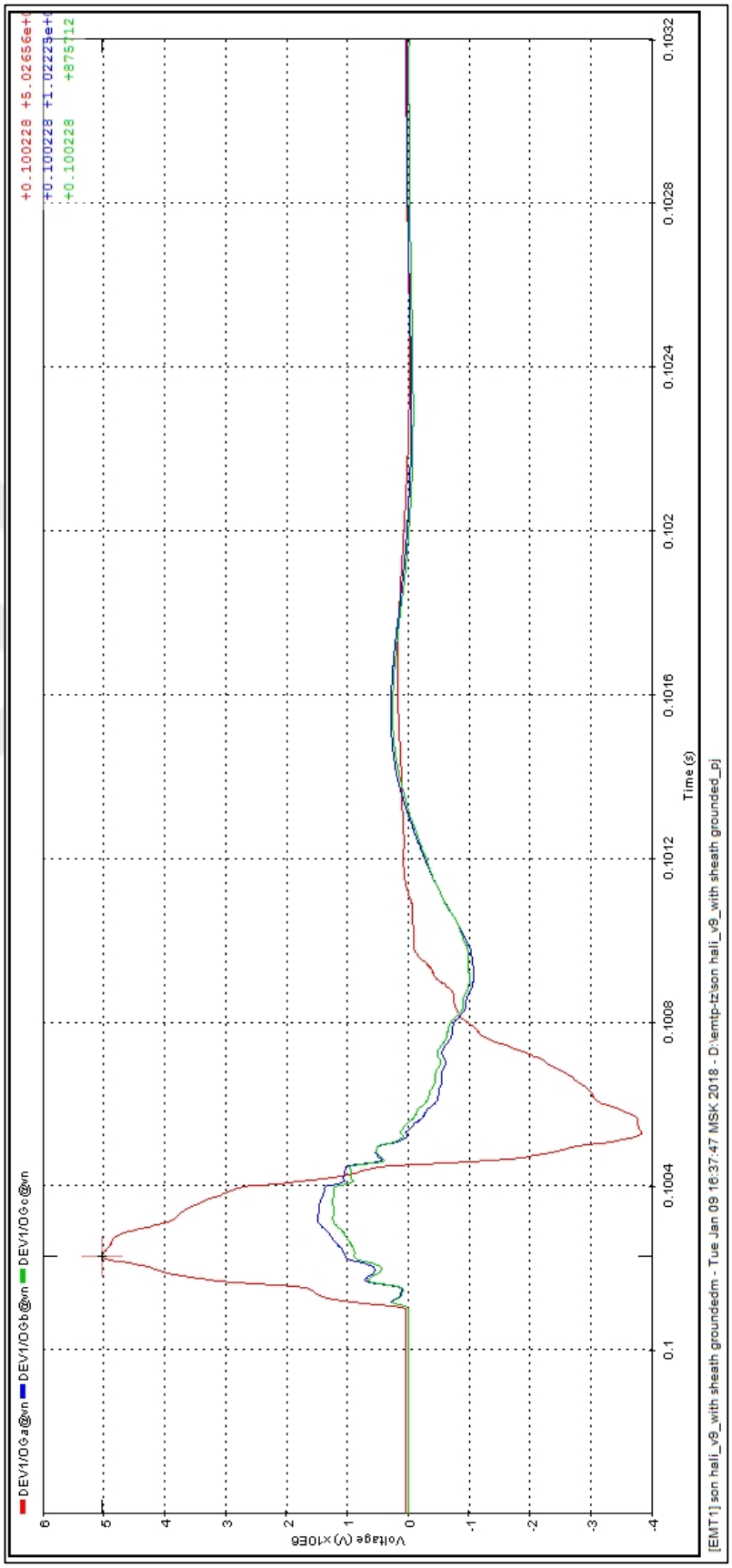

Figure 5.21: Voltage Graph Bus 6

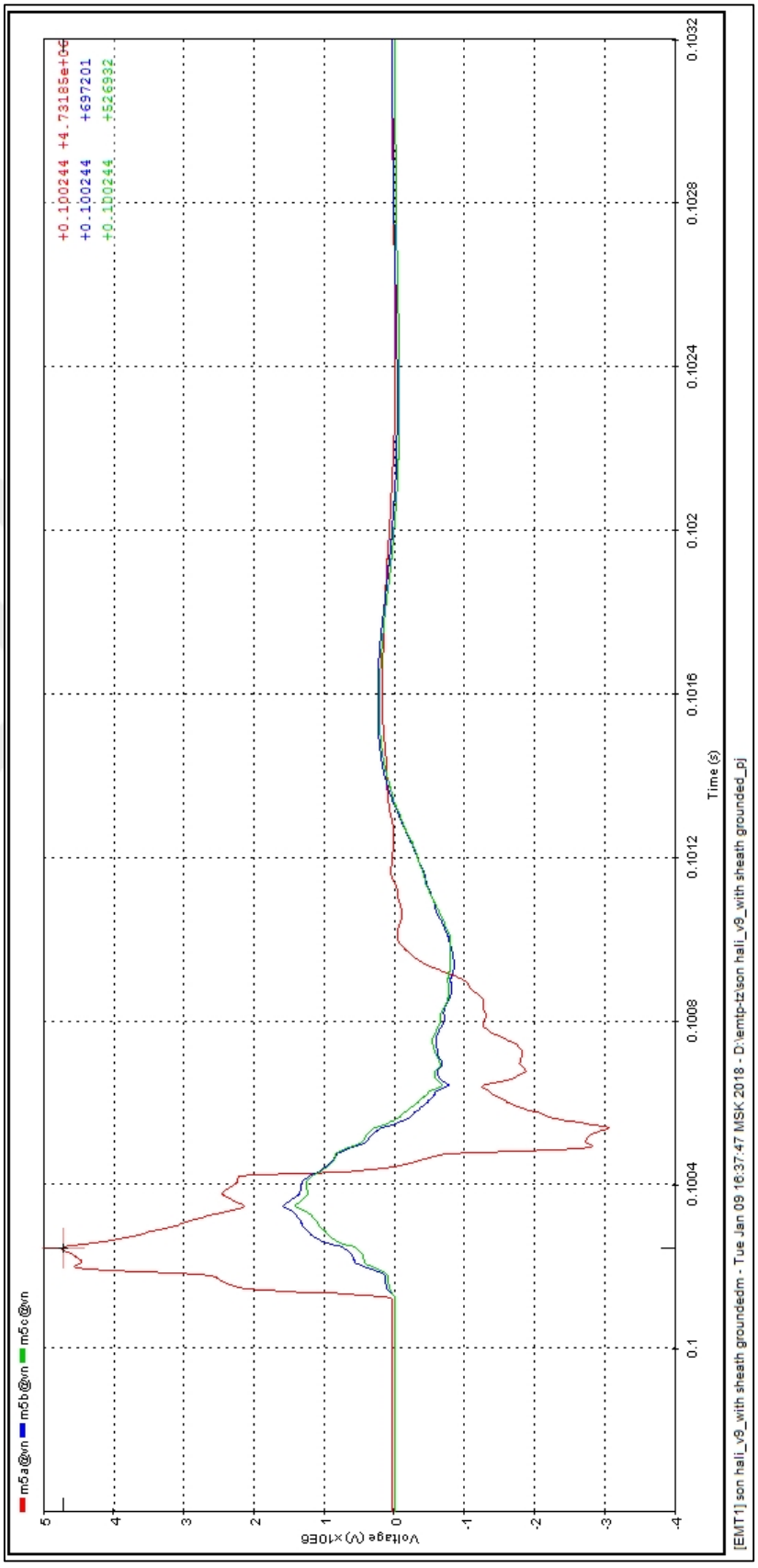

5.3 FAULTS EVENTS

5.3.1 Single Phase Fault at Grid with Frequency-Dependent Model

In the third case, one phase to ground fault is applied to phase A at the location of the main bus named Bus 7. It can be seen from Figure 4.2. This one phase to ground fault is occurred at 0.2 second and lasted 0.15 second. Voltage scopes are located at Buses named 7 in and 6 in Figure 4.2 and Bus 1 in Figure 4.1. Voltage shapes obtained for these different buses are given below as Figure 5.22 (Bus 6), Figure 5.23 (Bus 7) and Figure 5.24 (Bus 1). From the figures, it is obvious that one phase to ground fault seen as a voltage sag in other buses. Depending on the location of the bus, effects of voltage sag is changed. When bus location is close to fault location voltage sag value became higher. It can be deducted from Figure 5.22 and Figure 5.24. In order to show effects of micro-grid, the same fault is applied when all DERs are connected and when all DERs are excluded from the model. For DERs connected case, more than one micro-grid is included to model. Obtained graphs are indicated in below as Figure 5.25 and Figure 5.26.

Figure 5.22: Voltage Graph at Bus 6 Where Located Near the Fault

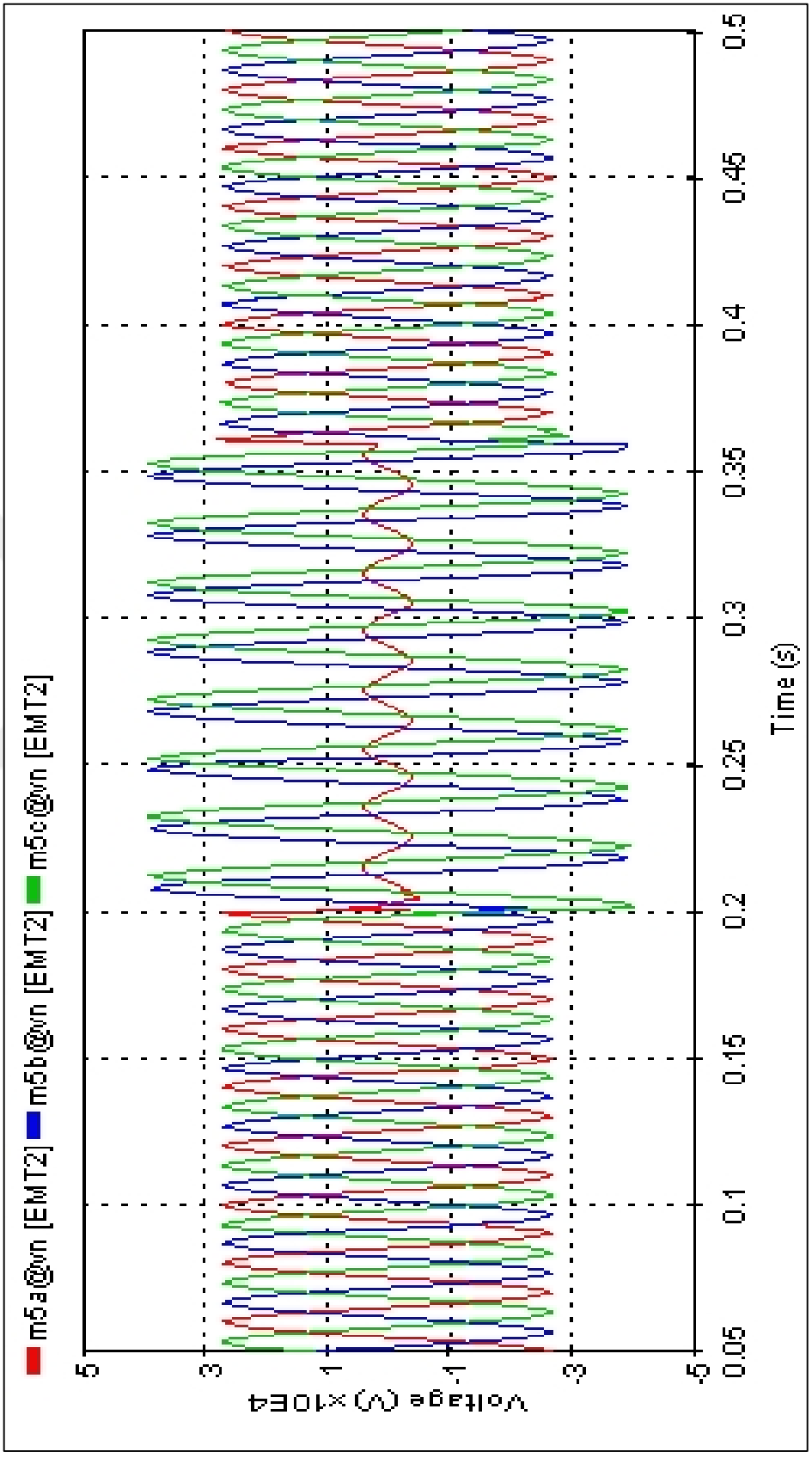

Figure 5.23: Voltage Graph at Bus 7 (Fault Location)

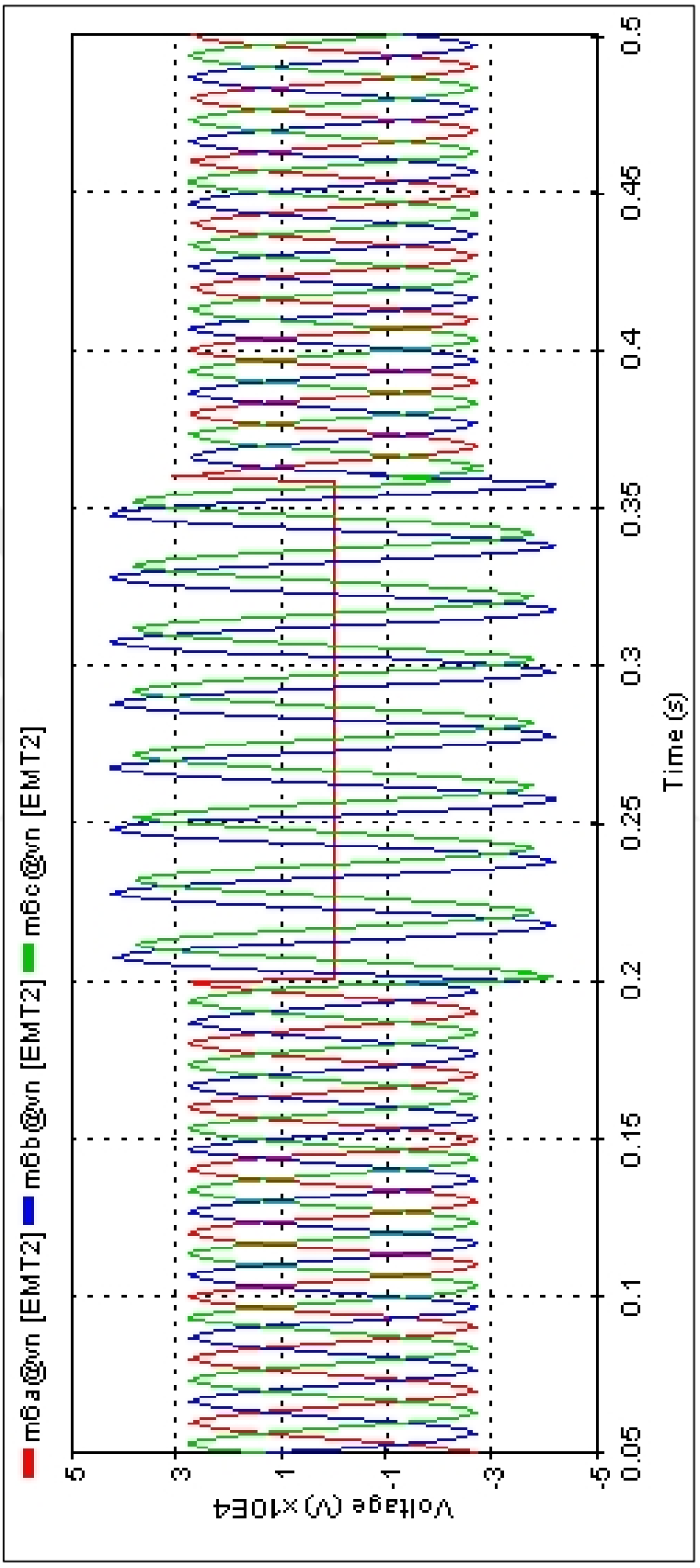

Figure 5.24: Voltage Graph at Bus 1 Where Located Far From Fault

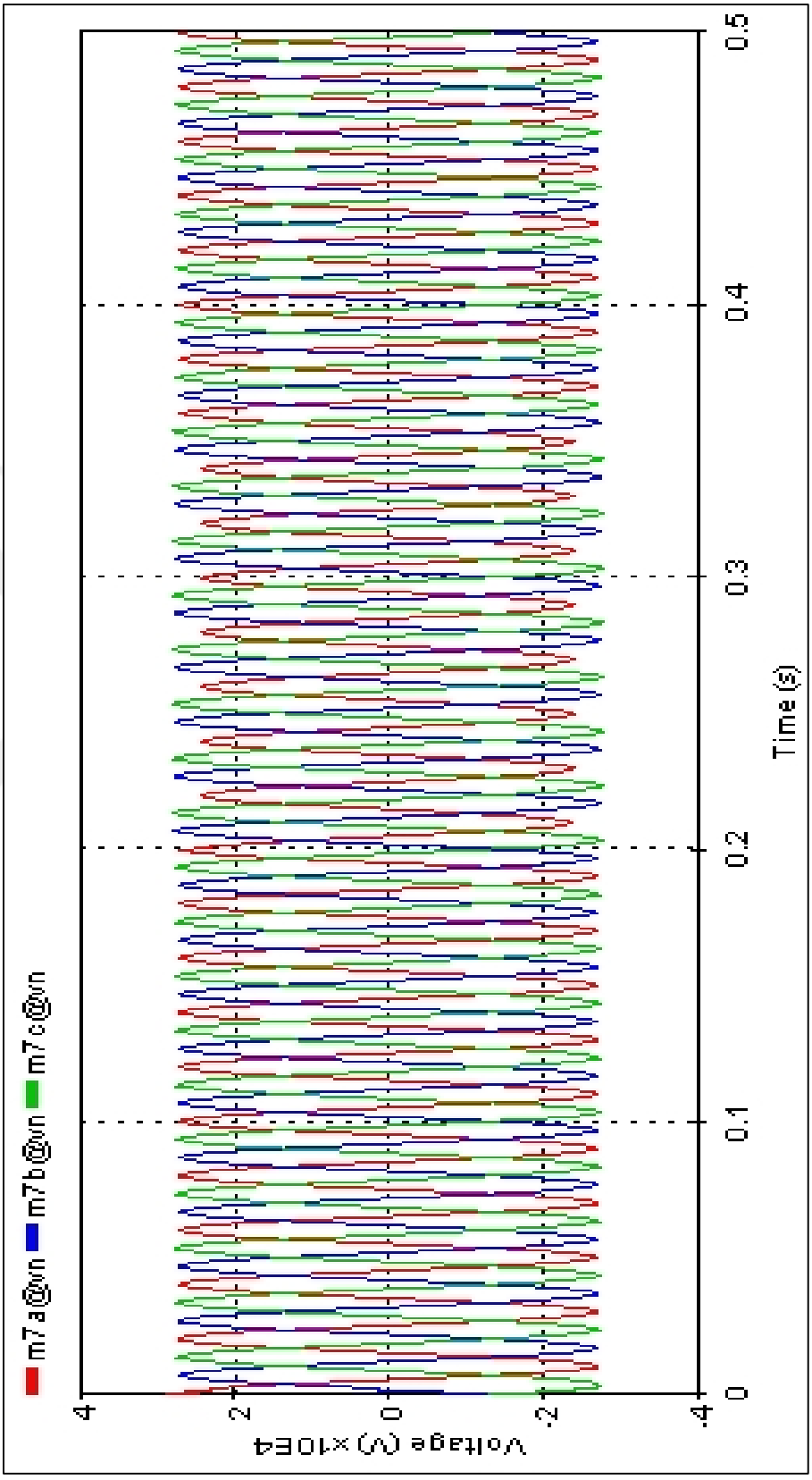

Figure 5.25: Voltage Graph at MV side of MG Bus When More Than 1 Micro-Grid are Connected

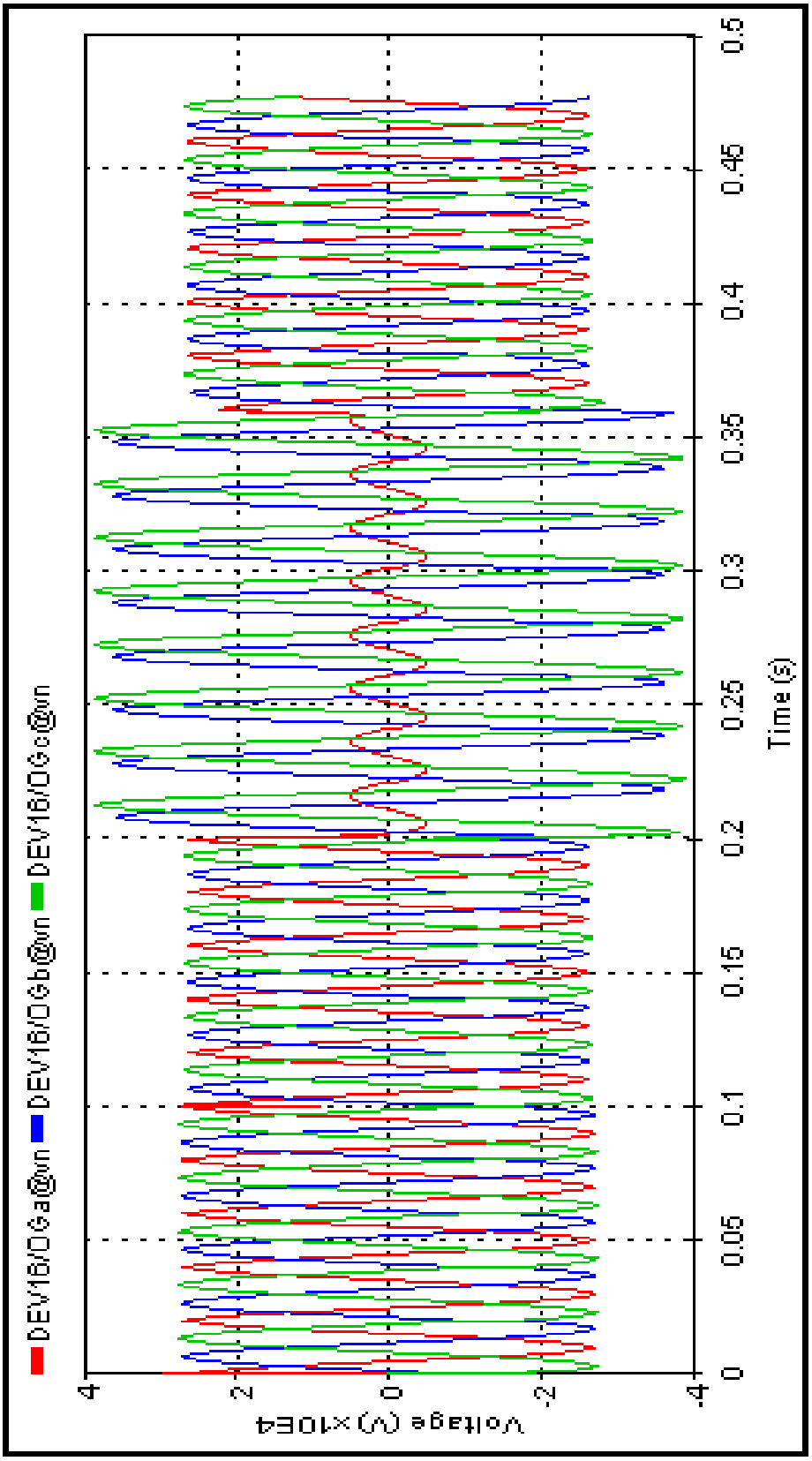

Figure 5.26: Voltage Graph at MV side of MG Bus When Micro-Grid is not Connected

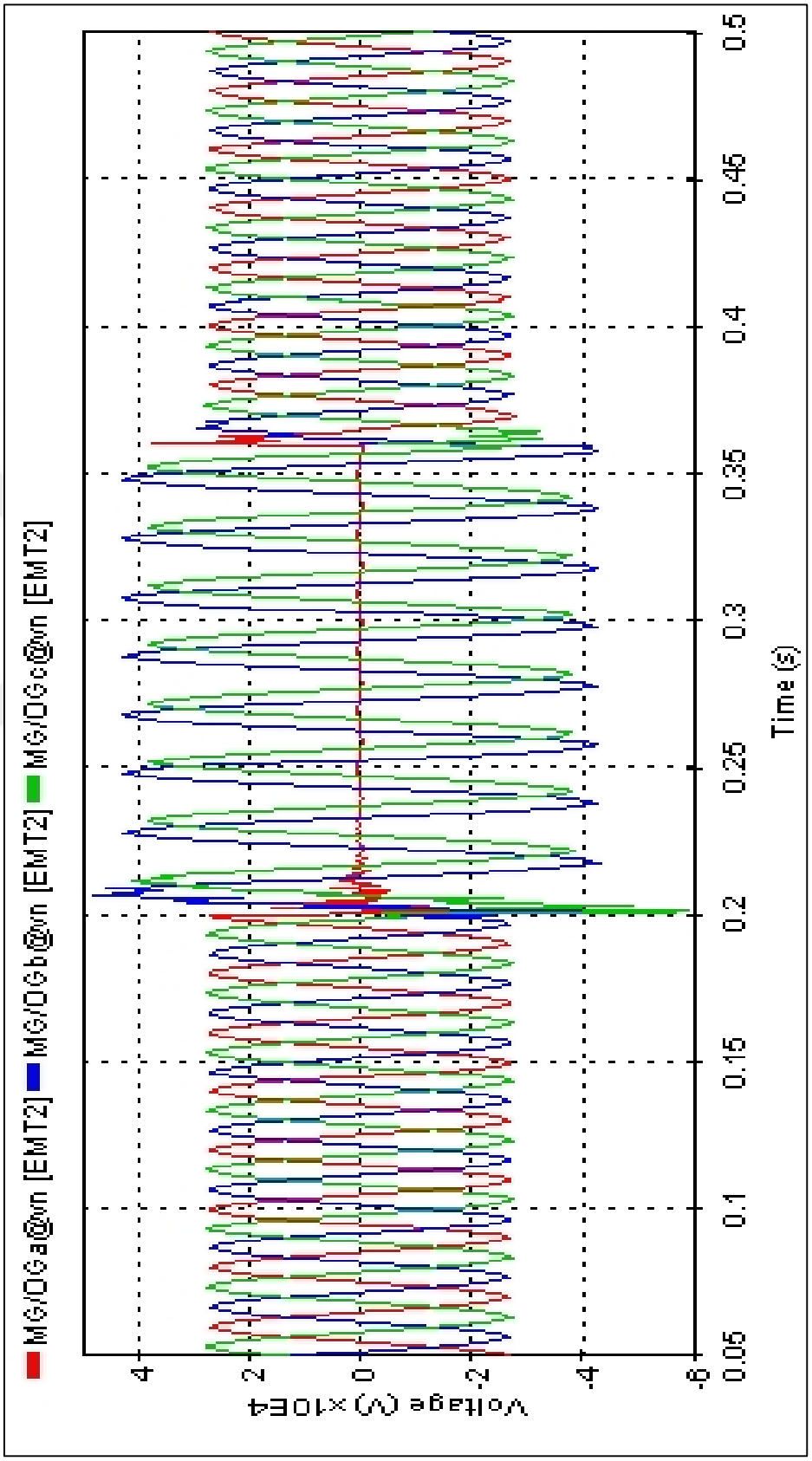

When voltage graphs are compared for DERs are included and DERs are excluded, improvements at the MV side of MG can be seen clearly. Also, voltage swell magnitudes at other two phases are affected positively when micro-grid is connected to the main grid. While maximum voltage magnitude is around 44 kV without micro-grid, with micro-grid this maximum voltage magnitude is becoming less than 39 kV.

5.3.2 Single Phase Fault at Grid with Constant Parameter Model

Figure 5.27: Voltage Graph at Bus 6 (Near the Fault Location)

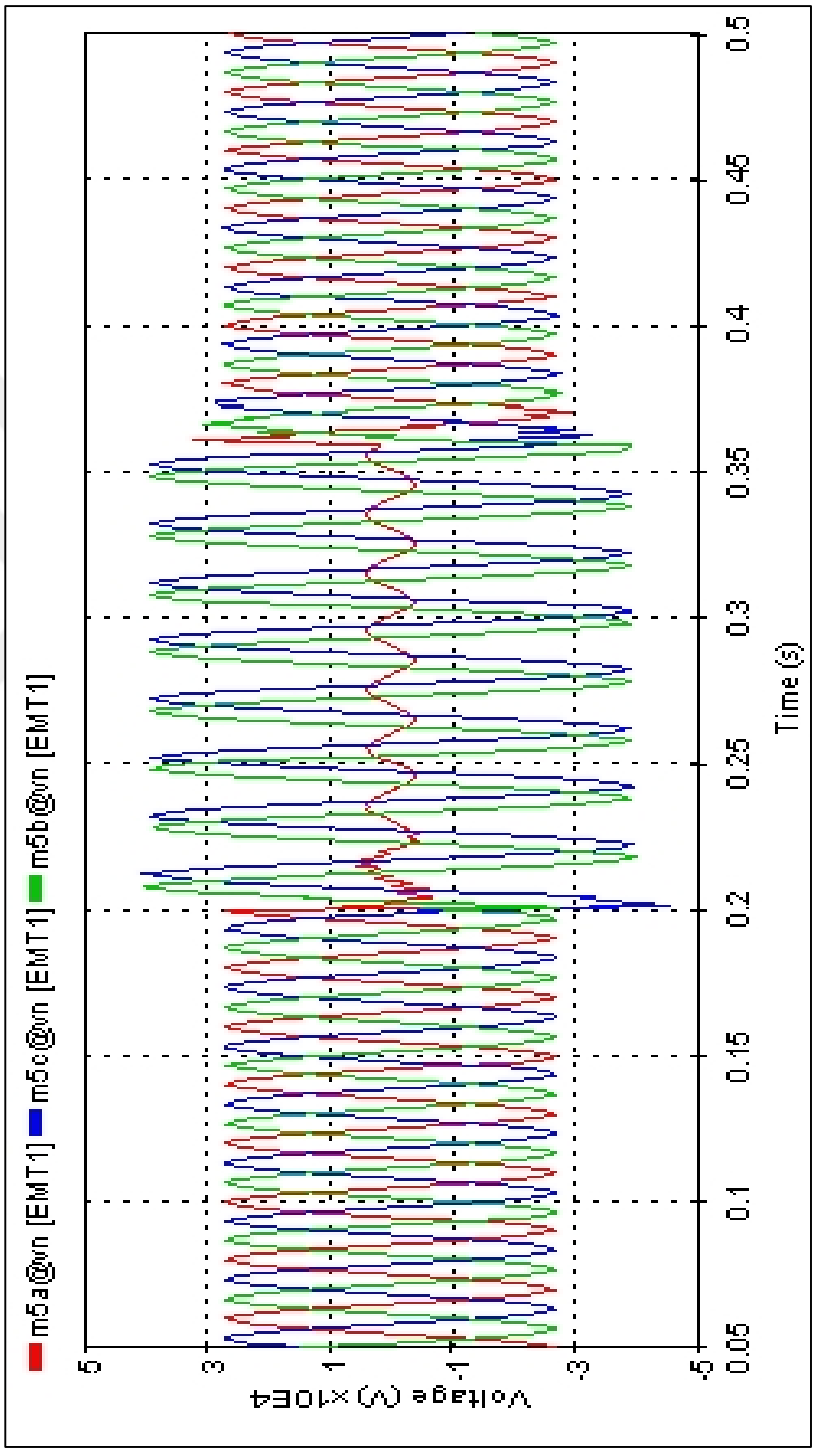

In this case, the same fault applied for the same locations which are explained in the 5.3.1 subsection. Voltage measurements are obtained again for exact same buses. The purpose of this case is to show simulation differences between models which are consist of only FD lines or CP lines. In this case, all underground cables and overhead lines are modeled as CP model. One of the obtained voltage shapes is indicated below as Figure 5.27 (Voltage graph of FD model for the same location is given in Figure 5.22). In order to see the difference between models, other voltage graphs are given together for the fault location and MV side of MG as Figure 5.28 and Figure 5.29 respectively.

When these figures are evaluated, differences are seen not only voltage magnitudes and angles but also voltage shapes. Especially for the first cycle after the fault is occurred and when it finished, variety between voltage shapes can be seen clearly. The main reason of this the distinctness of their impedance calculation of lines. It can be deduced that this difference is caused by mainly inductance value (especially in the overhead line) in the impedance estimation which is explained in Section 4.2. Thus, it can be said that although CP models have faster computing time and most accurate results, for transient events FD models give more precise results.

Figure 5.28: Voltage Graph at MV Side of Micro-Grid Bus

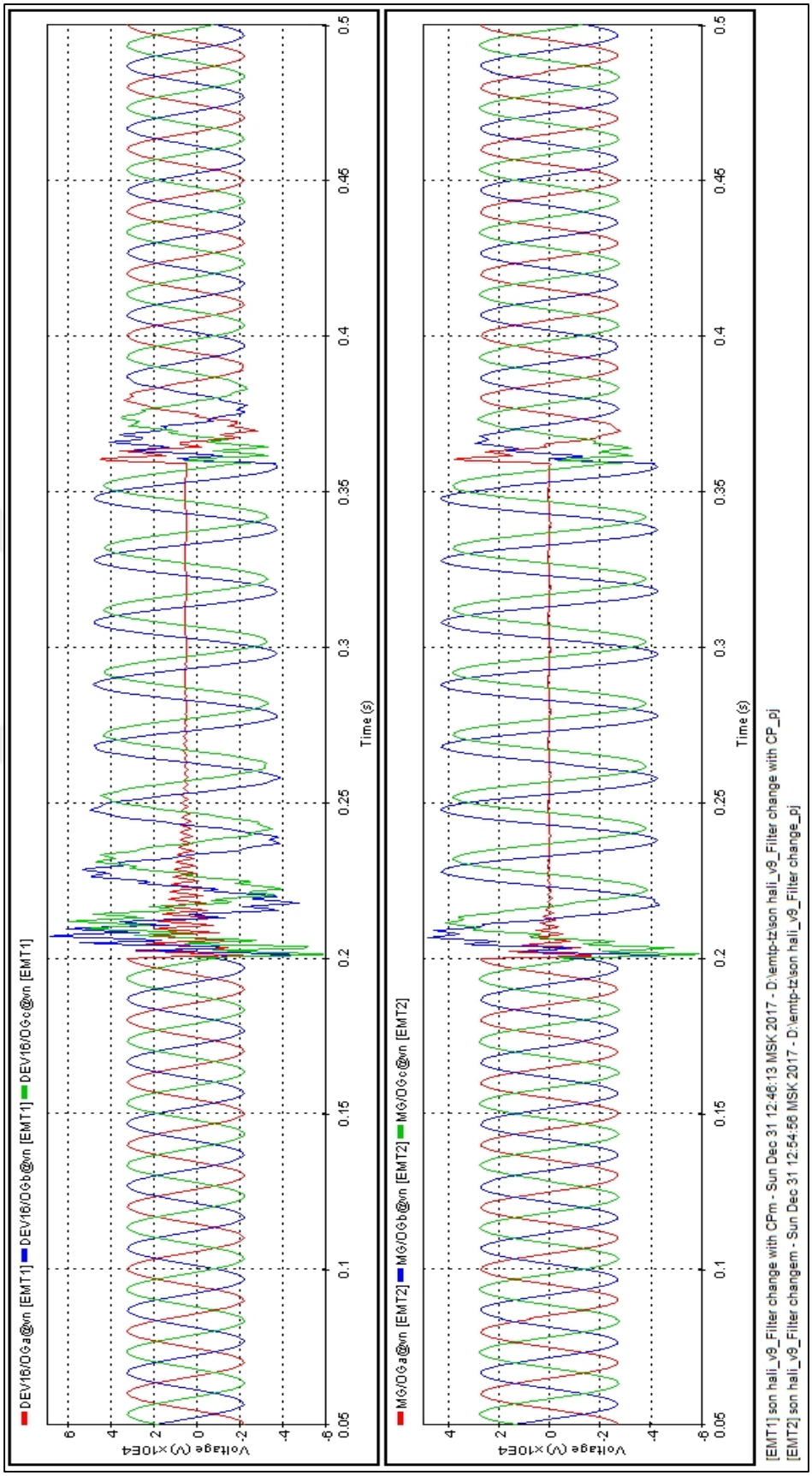

Figure 5.29: Voltage Graph at Fault Location

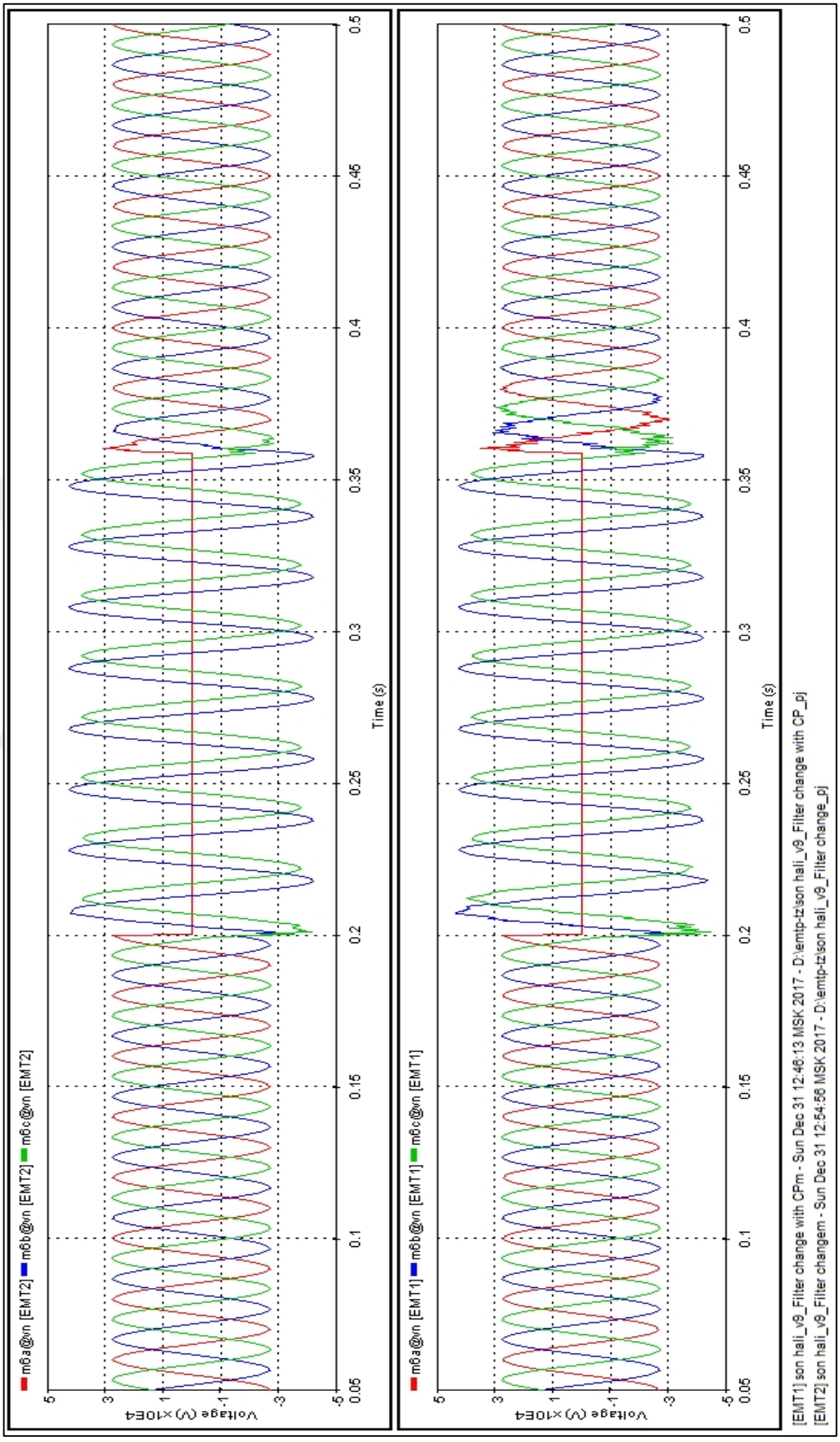

6. CONCLUSION AND RECOMMENDATION

The main aim of this thesis is to model the grid-connected AC micro-grid that, covers PV system, WES, and ESS, and evaluate the effects of modeled system under transient events on the power system. In order to obtain the model that represents the real AC Micro-grid system, two necessities are considered. The first one is that frequency dependent models are used for overhead lines and underground cables to simulate the actual system. The second one is that underground cables are modeled with their metallic sheaths which are double side bonded. Besides these, two LC filters are used to eliminate harmonics and distortions caused by power electronic systems which are used for PV and ESS.

Three case studies which deal with switching, lightning and faults are simulated and evaluated. From these cases, it can be concluded that micro-grid increases the reliability of the power system when a fault occurs. Depending on the importance of loads, the operation mode of micro-grid can be changed. For instance, it can be disconnected from main grid to protect its own load and remove the effects of faults. Besides, the micro-grid may help to decrease the voltage sag level at other buses and increase the voltage magnitude by supplying energy to the main grid. Especially when more than one micro-grid is operated as a grid-connected, such positive effects can be seen more clearly. It also improves the voltage magnitude by decreasing losses and supplying energy. Although micro-grid has general advantageous especially for voltage sag events, when transient events are considered, it seemed that micro-grid is affected substantially and became more vulnerable than other buses in the power system. Thus, when the micro-grid system is designed, transient events and their influences on micro-grid should be investigated to provide the reliability of the system. Moreover, all necessary protection devices should be used depending on these study results.

REFERENCES

Books

Dorf, R., 2005. The engineering handbook. Boca Raton [Fla.]: CRC Press.

Heier, S., 2009. Grid integration of wind energy conversion systems. Chichester [u.a.]: Wiley.

Manwell, J., McGowan, J. and Rogers, A., 2011. Wind energy explained. Chichester: John Wiley & Sons.

Willis, H., 2004. Power distribution planning reference book. New York: M. Dekker.

Willis, H., 2002. Spatial electric load forecasting. New York: Marcel Dekker.

Periodicals

Bradford, R., 2009. Capturing grid power. *IEEE Trans Power Energy*. **7** (4), pp. 32‑41.

Eghtedarpour, N. and Farjah, E., 2014. Power Control and Management in a Hybrid AC/DC Micro-grid. *IEEE Transactions on Smart Grid*. **5** (3), pp. 1494-1505.

Esram, T. and Chapman, P.L., 2007. Comparison of Photovoltaic Array Maximum Power Point Tracking Techniques. *IEEE Transactions on Energy Conversion*. **22**, 439-449.

Faranda, R. and Leva, S., 2008. Energy Comparison of MPPT Techniques for PV Systems. *WSEAS Transactions on Power Systems*. **3**, 447-455.

Hansen, A., Iov, F., Blaabjerg, F. and Hansen, L., 2004. Review of Contemporary Wind Turbine Concepts and Their Market Penetration. *Wind Engineering*. **28** (3), pp. 247-263.

Hossain, E., Kabalci, E., Bayindir, R. and Perez, R., 2014. A Comprehensive Study on Micro-grid Technology. *International Journal Of Renewable Energy Research*. **4**, (4).

Jacobson, M., Z., 2009. "Review of Solutions to Global Warming, Air Pollution, and Energy Security". *Energy & Environmental Science*. **2** (2): pp. 148–173.

Jansuya, P. and Kumsuwan, Y. 2013. Design of MATLAB/Simulink Modeling of Fixed-pitch Angle Wind Turbine Simulator. *Energy Procedia*. **34**, pp. 362-370.

Lacal-Arrntegui, R., 2014. 2013 JRC Wind Status Report. *SSRN Electronic Journal*.

Lal, N. and Mubeen, S., 2015. Voltage Dependent Load In Power Flow Analysis. *Electrical and Electronics Engineering: An International Journal*. **4** (2), pp. 65-77.

Lasseter, R., 2010. Micro-grids And Distributed Generation. *Intelligent Automation & Soft Computing*. **16** (2), pp. 225-234.

Liu X., Wang, P. and Loh P. C., 2011. A Hybrid AC/DC Micro-grid and Its Coordination Control. *IEEE Transactions on Smart Grid*. **2** (2), pp. 278-286.

Majumder, R., Ghosh, A., Ledwich, G. and Zare, F. 2010. Power Management and Power Flow Control With Back-to-Back Converters in a Utility Connected Micro-grid. *IEEE Transactions on Power Systems.* **25** (2), pp. 821-834.

Majumder, R., Ghosh, A., Ledwich, G. and Zare, F., 2009. Load sharing and power quality enhanced operation of a distributed micro-grid. *IET Renewable Power Generation*. **3** (2), p. 109.

Mariam, L., Basu, M., and Conlon, M. F., 2013. A Review of Existing Microgrid Architectures. *Hindawi Publishing Corporation Journal of Engineering*. **2013**, pp. 1-8.

Pandiarajan, N., Ramaprabha, R. and Muthu, R., 2012. Application of Circuit Model for Photovoltaic Energy Conversion System. *International Journal of Photoenergy.* **2012**, pp. 1-14.

Plett, G., 2004. Extended Kalman filtering for battery management systems of LiPB-based HEV battery packs: Part 2 Modeling and identification. *Journal of Power Sources*. **134** (2).

Ramos, H., J., Campayo J., J., Larrañaga, J., Zulueta, E., Barambones, O., Motrico, J., Fernandez, G., U., and Zamora, Z., 2012. Two Photovoltaic Cell Simulation Models in Matlab/Simulink. *International Journal of Power Electronics (IJTPE).* **4** (1), pp. 45-51.

Riegler, H., 2003. HAWT versus VAWT VAWTs Find a Clear Niche. *Refocus.* **4** (4), pp. 44-46.

Sharma, H., Pal, N., Singh, Y. and Sadhu, P. 2015. Development and Simulation of Stand Alone Photovoltaic Model Using Matlab/Simulink. *International Journal of Power Electronics and Drive Systems (IJPEDS).* **6** (4), p. 703.

Shikha, Bhatti, T. and Kothari, D., 2005. Early Development of Modern Vertical and Horizontal Axis Wind Turbines: A Review. *Wind Engineering*. **29** (3), pp. 287-299.

Su, W. and Wang, J., 2012. Energy Management Systems in Micro-grid Operations. *The Electricity Journal*. **25** (8), pp. 45-60.

Villalva, M., Gazoli, J. and Filho, E., 2009. Comprehensive Approach to Modeling and Simulation of Photovoltaic Arrays. *IEEE Transactions on Power Electronics*. **24** (5), pp. 1198-1208.

Other Publications

Belkacemi, R., Babalola, A. and Craven, R., 2015. Experimental Transient Stability Analysis of Micro-grid Systems: lessons learned. Power & Energy Society General Meeting. 2015, IEEE.

Davodi, M., Norouzizadeh, R., Davodi M. and Reihani, E., 2010. Simulation and Analysis of A Micro-grid With Distributed Generation Units Under Unbalanced Conditions. Power and Energy Engineering Conference (APPEEC). 2010 Asia-Pacific.

Engineering.com., 2017. ENGINEERING.com | Photovoltaics. [online]. http://www.engineering.com/SustainableEngineering/RenewableEnergyEngineering/SolarEnergyEngineering/Photovoltaics/tabid/3890/ [Accessed 12 Dec. 2017].

Ghosh, L., Majumder, R., Ledwich, G. and Zare, F., 2009. Power Quality Enhanced Operation and Control of a Microgrid based Custom Power Park. International Conference on Control and Automation. 2009, Christchurch, New Zealand.

Goyal, M. and Gupta, R., 2012. Operation and control of a distributed micro-grid with hybrid system. IEEE 5th India International Conference on Power Electronics (IICPE). 2012, Delhi, India.

Gwec.net., 2017. GLOBAL STATISTICS | GWEC. [online]. http://gwec.net/global-figures/graphs/ [Accessed 12 Dec. 2017].

Hoffmann, R., (2002). A comparison of control concepts for wind turbines in terms of energy capture. Thesis for the Ph.D. Degree. Wien: Elektrotechnik und Informationstechnik der Technischen Universit.

Kumar, V. and Gupta, R., 2016. Voltage Control and Power Balance in a Standalone Micro-grid Supported from Solar PV System. IEEE Region Conference (TENCON). 2016, Singapore.

Larsson A., (2000). Power quality of wind turbines. Thesis for the M.A. Degree. Göteborg, Sweden: Chalmers University of Technology.

Miron, A., Cziker, A., Chindriş, M. and Sacerdotianu, D., 2016. Impact of distributed generation on weak distribution networks: Study case on a Romanian micro-grid. International Conference on Applied and Theoretical Electricity (ICATE). 2016, Romania.

NREL, 2013. National Renewable Energy Laboratory. [online]. http://www.nrel.gov/ncpv/images/efficiency_chart.jpg [Accessed 13 Dec. 2017].

Priyadarshanee, L., (2012). Modeling and Control of Hybrid AC/DC Micro-grid. Thesis for the M.A. Degree. Rourkela: National Institute of Technology.

Rasheed, B., M., Awais, M. and Jawaid, N., 2016. Transient stability analysis of an islanded micro-grid under variable load. 19th International Conference on Network-Based Information Systems. 2016, Ostrava, Czech Republic.

Sera, D., Kerekes, T., Teodorescu, R. and Blaabjerg, F., 2006. Improved MPPT Method for Rapidly Changing Environmental Conditions. IEEE International Symposium on Industrial Electronics. 2006, Montreal, Que., Canada , 2, 1420-1425.

Seritan, G., Triştiu, I., Ceaki, O. and Boboc, T., 2016. Power Quality Assessment for Microgrid Scenarios. International Conference and Exposition on Electrical and Power Engineering. 20-22 October, 2016, Iasi, Romania.

Singh, A., Karandikar, P. B. and Kulkarni, N. R., 2016. Feasibility Of Energy Storage Systems In Different Applications For Sustainable Energy. International Conference on Emerging Technological Trends [ICETT]. 2016, Kollam, India.

Singh, R. and Kirar, M., 2016. Transient Stability Analysis and Improvement in Micro-grid. International Conference on Electrical Power and Energy Systems (ICEPES) Maulana Azad National Institute of Technology, Dec 14-16, 2016, Bhopal, India.

Sorensen, P., Bak-Jensen, B., Kristian, J., Hansen, A.D., Janosi, L. and Bech, J., 2000. Power plant characteristics of wind farms, in Wind power for the 21st century, Proc. of the Int. Conf. 2000, Kassel, Germany, p. 176-179.

Tuffana, T. and AlMuhaini, M., 2015. Reliability Assessment of a Micro-grid Distribution System with PV and Storage. International Symposium on Smart Electric Distribution Systems and Technologies (EDST). 2015, Vienna, Austria.

Watson, R., (2007). New Techniques in the Design of Distributed Power Systems. Thesis for the Ph.D. Degree. Virginia: VirginiaTech.

Wong, Y.S., Lai, L.L., Gao, S., and Chau K.T., 2011. Stationary and Mobile Battery Energy Storage Systems for Smart Grids. 4th International Conference on Electric Utility Deregulation and Restructuring and Power Technologies (DRPT). 2011, Weihai, Shandong, China.

Zhang, J., Guan, L. and Wang, X., 2016. Impacts of Island Load Shedding and Restoration Strategies on Reliability of Micro-grid in Distribution System. IEEE PES Asia-Pacific Power and Energy Conference. 2016, Xi'an – China.

Zheng, D., Wei, D., Zhang, W. and Meng, Z., 2015. The study of supercapacitor' transient power quality improvement on Micro-grid. PowerTech, IEEE. 2015, Eindhoven, Netherlands.